Doctoral Dissertation
Doctoral Program in Electrical, Electronics and Communications Engineering
(32.th cycle)

New methods for Frequency Signal Modelling and Impact Evaluation of New Resources

Francesco Arrigo
* * * * * *

Supervisors
Prof. Ettore Bompard, Supervisor
Prof. Federico Milano. Co-supervisor

Politecnico di Torino
February 29, 9999

I hereby declare that, the contents and organisation of this dissertation constitute my own original work and does not compromise in any way the rights of third parties, including those relating to the security of personal data.

. . . . . .

Francesco Arrigo

Turin, February 29, 9999

Summary

Power systems are increasingly gaining importance. Progressive electrification is happening all over the world in order to enhance energy efficiency and integration of Renewables Energy Sources (RESs). Electricity consumption is growing more than the other energy vectors.

My research work deals with the stable operations of electricity systems. Specifically I asked myself: what is and how can we measure the impact of Battery Energy Storage Systems (BESSs) performing fast frequency control? This question is inserted in the wide area of problems related to the decrease of rotating inertia in the electric grid. Since RESs presence continue to increase, synchronous generators are being replaced by converters which will change the fundamental dynamics of the power system. Regulating energy from conventional fossil fuels sources will continue to decrease and BESS can provide the fast control needed by power system to remain stable. In chapter 3, I present the literature about BESS performing frequency control and propose a novel categorization of the studied papers . In chapter 4, modelling the power system with a low order model, I perform simulations to quantify the impact of BESSs during a contingency. BESSs fast answer was divided in two services: fast Primary Frequency Control (PFC) and RoCof (Rate of Change of frequency) control which mimics the behaviour of physical inertia. A correct dimensioning of the two services has been assured imitating the behaviour of synchronous generators through the use of an Equivalent Saturation Logic (ESL). Both components of the control are fundamental to stop the frequency decay.

Another part of the Thesis is focused on the impact of BESSs during normal operations of the grid, when frequency is bounded in a strict operating range. In order to address this problem, a closed loop model must be used. In such a model frequency can vary realistically for a long period of time and BESSs influence the frequency signal. In chapters 5 and 6 are developed two different methodologies to simulate a closed loop system: the first one based on the explicit computation of the load mismatch which creates the frequency deviation, the second one based on the use of the Fourier Transform Theorem (FTT) in order to reproduce the main power disturbances harmonics which are present in the grid. In such a way

It has been possible to quantify the impact of BESSs making use of specific defined indexes. Besides an additional analysis with the low order model is performed in the frequency domain.

Due to the slow nature of the frequency signal in normal operations, RoCof control cannot improve frequency deviations. Even PFC produced by BESSs is not particularly more efficient with respect to Conventional Generation (CG). Moreover, I conduct an investigation on the main effects of frequency control on BESS State of Charge (SoC) dynamics: the main result is that the impact of BESS inefficiency is negligible with respect to the effects caused by intra-day and average frequency dynamics. Also, I simulate a Variable Droop Strategy (VDS) to find out its consequences on the system: the strategy improves the SoC profile without causing frequency unbalances.

Finally, in chapter 7 I focus on the evaluation of the impact of Electric Vehicles (EVs). Due to their expansion, EVs could represent the most part of batteries systems operating in the electric grid, therefore there is a great interest to study their potential for fast frequency control. However, EVs present additional modelling challenges with respect to BESSs for their correct characterization: they are not always attached to the electrical grid and need to recharge after a travel, besides they are connected to the distribution system which is more easily subject to congestion with respect to the transmission system where BESSs are usually installed. I present a framework to study the mentioned problems and develop the first steps.

Acknowledgements

And I would like to acknowledge ...

Dedication ...

Contents

List of Tables

List of Figures

List of Abbreviations

ACE	Area Control Error
BESS	Battery Energy Storage System
CG	Conventional Generation
COI	Centre of Inertia
DFT	Discrete Fourier Transform
DSO	Dystribution System Operator
ESL	Equivalent Saturation Logic
EV	Electric Vehicle
FDS	Fixed droop strategy
FTT	Fast Fourier Transform
ICT	Information and communication technologies
MPC	Model Predictive Control
PDF	Probability Distribution Function
PFC	Primary Frequency Control
PI	Proportional Integral
PID	Proportional Integral Control
PLL	Phase Locked Loop
RES	Renewable Energy Source
RoCof	Rate of Change of frequency
SGAM	Smart Grid Architecture Model
SFR	Secondary Frequency Control
SFRM	System Frequency Response Model
SG	Synchronous Generator
VDS	Variable Droop Strategy

Introduction

This Introduction provides a brief description of the content of each chapter. In a parallel way, at the end of the Thesis, the Conclusions gather the main results, lessons learned and suggestions coming from my studies. Few notes are added concerning the scientific works I was involved with, the tools that I have used and the other activities I conducted during my PhD-

Thesis Structure

The work can be divided in three parts:

First part - Background, composed by three chapters. In particular we have:

- **Chapter 1 - Power System Fundamentals.**

  Key data are gathered on the energy transition happening today by using the most recent countries reports. This is a non-technical presentation, but important to contextualize the role of electricity in the energy sector. The electric grid is then presented in its basic structure and components by using SGAM methodology. Finally, are described the stability issues of the grid considering the increase of RESs resources. Part of the content of the chapter was used in the deliverable D1.1 of the European project RESERVE [176] [1]. Besides I in order to describe the RESERVE projects use cases [175], I applied SGAM methodology .

- **Chapter 2 - Frequency Dynamics and Control Modelling.**

  A critical description of the grid frequency dynamics is presented along with the main parameters influencing this variable. The classical view of frequency control is presented in the first part, while a general discussion on the impact of RESs and the potential of new resources for frequency control is presented in the second part.

[1] https://www.re-serve.eu/

- **Chapter 3 - Literature Review on Frequency Control.**

  This chapter provides a rigorous and in-depth review on the papers dealing with the impact of BESSs performing fast frequency control. The read works are divided in 3 groups: studies on open loop where the effect of BESS into the grid cannot be evaluated, studies of the impact of BESS after a sudden contingency in the grid, studies of the impact of BESS during normal operations. The papers are sub-divided according to the methods and the main research questions to highlight differences and improvements among them. The chapter (with the addition of chapter 2) works as a basis for a future literature review paper.

Second part - Evaluating the impact of BESSs on frequency dynamics. Also this part is divided into three chapters:

- **Chapter 4 - Impact of BESS fast frequency control after a contingency**.

  The first two studies on BESS impact on frequency control are developed in this chapter. Two channels of control (RoCof and PFC) are simulated using two different grid models considering different analysis and highlighting the most influent parameters. The two studies were published respectively in [174] and [119] in collaboration with other researchers. In [119] I built a basic version of the grid model used in Chapter 5 and the Equivalent Saturation Strategy to dimension frequency Reserves from BESSs. Models are developed in Simulink and the data analysis is performed in Matlab.

- **Chapter 5 - Impact of BESSs in normal grid conditions: a System frequency response model approach**.

  The model of last chapter is expanded and reversed in order to compute the load mismatch which cause the frequency to change during normal conditions of the grid. BESSs are then added to evaluate their impact on the grid. The System Frequency Response Model (SFRM) is studied also in the frequency domain. The results of this part will serve as a basis for a paper to be submitted shortly. Finally, notes on SoC dynamics, on BESSs modelling and on the frequency signal characteristics are introduced based on the frequency data of the Irish system.

- **Chapter 6 - Impact of BESSs in normal grid conditions: a Fourier Transform approach.**

  The second approach uses FFT to analyze the real frequency signal and its harmonic content. Relevant power disturbances are reproduced in order to

recreate frequency deviations in a simulated environment which is compared with the harmonic content of the original frequency data (in this case the Irish signal is used). The study is performed in DOME, a transient power system simulator created by Professor Federico Milano. Beside the classic fixed frequency droop control, VDS is used for BESSs and the impact of this strategy on the grid can be explicitly evaluated. For the data analysis I have used Python programming language. Relevant papers associated with this research are [12, 13].

Third part - This last part is composed just by one chapter and deals with Electric Vehicles.

- **Chapter 7 - Electric Vehicles Studies**.

  This chapter aims to evaluate the impact of EVs performing frequency control when connected to the grid. The final goal is to study the possibility of bottlenecks in the distribution system which can be provoked by frequency control and how Distribution System Operator (DSO) can intervene to secure the grid. In this chapter only two intermediate steps are presented: in particular an agent based modelling framework is built to recreate scenarios with thousand of cars moving in a realistic road network and charging in different points of the electrical grid. The models of this framework were designed and developed in Matlab and presented in [60]. A second part deals with the construction of a sound smart charging strategy for the EVs before performing frequency control. A priority based logic was implemented and proved in a simple case study. The results are accepted for publication in ISGT Conference 2020 (Washington).

During my PhD I had the opportunity to work on real time simulation [117] developing models in Simulink-Sympowersystems for the RESERVE project. Finally, I am collaborating in a paper currently under revision about the modelling and the simulations of Power to Gas plants in the distribution networks.

In this Thesis when writing about works conducted in collaboration with other researchers, I focus more on my personal contributions.

Chapter 1

Power system Fundamentals

In section 1.1 current and future energy scenarios are presented in order to highlight the important role of electricity to increase the production from renewable sources. European perspective will be explained in detail. Since electric grid is a complex industry, an holistic view on its main features is briefly presented in 1.2 through the description of the SGAM model. Finally in section **??**

1.1 Energy and Electricity Scenarios

1.1.1 World Energy Transition

Today, energy is at the center of modern society. Several international agencies propose [182] the use of a set of indicators called Energy Indicators for Sustainable Development. These indicators are 30 and divided in 3 dimensions: social, economic and environmental. Moreover the importance of energy is highlighted in the Goal 7 of the Millennium Development Goals ratified by UN: "Ensure access to affordable, reliable, sustainable and modern energy for all". These goals are a synthesis of the countries' political will and have to be implemented in practical actions in the period 2015-2030 all over the world.

Energy sources and technologies have drastically changed during the years. For example total final energy consumption (TPES) continues to increase passing from 6101 Mtoe [1] in 1973 to 13972 Mtoe in 2017 [3]). In the current state, the increase of energy consumption comes from development countries while industrialized nations tends to flatten or even decrease their energy demand. Energy intensity

[1] Mtoe stands for Mega tonnes of oil equivalent which is computed as the energy produced by burning one tonne of crude oil equivalent to 41.868 GJ or 11.63 MWh.

(which is evaluated as energy consumption divided by the value of the Gross Domestic Product) continues to decrease thanks to an improvement in efficiency, technologies and better industrial processes management. New renewable energy sources (mainly solar and wind) are just starting to reach significant amounts in the system, while fossil fuels still covers most of the production. Enormous efforts are still needed to decrease climate change.

In the electricity sector, electricity consumption increases proportionally faster than energy demand. In 2000, electricity accounted for 15% of the total TPES, while in 2017 was already 19% and it is still expected to increase. Electricity is in fact a high value energy carrier for several reasons:

- in the presence of a good infrastructure, it is very easy to transport in big quantities with low losses and used in the most part of domestic, commercial and industrial appliances.
- Electricity eliminates the pollution in the place of consumption. Moreover, power plants using fossil fuels for electricity production have very efficient filters and pollution abatement systems.
- It helps and sustains the increase of renewable energy sources (RES) such as Wind (Offshore and Onshore) and Photovoltaic power. These naturals sources are usually sparse in the country territory and the electric infrastructure is essential to transport the energy produced to consumption centers.
- Electricity can also be a driver for energy efficiency and low environmental impact technologies like heat pumps and electric vehicles.

For all these reasons, industrialized countries are wired with a strong, meshed electric network. However today still a little less of one billion people does not have access to electricity at home. In the last years the Asian and African progress in energy and especially electricity consumption allowed to raise the human standard of living, but on the other hand it is a serious cause for environmental concern as green-house gases (GHG) emissions are still rising and reached 37.1 Gtonnes in 2018.

China and USA objectives

China is today the biggest energy user and GHG emitter, responsible for the 20.8 percent of the total global emissions and it is still growing at enormous pace. China still heavily depends on coal plants and coal use for its energy needs covering more than 55 % of its internal demand. The situation started to change in 2015 with the 13th Five-year Development Plan 2011-2015 and especially during the

19th National Congress of the Communist Party of China in 2017, were Chinese government decide to work towards the construction of an ecological civilization within 2050 and agreed to participate to Paris Agreement [36]. By 2050 if the Paris agreement is to be respected, electricity is expected to represent around 50 % of the final demand and to be produced mainly by RES. China aspire to overcome Europe and USA and become the world leader of the renewable world and its pushing very strongly for changing its society.

USA is responsible for the 20.1 percent of total global emissions. In recent years it has become a net exporter of oil, oil products and naturals gas thanks to the use of environmental controversial fracking techniques. In 2017 the portion of renewable in total energy demand was just 11 %, a much lower starting point than Europe. Nevertheless while at the federal level, Trump administration is slowing the pace of reforms, at the state level the increase of renewables is being fostered by local government initiatives. However the USA Reference Energy Scenarios towards 2050 [11] projects an energy demand slightly increasing, a big share of gas, still some coal power plants in the power sector and not enough increasing electricity penetration.

1.1.2 The European Perspective

The Europe Objectives

European Union is a leading force for what concerns the energy transition to a de-carbonized economy. The goal is to take an holistic and quantifiable approach in order to assure security of supply, competitiveness, sustainability of the energy and industrial system. Europe wants to achieve this goal by strengthening the Energy union under five important dimensions [2]:

- Security, solidarity and trust. Europe still heavily depends on imported fossil fuels in order to sustain its energy production. Fossil fuels (solid fuels, gas, petroleum, etc.) represented in 2016 the 71 % of total primary energy consumption. 54 % of fossil fuels used are imported from abroad (from the 52 % in 2005) and represents an high geopolitical risk. RES are expected to play a key role.

[2] if the reader is interested, more news, documents and data can be found online at the European Commission website in the page for energy: https://ec.europa.eu/info/energy-climate-change-environment_en and in the page for statistics data https://ec.europa.eu/eurostat/data/database

- a fully integrated energy market, in order to foster efficiency and transnational connections between the countries. This is happening especially for the two biggest energy infrastructures: gas and electricity transmission networks, which are reaching a more strict technical and economical coupling for example through the joint construction and update of the Ten Year Network Development Plans (TYNDP). These and other actions are fostered and harmonized by ENTSO-E and ENTSO-G, which are the European agencies gathering the gas and electricity transmission system operators.
- Energy efficiency in order to reduce the energy demand and drive the increase of high tech jobs and growth. This is done mostly by improving the efficiency of house appliances and the reducing the energy needs of buildings. The deployment of millions of smart meters is also considered part of the strategy
- Climate action - decarbonising the economy. While energy sector produces the most amount of carbon emissions (1,28 billion of tonnes of CO2 equivalent), it just represents around the 25 % of the European emissions. Industry, transport and building are the other sectors causing big GHG emissions.
- Research, innovation and competitiveness. Europe is investing in programmes of research in helping patent creation from battery storage to bio-energy and smart cities.

The first accountable objective for Europe was established by the **2020 climate & energy package** in 2007.The Goals to reach are those of the 20-20-20; 20% decrease of GHG emissions with respect to 1990 levels; 20 % of energy coming from renewable sources (with at least a 10 % share of renewable in the transport sector) and finally 20% of consumption decrease due to increase in energy efficiency. Numerous initiatives were taken to ensure these goals:

- ETS (Emission Trading Scheme) for energy and large polluting industries and binding annual targets for other sectors in order to cut GHG emissions.
- National targets for renewable production.
- Support for the development of low carbon technologies for example through the NER300 programme for renewable energy technologies and carbon capture & storage and the Horizon 2020 fundings for research & innovation.
- Energy efficiency measures through the Energy efficiency Plan and Directive.

The emissions were cut by 23% between 1990 and 2018, while the economy grew by 63% over the same period. Energy consumption continued to decrease

until 2014, but increased in the years 2014-2017 due to economic growth related emissions. So while energy efficiency is actually increasing at an high rate (more than 30 % [3]), new appliances and increasing energy demand slow down the decrease in energy consumption. In 2017 the final energy consumption was 3.3 % above the respective 2020 target. Finally, renewable sources represent 18.9 % of energy consumed in 2018 and in the transport sector this percentage reached 8.3 % in the same year in line with 2020 goals.

Europe continues its efforts also in the period 2020-2030 under the 2030 climate & energy framework.The key targets for 2030 are:at least 40% cuts in greenhouse gas emissions (from 1990 levels). At least 32% share for renewable energy. At least 32.5% improvement in energy efficiency. Finally in 2018 the European Commission presented its strategic long-term vision for a prosperous, modern, competitive and climate-neutral economy by 2050. The vision is compliant with with the Paris Agreement objective to keep the global temperature increase to well below 2°C and pursue efforts to keep it to 1.5°C. The detailed plan and the single national efforts are still under discussion.

Electricity sector status and future trends

Various scenarios can be formulated to consider the future trends of Europe RES production increase. The energy scenarios are a representation of possible pathways that a place will undergo to fulfill its ever growing demand for energy. Each scenario is described by a coherent set of assumptions on the current trends or possible different future constraints, like environmental awareness, policy intervention, socio-economic and technological trends. These features are quantitatively linked together through the use of key relationships and models mixing several scientific disciplines [122]. Keep in mind that scenarios are not predictions or forecasts of the future but a way to show all interested people from policy, technical and research environment how the future could unfold as a consequence of certain choices and natural dynamics into society. The task is extremely difficult considering the enormous complexity of today energy systems and societies.

The most interesting scenarios are the EU Reference Scenario 2016 [30] and the EUCO scenarios [167] . The latter was built starting from the EU Reference Scenario 2016 and designed to achieve the 2030-2050 targets agreed by the European Council. instead EU Reference Scenario for 2030 and 2050 was built as a benchmark of current policy efforts and market trends. The EUCO3232.5 [147]

[3]https://www.eea.europa.eu/data-and-maps/indicators/progress-on-energy-efficiency-in-europe-3/assessment

scenario was constructed in compliance with the new 2030 objectives developed in 2018. EUCO scenarios were used by European commission to propose a recast of the current European policies in order to achieve better results under Effort Sharing Decision procedure of the winter package.

In Figure 1.1 the historical data about 2000 and 2010 and the projection of electrical consumption for Europe in year 2020,2030 and 2050 are shown. For 2020 only EUCO3232.5 was shown as the number are very similar to the Reference Scenario. The 2050 is shown only for the Reference Scenario and the EUCO30 as found in [31]. EUCO30 with respect to EUCO3232.5 present similar assumptions but slightly less ambitious.

Table 1.1: Electricity production statistics in Europe. The EUCO scenario 2050 refers to the scenario EUCO30 indicatively very similar to EUCO3232.5

	- 2000	- 2010	EUCO 2020	EUCO 2030	Ref. 2030	Ref. 2050	EUCO 2050
Generation [TWh]	3005	3332	3378	3498	3527	4063	4300
Fossil fuels [pu]	0.54	0.515	0.42	0.23	0.36	0.27	0.14
Renewable[pu]	0.145	0.21	0.36	0.56	0.42	0.55	0.64
Nuclear [pu]	0.315	0.275	0.22	0.21	0.22	0.18	0.22
El. pen. [pu]	0.15	0.163	0.177	0.217	0.25	0.28	0.381

In all future scenarios coal (which is the main part of solid fuels) is substantially substituted by gas sources. Gas sources are still needed even in 2050 to add flexibility and back-up capacity to the system: it is therefore forecasted that there will be still a not negligible presence with a much lower capacity factor. To avoid GHG emission carbon capture and storage technologies could be used or the plants could burn bio-methane with almost zero impact for the environment. Nuclear sources are expected to decrease until 2020 and then remain substantially stable. Finally, except for Hydro (which in Europe already reached an high level of maturity) all other renewable sources will undergoes a substantial increase depending on the scenarios. Geothermal will remain low as it is usually exploited for heat production and not electricity and present important natural constraints for efficient exploitation. The limited growth of Biomass and its possible decrease in the long run is due to the competition from the biofuels industry which is supposedly a more lucrative alternative and it is needed to de-carbonize the transport sector. Wind will be the biggest source especially in the case of a big off-shore wind deployment with the construction of the DC super-grid connecting the North Sea. To compute 2030 scenarios and especially for 2050 scenarios many assumptions on the diffusion of Power-to-Gas and Power -to-Hydrogen technology process were

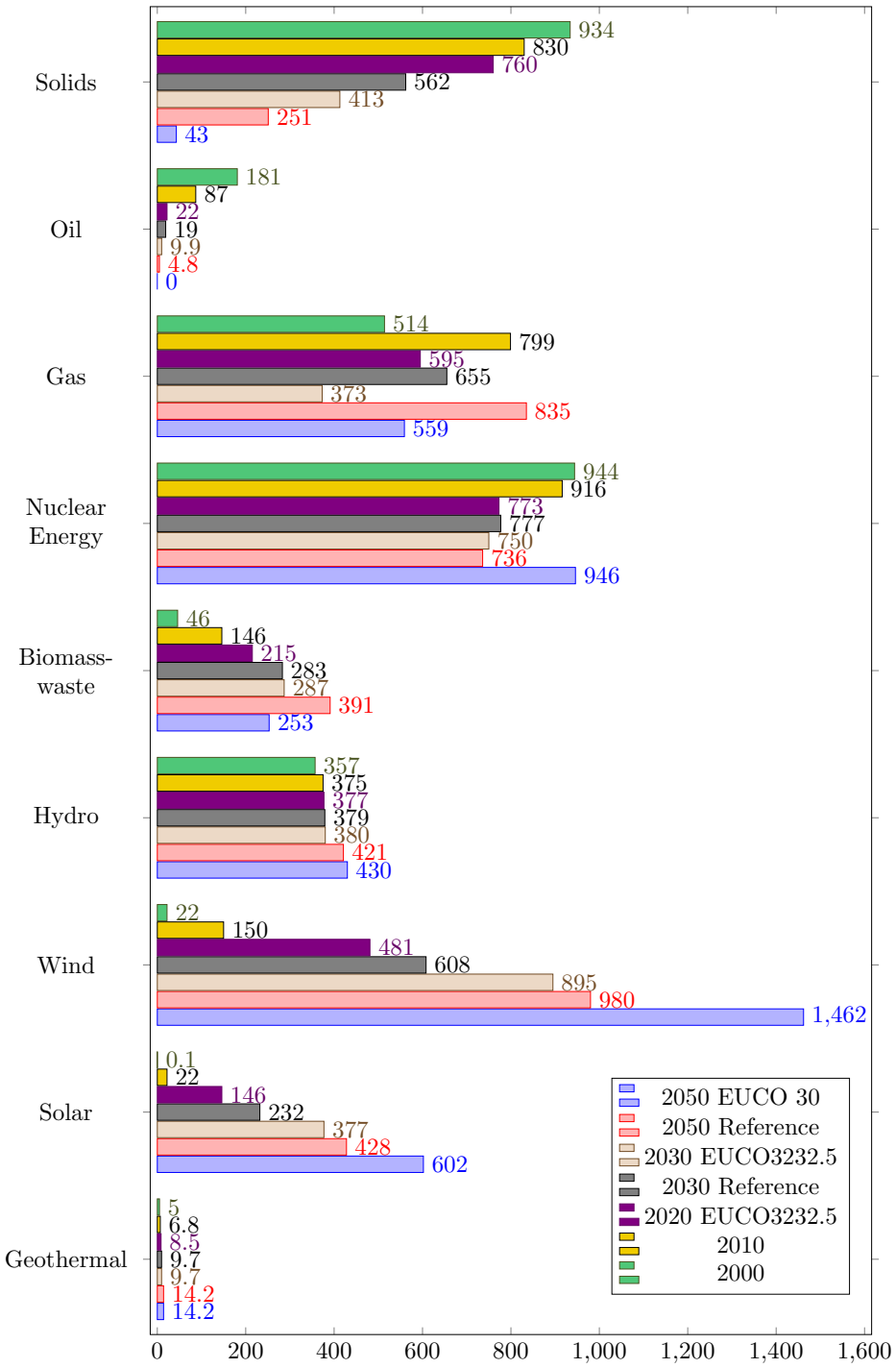

Figure 1.1: Yearly electricity production in Europe by source [TWh] in different scenarios

made that leave space for different future scenarios. As seen from Table 1.1 total electricity consumption and penetration increases thanks to the diffusion of electrical transport, heat pumps and Power-to-X technologies even if Reference Scenario is substantially under the EUCO scenarios. Note that while EUCO scenarios are evaluated with the goal of reaching European objectives, Reference Scenarios are built by trying to intercept the current trends and possible outcome of environmental policies adopted by European countries. The close proximity between the EUCO3232.5 for 2030 and the 2050 Reference Scenarios is due to the biggest role energy efficiency has in the EUCO scenarios and the bigger deployment of energy sources and it is indeed a pressing remark which shows how much additional effort still has to be put to decarbonize the energy sector. However the electricity energy carrier is considered to be the best vector for this transition.

1.2 The Electric Grid Structure

1.2.1 A Paradigm shift

The electric grid is the biggest industrial system built by humans. It continuously provide energy and for its optimal operation needs continuous control in all time ranges from milliseconds up to years. Historically the system has been run in a vertical fashion with big plants connected to Transmission Grid optimized to follow the loads at the distribution levels. With the liberalization of the power system sector the system faced numerous changes from the introduction of thousand of new non dispatchable renewable generators to the possibility for industrial, commercial or private consumer to regulate their loads with renewable sources or even storage. The active player of the grid are not anymore hundreds of big power plant situated at the transmission level, but thousands or even more renewable producer or prosumer (consumer with installed renewable plants and possibility to at least partial control its overall consumption profile). In order to make all the players interact in a market environment with velocity and precision an expansion on the Information and Communication Technologies (ICT) infrastructure of the grid is of fundamental importance. The electric grid is growing extremely complex and it is also referred as the Smart Grid.

1.2.2 SGAM approach

In order to systematically describe new architectures or standards to make the grid more efficient and connect all the players, Smart Grid Architecture Model (SGAM) [32] is used. SGAM is very useful especially for use case design in which

interoperability of different layers are well represented in a technology neutral manner for both existing and future power systems.

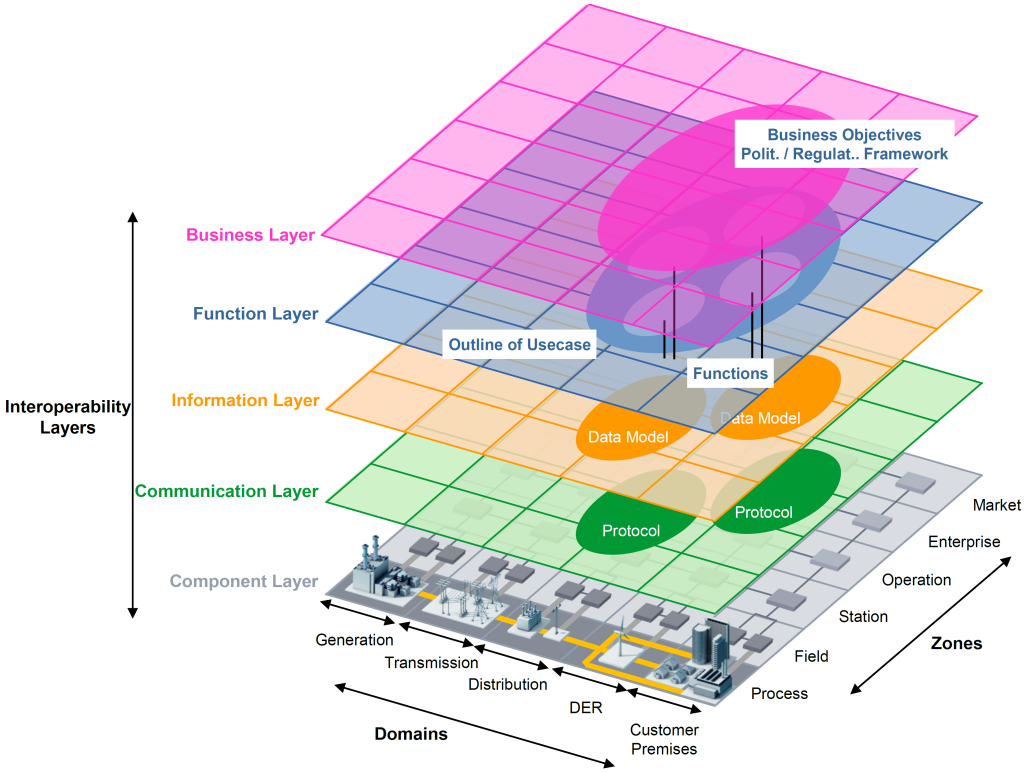

Figure 1.2: Smart Grid Architecture Model (SGAM) - Source: CEN-CENELEC-ETSI Smart Grid Coordination Group

SGAM is a three-dimensional model (see Figure 1.2)that is merging the dimension of 5 interoperability layers including component, communication, information, function and business, with the 2 dimensions of the Smart Grid Plain consisting of zones and domains. Zones represent the hierarchical levels of power system management while domains cover the complete electrical energy conversion chain from bulk generation, transmission, and distribution, to distributed energy resources and customer premises. All classical components and function of the grid and new entries can be introduced and well localized inside the SGAM framework. This would support gaps identification in Smart Grids standardization, and migration scenarios to improve existing/installed architecture.

SGAM Layers

- Component layer. The physical distribution of all participating components in the smart grid context, including system actors, applications, power system equipment, protection and tele-control devices, communication network infrastructure and any kind of computers.
- Communication layer. In this layer, data exchange procedure, technologies, protocols and standards are described for the specific use case, functions, and information objects.
- Information layer. This layer represent messages, measurements, alarms, and in general all data and information which are exchanged between actors of component layer and function layer. It includes information objects and considered canonical data models which ease communication between different data formats.
- Function layer. It includes functions along with their relationships from an architectural viewpoint. The functions are independent from actors and physical implementations in applications, systems and components.
- Business layer. The business layer represents the business view on the information exchange related to smart grids. It supports business executives in decision making related to business models and specific business projects (business case) as well as regulators in defining new market models.

SGAM domains

- Bulk generation. It includes all types of electricity production in bulk quantities, such as hydro power plants, fossil and nuclear power plants, off-shore wind farms, large scale solar power plant, etc.
- Transmission. Infrastructure and organization which are in charge of electricity transportation over long distances.
- Distribution. Infrastructure and organization which distributes electricity to customers.
- Distributed Energy Resources (DER). DERs are small-scale power generation which are directly connected to the public distribution grid with typical production in the range of 3 kW to 10 MW.

- Customer Premises. Hosting prosumers including industrial, commercial, and residential facilities. Prosumers can be either pure consumers or producers such as micro turbines, photovoltaic generation, etc. Electric vehicles storage and batteries are also hosted in this domain.

SGAM hierarchical zones

- Process. It covers all types of energy transformations processes and the physical equipment which is directly involved. Equipment examples in the process zone are generators, transformers, transmission lines and cables, circuit breakers, electrical loads, and any kind of sensors and actuators, etc.

- Field. Protection, control, and monitoring equipment of the power system process are all considered in the field zone. Any kind of intelligent electronic devices which acquire and use process data from the power system, protection relays, and bay controllers are some examples of the field components.

- Station. The area aggregation level for field components falls in the station zone. Station includes substation automation, local SCADA systems, data concentration, plant supervision, etc.

- Operation. Systems which are actually hosting power system operation are considered in operation zone. Some examples of operation systems in different domains: Energy Management Systems (EMS) in generation and transmission systems, Distribution Management Systems (DMS), Virtual power plant management systems (aggregating several DER), Electric vehicle (EV) charging management systems in customer premises.

- Enterprise. Management entities, commercial and organizational processes, services and infrastructures for enterprises (utilities, service providers, energy traders, etc.) are considered in the enterprise zone. Some examples are staff training, customer relation management, asset management, billing and procurement, logistics, etc.

- Market. Energy trading and all possible market operations as either mass or retail market are put in the market zone.

Insert the new actors examples that enters the frame using reserve deliverables (cite d1.1,d.1.2,d1.6)

1.3 Technical issues of the grid

1.3.1 Stability of the grid

The electrical management of the grid is characterized by different phenomena which appears at different time frames. A typical scheme of phenomena and time ranges can be seen in Figure 1.3 where power system phenomena depends on the typical disturbances and physical nature of power system components. In power system controls are listed the typical actions which were devised in the course of time in order to stabilize and optimize the power system operations. Usually automatic continuous control or automatic triggered actions are used to maintain stability in the short time frame normal operations or after a contingency. Long term ranges decision instead usually depends on a technical-economic optimization of the power system generation and reserves.

Many definitions and classification to define stability in a power system were used during the years. Definition should have a consistent and general mathematical underpinning description but, at the same time, it has to have a clear and physical motivated meaning. An attempt was done in 2004 [95]. The proposed definition for the general power system stability is:

> Power System Stability is the ability of an electric system, for a given initial operating condition, to regain a state of operating equilibrium after being subject to a physical disturbance, with most system variables bounded so that practically the entire system remain intact.

Power system is a highly nonlinear system that operates in a constantly changing environment. Disturbances can be of various nature and various intensity, like load stochastic changes or short circuit or big generator trips.Due to its complexity, it is the norm to make simplifying assumption and isolated more specific kind of instabilities based on (i) consideration on physical nature of the instabilities and main system variable involved, (ii) size of the disturbance and (iii) time span that must be taken into consideration.

In particular three stability were defined:

- **Voltage stability**. Voltage stability refers to the ability of a power system to maintain steady voltages at all buses in the system after being subjected to a disturbance from a given initial operating condition. The main driving force usually resides in the increment of reactive power flow from the loads, which cannot be sustained by generators without decreasing voltage level at the corresponding buses. Voltage stability may be studied in case of large disturbance referring to the ability to sustain large disturbance such as system faults, loss of generation, or circuit contingencies or in case of of small

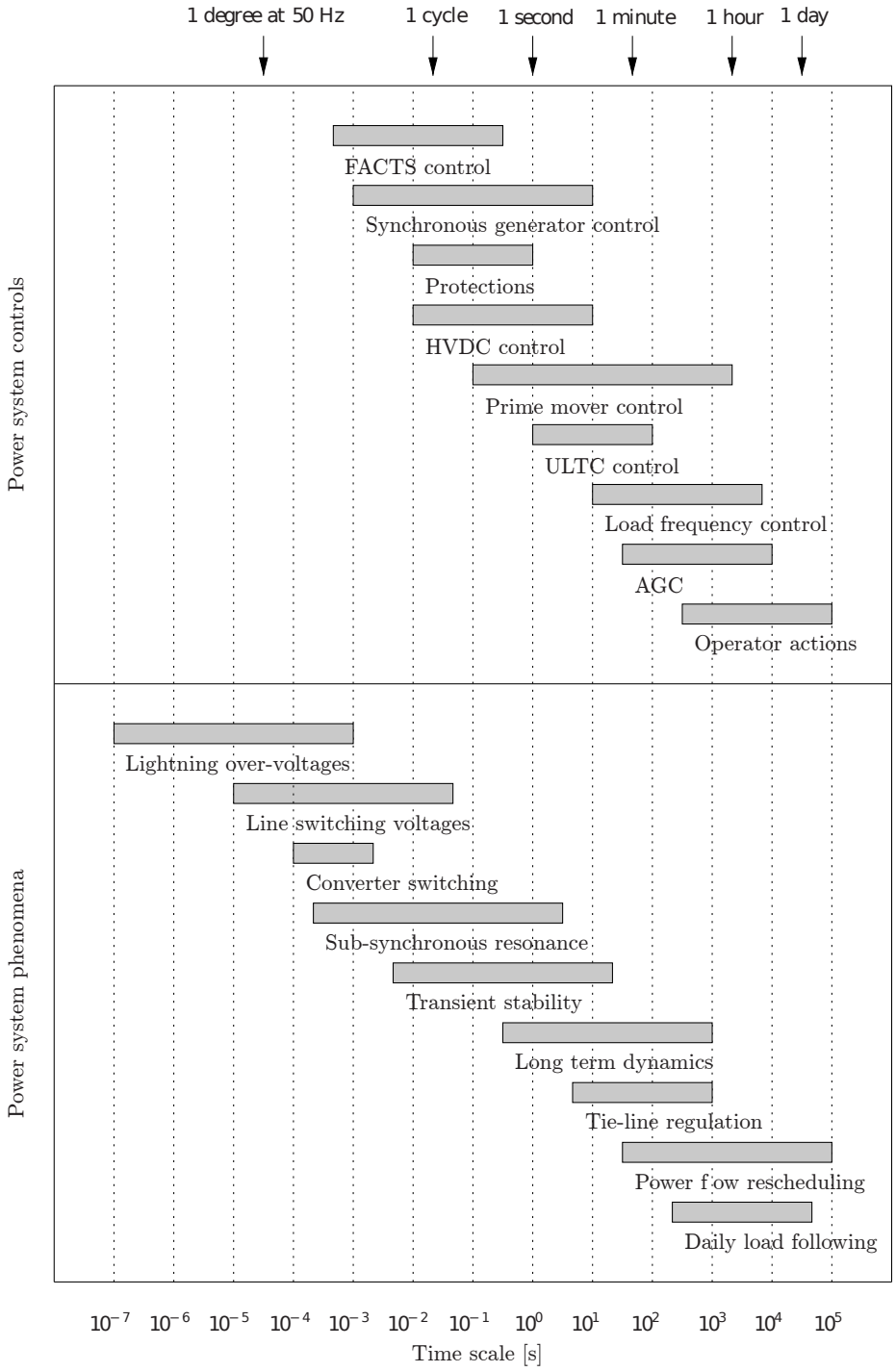

Figure 1.3: Time scales of relevant power system dynamics. Figure modified from [114]

disturbance, due to small perturbations such as incremental load change in the system load. Both kinds can be regarded as short term or long term phenomena depending on processes and components involved.

- **Rotor angle stability**. Rotor angle stability is the ability of the interconnected synchronous machines running in the power system to remain in the state of synchronism. In equilibrium condition there will be equilibrium between the input mechanical torque and output electrical torque of each machine (generator) in the power system and speed of the machines will remain same. If the equilibrium is upset, it results in the acceleration or deceleration of rotors of the machines. This oscillation can bring the machine to lose their synchronism due to the non-linear Power-angle characteristics of synchronous generators. Small signal stability refers to the stability of the machines under normal stochastic oscillations due to load noise. Transient stability refers to the ability to withstand synchronism under large grid faults.

- **Frequency stability**. Frequency stability refers to the ability of a power system to maintain steady frequency following a severe system upset resulting in a significant imbalance between generation and load. Instability occurs in case of big contingencies in the form of sustained frequency swings induced by the tripping of generating units. Frequency stability may be studied in short term corresponding to the characteristic time response of devices such as under frequency load shedding and generators control and protection, or in long term corresponding to the response of prime mover energy supply systems and load voltage regulator.

1.3.2 Renewable sources issues and solutions

The impacts of Renewable Energy Sources (RESs) is profound and involve the electric grid at all layers and all time ranges. The problems caused by RES are many. A list of issues and possible solutions is presented below:

- as we will discuss in next chapter, renewables have a double impact on frequency stability: it lowers inertia and increase short and medium term variability.

- Moreover RES variability affects the Net Load profile to be covered by conventional sources in the hour-day time range. Faster and longer ramps will be needed in order to follow the Net Load and avoid the unbalance of the grid. The typical expected situation is summarized in the duck curve (see

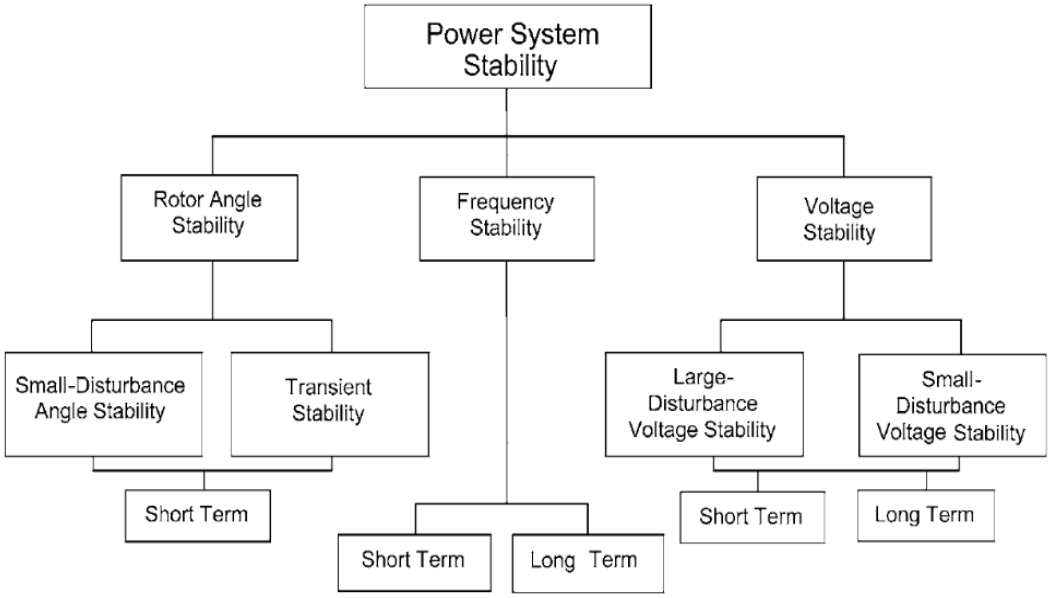

Figure 1.4: Classification of power System Stability [95]

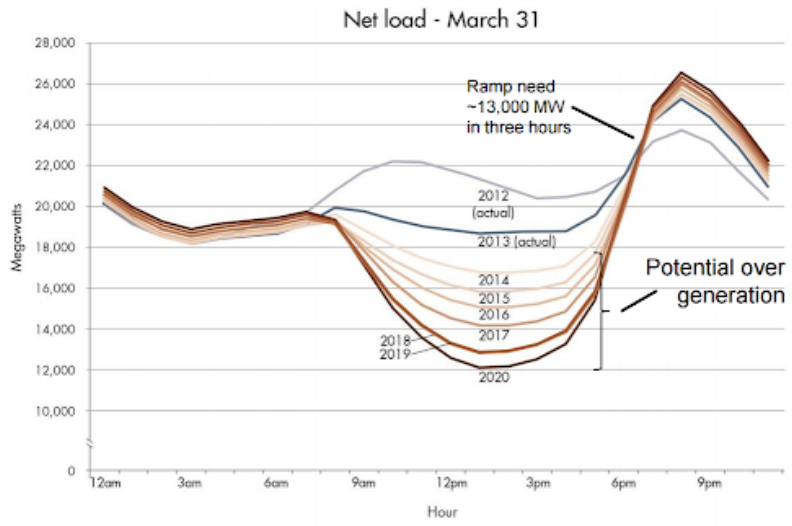

Figure 1.5: Duck curve example of the Californian system. Image taken from [81]

figure 1.5: this scenario comes true in the case of big PV production during the day, followed by a sudden decrease in energy after the twilight when the load is at its peak. The system will need to assure a fast ramp of dispatchable generation in order to avoid an energy unbalance. Some of the phenomena (like sun rise and twilight) are predictable and Reserves can be dimensioned

accordingly while wind is not forecastable with high precision and could create dangerous situations. The big number of plants and their geographical dispersion tends to smooth the output variability. Major flexibility could be achieved by the use of modern Combined Cycle Gas Turbine plants, more interconnection between countries in order to share power reserves and finally the Demand Response: the possibility for consumer to vary their load profile thanks to the use of ICT technologies and coordinated by proper resource aggregators. Moreover RES plants in the distribution grid are difficult to monitor and therefore their present and future production is unknown to the Transmission System operator (TSO).

- Weekly and seasonal variability. In the future there is a possibility to have long period of energy excess or deficit due to RES long term variability become a serious security issue (for example the 2018 July UK wind drought or the typical sun radiation differences between summer and winter). In order to overcome this variability, storage facilities (like pump hydro plants or innovative battery energy storage systems) could be used. Also the possibility of Power-to-X technologies (Power-to-Gas,Hydrogen,Heat) could be used to give more flexibility to the electric grid and give rise to a strict coordination between electric-gas and district heating systems.

- The replacement of synchronous generators with converter-based RES decrease the magnitude of short circuit currents after a fault. This could make protections system and circuit breaker work less efficiently and worsen the voltage levels and stability of the grid. Moreover often converter based RES are free to disconnect in the case of contingency and low voltages worsening the situation (in the last years new stricter rules demanded to RES the Low Voltage Ride Through capability).

- Converters give rise to harmonics in the voltage field and to possible stability problems due to the interaction of a great numbers of units in distribution networks. Better filtering, procedure and new devices are needed to avoid distribution networks problems.

- the decrease in numbers of SGs attached to the grid means loosing points of control for voltage and frequency as this machines are used to provide frequency reserves,sustain grid voltages and provide black-start capabilities, provide inertia and high short circuit currents. Moreover synchronous generators possess naturally good physical synchronization, damping and load sharing mechanisms. If proper controlled and with enough back-up storage, every converter based resources could behave similarly to SGs and behave like a grid forming unit [166, 94, 185].

- In distribution networks massive number of distributed resources will be installed especially in the forms of PV small plants and new kind of loads. Due to the more resistive nature of medium and low voltage lines (especially in for underground cables), active power swings of renewable sources can cause severe voltage oscillations and instabilities. Moreover there is a risk of creation of unintentional electrical islands [94] during faults due to the high presence of embedded distributed generation. other possible problems are [19] the occurrence of Reverse power flow when distribution network act as a net generator of energy into the transmission system and over-currents along the grid branches which can affect a certain portion of the network depending on the relative load and RES position

Clearly no single and easy solution is available in order to integrate up to 100 % renewable sources in our grid. Several changes in technical, commercial and policy operations and regulations must be introduced to lower the techno-economical cost of introducing always more RES in the grid. Good summary and further insights can be obtained in [137, 94].

Chapter 2

Frequency Dynamics and Control Modelling

In this chapter we will focus our attention on the frequency control of the electric grid. First in Section 2.1 we will explain the basics of frequency control and present the main equations and parameters influencing its dynamics. Three different aspects of the problem are treated: first it is presented the equation describing the dynamics of the grid frequency; then a qualitative analysis of the generators oscillation around COI frequency and finally the analytical expression of the frequency profile after a contingency is presented. In Section 2.2 current hierarchical control structure typically used in power systems is described and the importance of a stable frequency signal is highlighted. Finally in Section 2.3 new resources that can be used for frequency control are introduced. These resources are based on the use of converter interfaces and they are capable of numerous and flexible control strategies

2.1 frequency control modelling basics

2.1.1 Frequency control basics

(a) Center of Inertia frequency computation

Both rotor angle and frequency instability can be explained starting from the swing equation. The swing equation describes the SG rotor dynamics which give rise to the electro-mechanical oscillation in power grids. At electrical rotor level we can write [9] (see Figure 2.1):

$$J\frac{d^2\theta_m(t)}{dt^2} = T_m - T_e \tag{2.1}$$

where J is the mechanical rotating inertia of the machine ($Kg.m^2$). J value depends on rotor physical structure and materials; θ_m is the mechanical angle of the rotor (rad); T_m is the mechanical torque given by the turbine to the machine and finally T_e is the electrical torque exchange with electric grid. If we multiply and linearize the equation by the nominal angular velocity ω_{mo} and then we make use of this two equalities $\omega_m = \omega_e/(p/2)$ and $H = 0.5J\omega_{mo}^2/S$ we can write:

$$\frac{2H}{\omega_o}\frac{d^2\theta_e(t)}{dt^2} = P_m - P_e \tag{2.2}$$

where p is the number of poles of the electrical machine, S is the MVA rating of the machine and ω_{mo} is the nominal steady state velocity of the generator; H is expressed in second and it is called the *inertia constant* and represents half the time for a generator or motor to reach steady state speed at full nominal power.

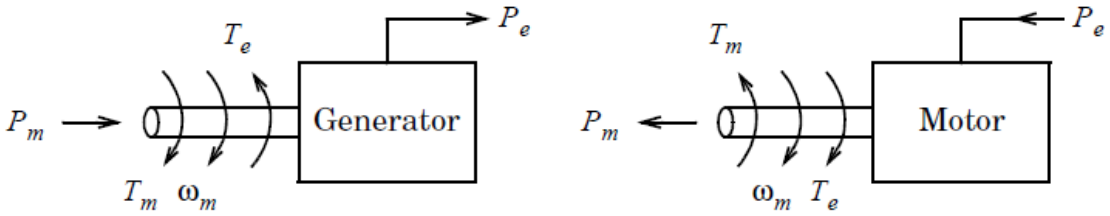

Figure 2.1: Rotor dynamic phenomena

The evolution in time of P_m and P_e of the single generator gives us an idea of the machine rotor angle stability. Under the hypothesis of well damped oscillations and good rotor angle stability, which is often true even in the case of a contingency [136], we can assume all the rotors in the grid to turn allmost at the same frequency. This frequency is called ω_{COI} where COI stands for Center of Inertia and it is computed as the weighted mean of all generators velocities. Since oscillations are very small, we can assume all rotors to turn at ω_{COI}. With this knowledge and normalizing equation 2.2 over a unique power system rating, we can write:

$$\frac{2}{\omega_o}\frac{d^2\omega_{\text{COI}}}{dt^2} = \frac{\sum_{g=1}^{N_g}(P_m)_g - \sum_{l=1}^{N_l}(P_e)_l}{\sum_{g=1}^{N_g} H_g + \sum_{l=1}^{N_l} H_l} \qquad [pu] \tag{2.3}$$

where N_g is the number of synchronous generators and N_l is the number of electric motors. Whenever there is an unbalance between the electric power requested by the loads and the mechanical power generated by the SGs, after a very brief time where a small amount of energy can be released or stored by the electric grid lines [115], the frequency of the grid will change following equation 2.3 with small negligible oscillations over this value for the single generators.

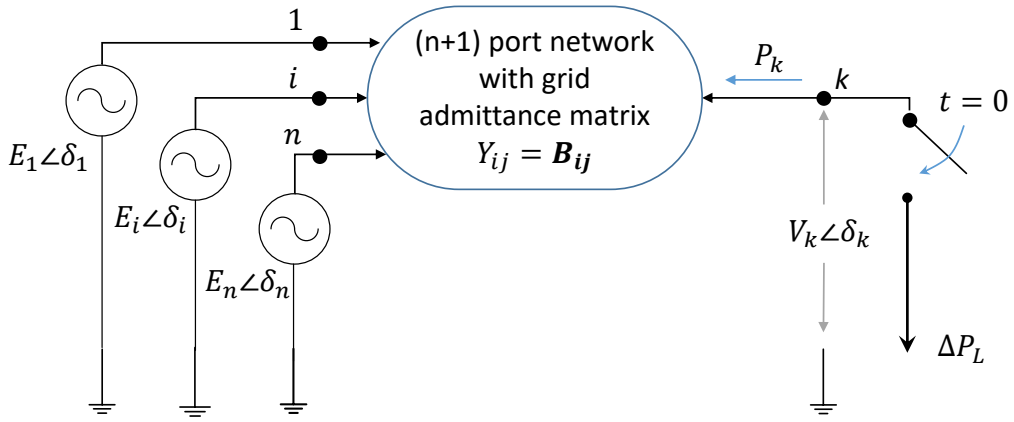

Figure 2.2: Network with ΔP_L applied at $t = 0$

(b) Generators rotors oscillations around COI frequency

The dynamics of the frequencies of the system generators can be qualitatively explained using the representation of synchronous generators as constant voltage sources plus a reactance and the electric grid connections as an admittance matrix connecting node i with node j with negligible resistance value (more details can be found in [7]). In such a system, let's consider the presence of a generic load k which at time $t = 0$ starts consuming a power ΔP_{load} .The active power in node i and node k can be computed as:

$$P_i = \sum_{\substack{j=1 \\ j\neq i,k}}^{n} E_i E_j B_{\text{ij}} \sin\delta_{\text{ij}} + E_i V_k B_{\text{ij}} \sin\delta_{\text{ik}} \tag{2.4}$$

$$P_k = \sum_{\substack{j=1 \\ j\neq i,k}}^{n} V_k E_j B_{\text{ij}} \sin\delta_{\text{kj}} \tag{2.5}$$

where E and V represent the voltages of the nodes,B_{ij} is the admittance matrix element value and $\delta_{\text{xy}} = \delta_x - \delta_y$ for whatever subscript in use. These expressions can be linearized for small ΔP_{load} values and the synchronizing torques of single generators can be introduced, obtaining:

$$P_{\mathrm{i}\Delta} = \sum_{\substack{j=1 \\ j\neq i,k}}^{n} E_i E_j B_{\mathrm{ij}} \cos\delta_{\mathrm{ij,o}}\delta_{\mathrm{ij},\Delta} + E_i V_k B_{\mathrm{ij}} \cos\delta_{\mathrm{ik,o}}\delta_{\mathrm{ik},\Delta} = \sum_{\substack{j=1 \\ j\neq i,k}}^{n} P_{\mathrm{s,ij}}\delta_{\mathrm{ij},\Delta} + P_{\mathrm{s,ik}}\delta_{\mathrm{ik},\Delta} \tag{2.6}$$

$$P_{k,\Delta} = \sum_{j=1}^{n} V_k E_j B_{\mathrm{ij}} \cos\delta_{\mathrm{kj,o}}\delta_{\mathrm{kj},\Delta} = \sum_{j=1}^{n} P_{\mathrm{s,kj}}\delta_{\mathrm{kj},\Delta} \tag{2.7}$$

where the subscript Δ represent the delta variation of the quantity due to the linearizzation process. A sudden ΔP_{load} in the grid can be modelled in node k by keeping fixed the magnitude of the voltage V_k and instead by changing its phase from $\delta_{\mathrm{k,o}}$to $\delta_{\mathrm{k,o}}+\delta_{\mathrm{k},\Delta}$, while SG cannot instantaneously change the phase due to the generator inertia. If we fix ourselves at time $t = 0^+$, we can rewrite Equations 2.6 and 2.7 knowing that $\delta_{\mathrm{ij},\Delta} = 0$, $\delta_{\mathrm{ik},\Delta} = \delta_{i,\Delta} - \delta_{\mathrm{k},\Delta} = -\delta_{\mathrm{k},\Delta}$, and we obtain:

$$P_{\mathrm{i},\Delta} = -P_{\mathrm{s,ik}}\delta_{\mathrm{k},\Delta}(0^+) \quad P_{k,\Delta} = \sum_{\substack{j=1 \\ j\neq i,k}}^{n} P_{\mathrm{s,kj}}\delta_{\mathrm{k},\Delta}(0^+) \tag{2.8}$$

moreover from Equ. 2.8 it can be noticed that $P_{k,\Delta} = -\sum_{\substack{j=1 \\ j\neq i,k}}^{n} P_{\mathrm{i}\Delta}(0^+)$ and moreover knowing (from fig.) that $P_{k,\Delta} = -\Delta P_{\mathrm{load}}$ we can finally write from Equ. 2.8:

$$\delta_{\mathrm{k},\Delta}(0^+) = -\Delta P_{\mathrm{load}} / (\textstyle\sum_{j=1}^{n} P_{\mathrm{s,kj}}) \tag{2.9}$$

$$P_{\mathrm{i},\Delta}(0^+) = (P_{\mathrm{s,ik}} / \textstyle\sum_{j=1}^{n} P_{\mathrm{s,kj}}) \cdot \Delta P_{\mathrm{load}} \tag{2.10}$$

Equ. 2.10 tells that in the first instants the delta energy to be served to the load is supplied by the energy stored in the magnetic fields of the synchronous generators and not by their inertia as the the generator rotor angles cannot move instantaneously due to their inertia. The needed energy is divided between SGs according on the amount of the synchronizing torque of each generator: generators which are electrically more connected to the source of ΔP_{load} will initially cover more of the load power regardless of their size. Immediately the single SGs rotors will start to decelerate/accelerate in case of a positive/negative ΔP_{load}. The incremental Swing equation governing the frequency dynamics can be written (from equation 2.2) as:

$$\frac{2H_i}{\omega_o}\frac{d\omega_{i,\Delta}}{dt} + P_D(\omega_{\mathrm{ij},\Delta}) + P_{\mathrm{i},\Delta}(t_1) = 0 \tag{2.11}$$

where $P_D(\omega_{\mathrm{ij},\Delta})$ is the damping torque of the synchronous machine and generally depends on the differences between rotors velocity in a multimachine system

[96, 159]. in the first instants after a ΔP_{load}, generators will start to oscillate lead by their inertias, damping and synchronizing torques. These oscillations will usually dampen after a certain time t_1 which will be usually lower to the time needed by prime governors of turbines (representing generators primary frequency control) to intervene. Load sharing between SGs at the end of these oscillations can be easily computed by using Equ. 2.11. Summing over all the generator i, remembering that at time t_i damping torque is zero as there is no velocity differences between generators and that velocities derivative are equal to each other we can write:

$$\frac{d\omega_{i,\Delta}}{dt}\sum_{i}^{n}\frac{2H_i}{\omega_o}+\sum_{i}^{n}P_D(\omega_{\text{ij},\Delta})+\sum_{i}^{n}P_{\text{i},\Delta}(t)=\frac{2H_{\text{TOT}}}{\omega_o}\frac{d\omega_{COI,\Delta}}{dt}+0-\Delta P_{\text{load}}(0^+)=0 \tag{2.12}$$

Finally we substitute the value of the velocity derivative of Equ. 2.12 into Equ. 2.11 at time t_1 and we obtain:

$$P_{\text{i},\Delta}(t_1)=({}^{H_i}/_{\sum_i^n H_i})\Delta P_{\text{load}}(0^+) \tag{2.13}$$

This means that after a brief transient the various machines will swing at the same velocity, sharing the additional load according to only their inertia constants.

(c) analytical expression of frequency after a contingency

After time t_1 the governor response from generators starts to be relevant and makes frequency stabilize. To analytically study this equilibrium, it is possible to study a single machine equivalent system (first presented in [8]) which is based on Equ. 2.3 where the dynamics of the governor system of the power plant can be simply modelled as a zero-pole transfer function and load posses a certain damping coefficient D $[MW/Hz]$. This coefficient represent the tendency of loads to increase or decrease their power consumption in the opposite direction off the frequency error. In order to be analytically solvable, dead-band and saturations are neglected (the system is depicted in figure 2.3). Now it is possible to give the analytical formula for the frequency profile considering a step input of magnitude ΔP:

$$\Delta f(t)=\frac{R\Delta P}{DR+1}\cdot(1+\alpha\exp^{-\zeta\omega_n t}\sin(\omega_r+\phi)) \tag{2.14}$$

with:

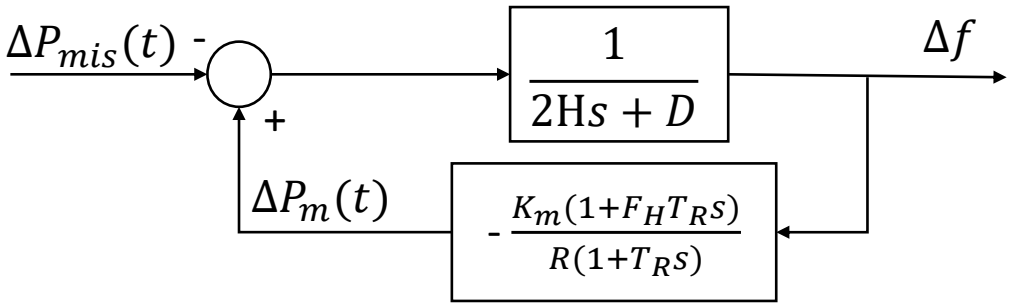

Figure 2.3: Low order single System frequency response model example

$$\omega_n^2 = \frac{DR + K_m}{2HRT_R} \qquad \zeta = \left(\frac{2HR + (DR + K_m F_H)T_R}{2(DR + K_m)}\right) \cdot \omega_n$$
$$\alpha = \sqrt{\frac{1 - 2T_R\zeta\omega_n + T_R^2\omega_n^2}{1 - \zeta^2}} \qquad \omega_r = \omega_n\sqrt{1 - \zeta^2}$$
$$\phi = \phi_1 - \phi_2 = \tan^{-1}\left(\frac{\omega_r T_R}{1 - \zeta\omega_R T_R}\right) \tag{2.15}$$

with Equations 2.14 and 2.15 it is possible to compute all quantities of interest. Interesting quantities for grid and machines stability are the frequency derivate, especially at the initial time when it is the highest value, Δf_{nadir} , which is the value of the frequency when the frequency derivative is zero and has the lowest/higher value (in the case of an under/over-frequency event) and its corresponding time t_{nadir} . Additionally it is also important to monitor the frequency and the time value at which the transient finishes (Δf_{reg} and t_{reg}). In equations we can write:

$$\frac{d\Delta f(t)}{dt} = \frac{R\Delta P}{DR + 1} \cdot \alpha\omega_n e^{-\zeta\omega_n t}\sin(\omega_r t + \phi_1) \tag{2.16}$$
$$t_{\text{nadir}} = \frac{1}{\omega_r}\tan^{-1}\left(\frac{\omega_r T_R}{\zeta\omega_n T_R - 1}\right) \tag{2.17}$$
$$\Delta f_{\text{nadir}} = \frac{R\Delta P}{DR + 1} \cdot \left(1 + \sqrt{1 - \zeta^2}\alpha\exp^{-\zeta\omega_n t_{\text{nadir}}}\right) \tag{2.18}$$
$$f_{\text{reg}} = \frac{R\Delta P}{DR + K_m} \tag{2.19}$$

and finally initial RoCoF at $t = 0$ is simply computed as $^{\Delta P}/_{2H}$ and depends on grid inertia alone.

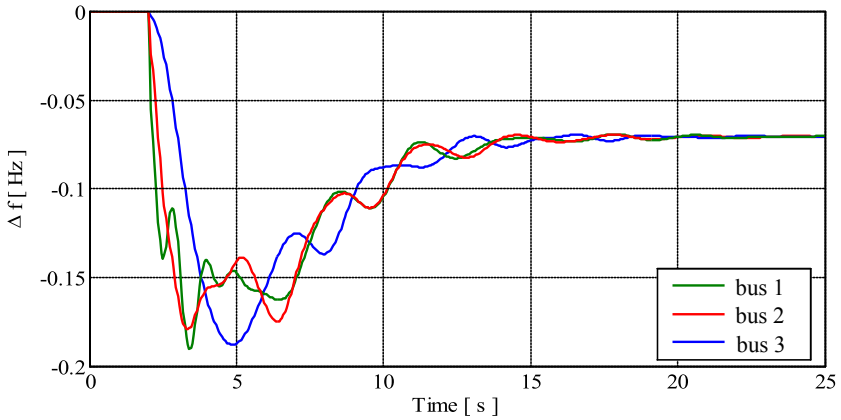

Figure 2.4: Simulation results. The figure was slightly modified from Fig. 14(a) of reference [160]

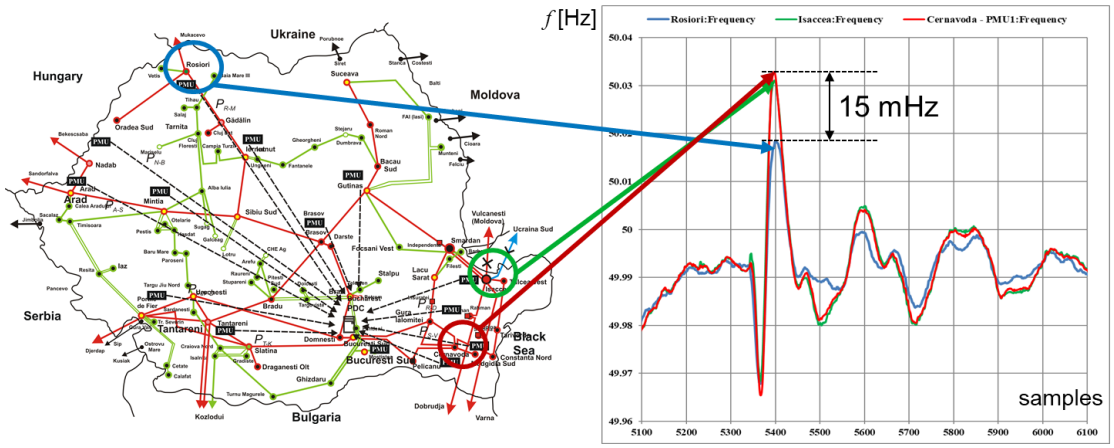

Figure 2.5: PMU measurements in Romanian power system after the disconnection of the Greece-Turkey interconnection line on 23 October 2017

To conclude I present 3 figures in order to explain and confirm previous concepts. In the first image (Fig. 2.4) different machine frequency profiles are shown resulting from a simulated contingency modelled in [160]. While the synchronous generators maintain synchronism even after a big contingency they can potentially continue to oscillate for a long time after the contingency event, well after primary frequency control intervention [1].

[1] In this situation a time t_1 (see Equ. 2.13) cannot be explicitly computed or visualized and generators continue to oscillate well after primary frequency control intervene to balance the frequency decrease. Nevertheless oscillations continue to decrease and Equ. 2.13 actually holds in

In the second image (Fig. 2.5), real Phasor Measurements Units of the Romanian power system are presented. These devices have different specifics and capabilities based on well known standards [78] which assures the quality of the measurements. The data are recorded after the disconnection of the Greece-Turkey interconnection line on 23 October 2017, which has resulted in well damped frequency oscillations in the whole European synchronized area.

Finally in the third image, the frequency signal recorded in Romania and Germany is shown during normal operation of the grid. It is clear how normal small deviations which causes second by seconds frequency dynamics are actually so small the no real difference in velocity between generators can be appreciated even in very far buses.

2.1.2 Fixed Frequency importance and low inertia/reserves challenges

The goal for Transmission System Operators (TSOs) is to keep the frequency as constant as possible. Frequency is of paramount importance as rotating machines (generator and loads) will work best at nominal velocity. Moreover some electronic loads are very sensible to frequency variations. A non constant and fleeting frequency is also dangerous for the mechanical stress and wear that can cause on the rotors of the generators regulating frequency [189]). Moreover if a contingency happens in the grid at a time frequency is already unbalanced, less reserves will intervene to counteract the power deviation.

If initial RoCoF is too high, severe problems can arise [125]. First of all the single synchronous generators could face a series of problem experiencing RoCof values higher than 1 $[Hz/s]$ [179]:

- Pole slip; this is directly connected to the rotor instability and the dynamics of the attractive forces between stator and rotor fields of the machine. This dangerous situation is reflected on the pole angle position between the stator and the rotor field. The machine will lose its synchronism if the angle becomes greater than 90 degrees. The pole angle dynamics will depends on type of contingency, RoCof levels, Inertia values, the power factor or/and the load of the machine.

- Momentary reverse power flows; important oscillations of the pole angle can temporarily produced negative output so that the generator will behave like

a "averaged" way. Infact, generators behaviour depend just as first approximation on Equ. 2.11 but actually an important role is also played by voltage profiles,controls and all other grid interactions

a Motor. The generator is generally protected against Motor operation by the reverse power protection. If triggered it will shutdown the unit. The triggering will depends on the amount of reverse power flow (usually this should be less than 5 % of the nominal power) and it will trigger after a certain period.

- Torque swings; the torque to be sustained after the contingency can be up to 160 % the nominal value. These values can have an effect on the wear and stress of the machines,but are actually well below the requirements of the current Fault Ride-Through. During voltage dips in fact, generators will have to sustain torques up to 300-500 % nominal value.

The tripping and/or the instability of a synchronous generators can possibly lead to the cascading tripping of the generators in the grid, causing load shedding, system islanding or system blackouts [47]. Another risk for SGs is to produce inter-area oscillations starting to swing and share load against each other decreasing the stability and the power quality of the system [134]. There are also other possible hazards for generators operations during high RoCof events due to particular plant layout and auxiliaries equipment reaction [50] such as torsional torque on rotor shaft train, flame and combustion control, hydraulic transients in hydro power plants, impacts on auxiliaries components (gas compressors, boilers feed pumps) etc....

It is also worth to remember that in distributions networks, RESs are equipped with loss-of-mains protection. These protection systems are important to prevent embedded generation supplying an electrical island when a loss of mains event has occurred. These protections are usually, but not exclusively, RoCof activated [48], in such a way that a loss of generation can be triggered without any real islanding event happening if measured RoCof is higher of a certain threshold.

ENTSO-E monitors the European situation trying to find minimum and suggested values for inertia in the grid to avoid load shedding or other emergency situations [66]. In particular, in cited study ENTSO-E suggests that every region after a split of the Synchronous Area should retain at least a time constant of the network of 12 seconds (nowadays European constant is about 15 seconds in continuous decrease). The time constant of the network is computed as $2 \cdot H$. To cope with this situation the local TSO will be forced to enlarge the capacity reserve for the grid (Primary, Secondary and spinning Reserve) increasing the costs of managing the grid (paid by the local community).

2.2 Current Frequency Control Structure

2.2.1 classical frequency control loops

In the world exists many definitions, technical solutions and market structures to control frequency but they are all based on three hierarchical levels of control. Definitions, services, rules and operations in Europe are being harmonized by ENTSO-E through the implementations of Network codes: until 2016, Load-Frequency Control and Reserves code [55] presented all the information about frequency control in European area. In 2016 it was merged with The System Operation Code and it is today entered into force in all single european countries [56]. Frequency controls characteristics and their functions can be summarized and visualized in Figs. 2.6. We distinguish:

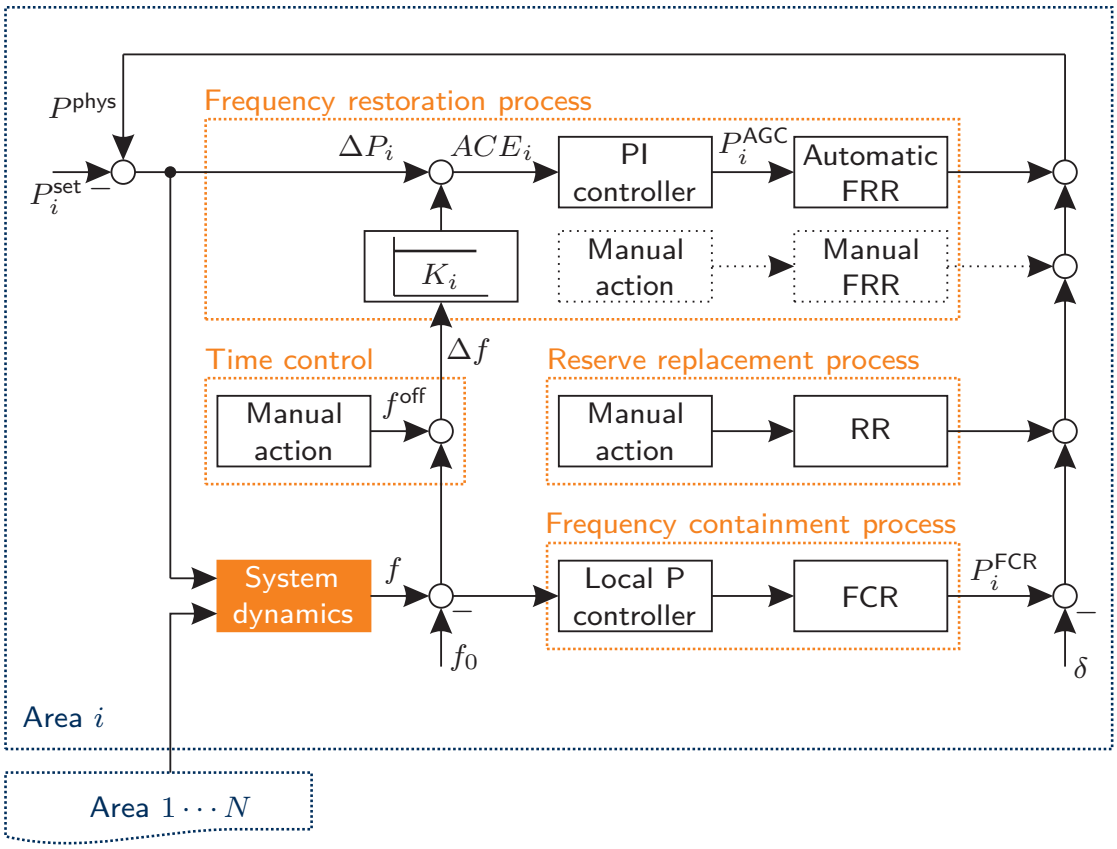

Figure 2.6: Four-level hierarchy of frequency control from a TSO perspective. Image taken from [155]

Frequency Containment Reserve (FCR) also called primary frequency control is the fastest control responding to a frequency deviation following a

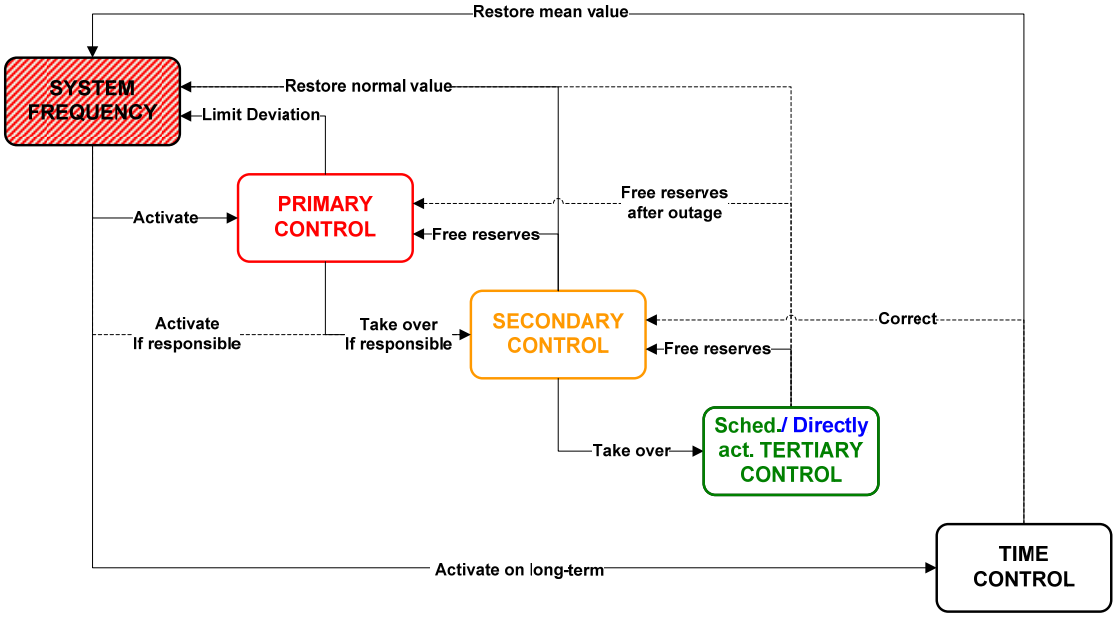

Figure 2.7: Frequency controls services relationships and functionalities [178]. The names of these services refers to the names used in the Continental Europe (see appendix B of [57] to map these names to the services of Fig. 2.6)

proportional rule between frequency deviation and power injection in the grid. The aim is not to restore frequency but to balance Power mismatch as soon as possible. Historically and until now this service is basically provided by all traditional synchronous generators from a minimum size (in Italy according to Italian grid code, all generators with Power rating more than 10 MW should obligatory take part in Primary Frequency Control [168]). Generators will measure the frequency signal and change consequently and immediately their Power reference set-point according to their Droop defined as:

$$s_g = -\frac{(f_t - f_{nom})/f_{nom}}{P_t - P_{nom}/P_{nom}} \qquad [\%] \tag{2.20}$$

where:

- f_t is the frequency signal as measured by generator measurement system;
- f_{nom} is the nominal frequency of the grid: 50 Hertz in Europe;

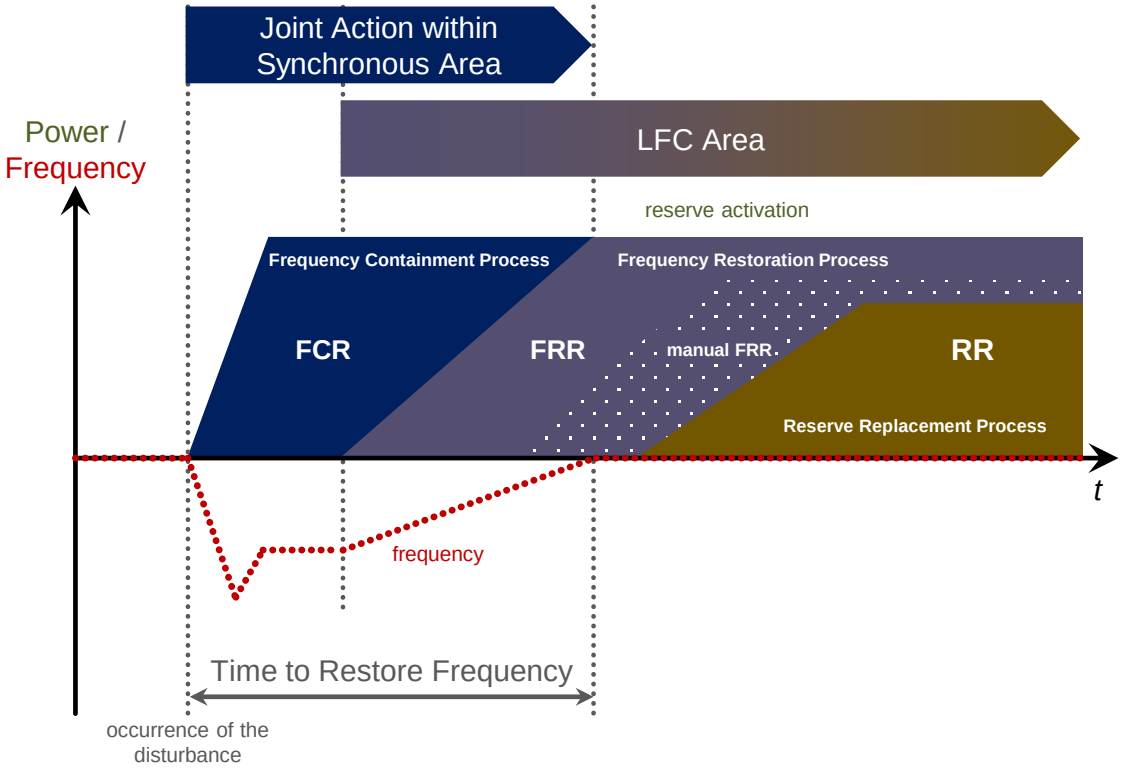

Figure 2.8: Dynamic hierarchy of Load-Frequency Control processes (under assumption that FCR is fully replaced by FRR). Image taken from [57]

- P_t is the new instantaneous Power-set-point due to Primary control in MW;
- P_{nom} is the Power set point due to normal market scheduling of the generator.

From Equ. 2.20, P_t point depends on frequency deviation and droop of a generator. Normal values of droop are from 2% (very stiff curve) to 7 % . Usually a Dead-band is applied to not overstress generator governor mechanisms and also to avoid set-point mistakes due to the limitation and error of the measurement system. Every TSO sets the rules. The main goal is that every area is able to guarantee a proper value of Regulating Energy defined as $\lambda_u = {}^{\Delta P_a}/_{\Delta f}[MW/Hz]$, where ΔP_a is the power disturbance and Δf is quasi steady-state frequency deviation after the disturbance. Every area should assure and contribute to this value with a coefficient C_i calculated on a regular basis (principle of Joint Action) based on country electricity generation. To find out the proposed value of λ_u a reference incident for the UE grid is simulated. Such an incident consists in the tripping of the two biggest

nuclear power plant with a power loss for the grid of 3000 MW. Simulation are performed under basic assumption for time constant and load conditions: Regulating energy of UE will be such that the frequency deviation does not fall lower than 800 mHz avoiding automatic load shedding operations. Finally, every TSO should check that Primary Reserve is deployed within a certain time (for example: full activation of reserve in Italy by generators is expected in no more than 30 seconds).

Frequency Restoration process or Secondary Control. After a disturbance has been balanced by PFC, frequency is not restored, but only stabilized. At this point other generators following another power signal restore nominal frequency. This two-step process (primary + secondary) is made to avoid instability and power sharing conflict between generators governors during a hypothetical one step frequency restoration process. The goal is double:

- Restore nominal frequency of 50 Hz;
- Restore Power exchange among Areas to their previous values.

For these reasons secondary control power set-point is of proportional-integral nature (PI) computed in such a way that it only activates in the area where the disturbance (ex. trip of a generator or big power deviation) has taken place. The secondary controller sends, in real time for each time step, a unique level signal to every generator in the area of the form:

$$L = 50 - \frac{100}{P_D}\beta_1 G_i - \frac{1}{T_r}\int G_i\, dt \qquad [\%] \tag{2.21}$$

where P_D is the total Secondary Band Reserve in the grid, β_1 is the proportional constant and T_r is the integral constant in seconds and usually quite big (from 100 seconds to 200) to avoid a too fast response and overshooting problems. G_i is the **ACE or Area Control Error** which takes into account the frequency deviation and the power tie-line exchange deviation. It is usually calculated as:

$$G_i = P_{meas} - P_{prog} + K_{ri}\Delta f \qquad [MW] \tag{2.22}$$

where $P_{meas} - P_{prog}$ is the difference between programmed power exchange between areas and actual power exchange due to activation of Primary Reserves; K_{ri} is the regulating energy of the whole synchronous area. The ACE, computed is such a way, is 0 for all areas except for the one in which the disturbance appeared. Level signal L goes from 0 to 100 % with 50 as base case, where Secondary band of the generator is half utilized.

Secondary reserves can be computed in different ways depending on characteristics of the Load and market rules (see section 2.2.2). Time activation depends on the nature of the generator used (gas,water and coal based generators have different ramp mechanisms and velocities). Different quality parameters are used to check the consistency and the intervention of secondary reserve. TSOs can also activate manually some reserves in case of need in the grid.

Reserve Replacement or Tertiary Control. Tertiary reserves are manually dispatched in order to restore secondary reserves. Least cost dispatching plants are used to fulfil the service.

RoCof control This new service is still yet to be used. Its principle lays in the fact the activation and Power modulation will depend on the value of frequency derivate and not on the frequency value itself. This is done in order to replicate the containing effects of the real rotating inertia. Due to the very fast expected response (ideally less than 10 ms or even less) only machines connected to the Grid through fast Power Electronics could participate to the Service.

Time control. It is an index used to measure and control the long term frequency deviation. It is computed as the difference between the nominal time computed by using the nominal frequency value and the electrical time computed as the integration of the actual frequency of the grid. Many devices are dependent on electrical time:

- meters of electrical energy which calculate different tariff periods in a precise time measurement
- power plants control energy
- power quality devices
- old industry's processes
- customers in textile industries and
- synchronous motors which drives the value of electrical clock.

in Continental Europe,time control is adopted since many decades. In practice the TSO raise or lower the Setpoint frequency for the other frequency services by a specific percentage so that electrical clock deviations stay within a certain amount of seconds.

2.2.2 Renewable impact on frequency stability

As seen in Subsection 1.1, the major renewable sources present in the grid will be Wind and PV technologies which are linked to the grid through a static converter (DC-AC) or a back-to-back (AC-AC) converter, which hold no rotating part and offer no inertia. The converter is usually operated in grid-tied mode reproducing voltage levels and frequency of the utility lines to which they are attached. Moreover, both technologies are non dispatchable: infact they continuously change their power set point, following the Maximum Power Point given by environmental external conditions (wind gust and cloud movements are the major phenomena affecting power output of the plants). In order to provide reserves to the grid the renewables energy sources. This is done to not waste the primary source and maximize renewable production which changes often during the day and even within short time windows. However for RES this means to run under the optimal production point and lead to a waste of primary energy source. In the case of wind turbines, frequency control is possible by making use of the kinetic energy stored in the turbine blades [45], but the amount of energy that can be released is limited and need to be restored after the transient, endangering the grid stability.

These two characteristics of RESs plants have a double effect on frequency dynamics as shown equation 2.3: numerator will have a produced power much more variable as primary source (wind or radiation) suffers from stochastic variability, denominator will decrease having less inertia from normal installed synchronous generators. Expected frequency oscillation will be higher and faster. Moreover The RES reduce the ability to forecast and increase the variability of the Net Load, forcing the TSOs to increase the reserve requirements against unbalanced periods increasing the cost of managing the grid

2.3 New resources for frequency control

In the future due to RES increase and market integration, European system can be subject to RoCoF of more than 2 Hz/s and in case of area splitting, power unbalance can reach up to of 40% (on Area Load) [53]. Also under normal operation, the degradation of frequency signal can affect power quality given to system loads. Various solutions and improvement of the grid are detailed in [80]:

Interconnection & market integration. Continental Europe is already a synchronous area so that SGs oscillates in the same manner and sudden variations of load and RESs partly compensate each other. However new interconnection lines and better cross-country reserves sharing mechanism can effectively improve the performance of frequency reserves (especially secondary

and tertiary reserves).

Flexible Dispatchable plants. Traditional Generation, except for Hydro turbines, are usually not very efficient in working outside nominal point and have ramp limitation. New CCGT (Combined Cycle Gas Turbine) plants have much more flexibility and moreover the study of components with better dynamic behaviour is constantly under research.

Demand side Managment (DSM) refers to the possibility for the controllable consumers loads to participate to frequency control at various levels. All type of loads can theoretically participate to new energy markets from big industrial loads to small residential consumers making use of local RES, storages, home automation, Information and Communication Technologies (ICT). New controllable loads examples are power-to-gas plants, electric vehicles, RESs (especially in under-production), cooling and refrigeration appliances [20], entire buildings [184], water heating units etc.

These resources are usually aggregated by new entities known as aggregators. Consumers becomes pro-sumer, both producer and consumer and they are capable to dispatch their load profile [26]. Different layouts are incentivized and regulated by DSO [39] and regulating authorities.

Synchronous compensator. They are essential synchronous motors run at no load and used to produce or absorb reactive energy. They also maintain some good intrinsic characteristic of synchronous machines like inertia or short circuit current production.

Storage refers to the the possibility to accumulate electrical current, usually in another kind of energy and then when useful, transform it back to its original form (producing some losses). The possibility of extensively using storage will mean a total revolution in the way grid is managed [91] [42]. In view of a liberalized and efficient market, like the European one, not good enough regulations of these new resource can create regulative and economic bottlenecks that even if here not discussed, are important as the technical problems [165]. For now **the only mature and largely installed technology is pumped hydro**: its installation is limited by the presence of a proper physical site and it is basically used for energy wide uses as peak levelling or energy arbitrage. But on the last years there is a great interest to develop new forms of storages for new technologies. Storage can be classified depending on type of energy transformation (we usually divide into electrical, electro-chemical, mechanical, thermal storage). In order to consider the possible grid application it is also useful to consider the typical Power-Energy

ratings of the various systems or the Ragone plots which give us information on the power-energy density of these systems (see Fig. 2.9). Other specific-technology characteristics like geographical limitation or special maintain ace need are also important in the storage technology decision (see [143]). Finally it is important to remember that these technologies are still in their "infancy" (except for pumped hydro) and great improvement and lower costs are to be expected.

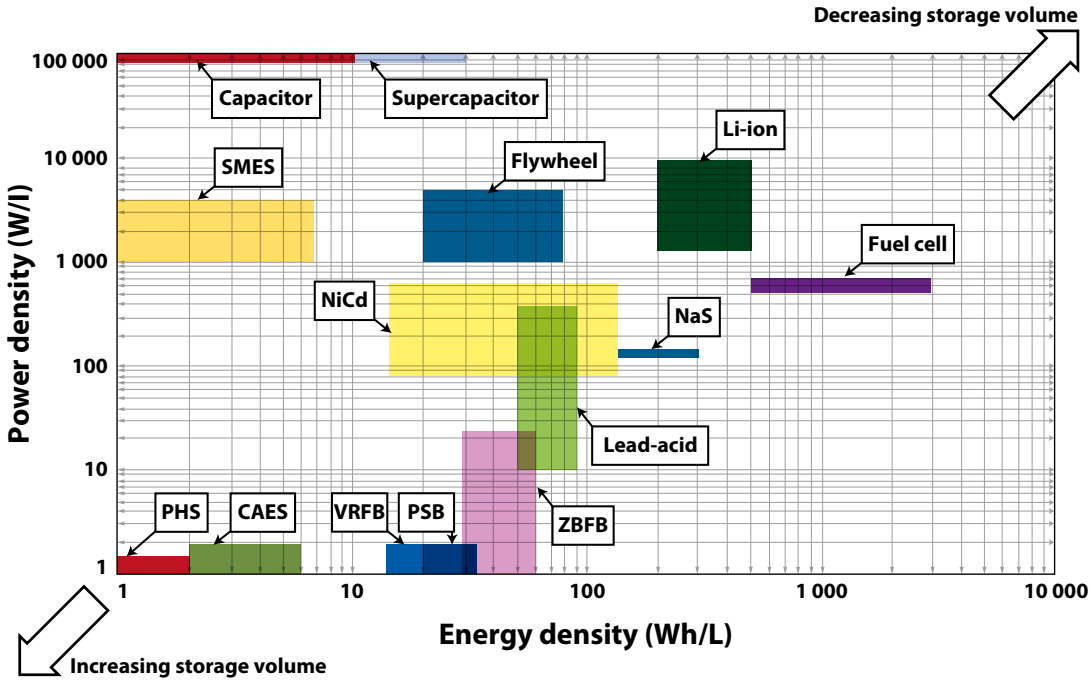

Source: Luo *et al.*, 2015.
Note: SMES = superconducting magnetic energy storage; NiCd = nickel cadmium; NaS = sodium sulphur; PHS = pumped hydro storage; CAES = compressed air energy storage; VRFB = vanadium redox flow battery; PSB= polysulfide bromine flow battery; ZBFB = zinc bromine flow battery.

Figure 2.9: Storage power and energy density characteristics [57]

2.3.1 battery energy storage systems uses

In the last few years the installations of batteries is gaining a certain momentum. As a matter of fact BESSs (especially but not exclusively lithium-ion technology) thanks to their velocity and at the same time good power and energy ratings are already being used in various application [143]. Moreover BESSs are easily scalable and packed in different dimension and they are not-site dependent like CAES (compressed air energy storage) or PHS (Pumped hydro storage). BESSs system are divided between utility grid storages and small home systems

installed in combination with PVs systems in order to increase the self-sufficiency of the owners. Also electric vehicles are equipped with batteries. [165] studies the most profitable services BESSs can provide to the grid. These are usually services connected to short term power regulation like frequency control. BESSs could also serve other services, but only if regulatory framework clarifies and helps the installation, management and remuneration for owner which is still not the case in most of countries. Beyond frequency control and self-consumption in combination with PV, some other real operating applications are [89, 10] :

Flexible ramping. Due to the diffusion of RESs especially PV, great power ramps are requested during the morning and in the afternoon when sun is quickly going down. BESSs thanks to their high power capability can lower the stress on the system and decrease the net load variance.

Island system. Batteries have a major role in system design optimization and real time operations and are essential to have a major RES penetration. Their role affects the energy balance (at wide time steps) and also the instantaneous power balance to keep the grid in equilibrium in case of mismatch. Nowadays, most off-grid system make use of expensive and polluting diesel generators which nevertheless present a lot of flexibility and management security. BESS system can help higher share of energy to be produced by clean and cheap methods. Hybrid system with short and long term storage (high power and high energy systems) can also be a cost effective solution. Moreover island are the first system where SGs can be zeroed and just converter based generation is present so that different techniques for the parallel connection of converters could be tried out in a smaller scale before being deployed eventually in bigger systems.

Transmission and distribution congestion relief . Depending on the grid structure, certain particular lines or stations can result to be saturated for a small number of hours due to RESs productions. The use of local BESSs can help desaturate the congestion without the costly need to upgrade the infrastructure.

Energy supply shift. BESS can be used for the practice of Arbitrage. This corresponds to accumulate energy in time when price is low and to resell it when price is high (peak consumption hours). Usually for large time interval other storing technologies can be used, batteries are used for 15-minutes to 1-hour time intervals, which can help the grid to level its peak consumption and avoid the use of expensive peak gas plant and the costly upgradee of the system infrastructure.

The installation of new type of storages (except pumped hydro which amount to 198 GW world-wide) have reached more than 3 GW of installed power in 2018, of which the most part consist of BESSs especially lithium ion technology with more than 85 % of new installation in 2018 represented by this technology. [2]. More than one third of installations comes from South Korea. Other countries in which there is a big increase are Japan (due to PV battery system and resilience against natural disasters), Germany, United Kingdom, China and USA. In the future more installation are expected with other technologies such as flow batteries to counter the lithium-ion market dominance. Additionally manufacturing capacity for lithium-ion batteries is expected to increase threefold by 2022, driven by the booming of the EV market and there is a serious possibility that technologies cost can further lower. As EV batteries expire for mobility applications, it can still used in the power sector by utilities and private owners. In his 2017 study [143] on future storage uses (with special focus on BESSs) IRENA predicts that main uses for stationary storage will be related to accumulation of electricity produced by home PV systems in order to increase self-consumption (more than half of the use), secondly frequency regulation (up to 15 % of systems) and finally renewable capacity firming (up to 14 %) in order to decrease utility scale RES production variability.

Frequency control regulation is today one of the most lucrative service to be offered by BESSs systems, especially for utility scales systems. With respect to conventional generation, BESSs present inherently advantages[93]: reserve provision from CG in fact reduces the maximum output a power plant can offer to energy market reducing profits and impose that plants run also when RES are high to provide frequency services limiting the exploitation of renewables. Batteries can offer control reserves power without producing energy, effectively decoupling power from energy provision. In addition, BESSs can offer upper and lower regulation with the same nominal capacity, while CG need to reserve the double amount of capacity. BESSs are more suitable for power based services due to theri velocity of presponse and it is not a case that in UK the tender for enhanced frequency response (the fast frequency service provided by BESSs) have being cleared at lower prices with respect to firm frequency response (traditional frequency control performed by slower resources like CG) [3]. Several markets have opened the possibility for BESSs to offer services like primary frequency control (FCR) responding to frequency disturbances with a linearly proportional power delivery and other similar

[2]source: https://www.iea.org/tcep/energyintegration/energystorage/

[3]https://everoze.com/what-7mwhr-for-efr-storage-explain/

In particular, we can count:

- Australian System: the Australian system operator publishes quaterly report on the market cost and grid dynamics [126]. Starting from the Tesla installation of 100 MW BESS (Hornsdale Power Reserve) in 2017, The frequency control ancillary services (FCAS) costs are reducing thanks to the use of BESSs and demand response services which accounted respectively for 17 % and 15 % of the whole supply mix in the first quarter of 2019. The Hornsdale Power Reserve (which is the oldest plant) has already avoided systems blackout and it is able to intervene in about 100 ms.

- UK market: IN UK, a new service called enhanced frequency response has been established [add cit], requiring a droop response form resources which are able to deliver full power in less than one second. In the 2016 auction in the transmission system operator contracted 200 MW of reserve capacity for four years. Even though the tender for this project was technology neutral, battery storage systems won the entire capacity on offer [10]

- In the United States, Federal Electricity Regulator Commission (FERC) Order 755 has mandated a separate compensation structure for fast-acting resources such as batteries, with respect to slower acting conventional resources.

- Central Europe. Many TSOs from Central Europe countries (France,Germany, Belgium, Switzerland, Netherlands nd Austria) gathers FCR in the same competitive market. The tendering period was changed from weekly to daily in 2019 according to [1] and is planned to be reduced further to 4 h in the beginning of 2020. In this market BESSs are strongly present (with more than 100 MW usually assigned) as revenues represent an important incentive even if it is decreasing in the last years.

- Italy has implemented a series of pilot projects [170] through its TSO, Terna, and installed already in 2014 several dozens of BESSs in Sardegna and South Italy to test power intensive and energy intensive use of BESS. Fast services are tried out primary frequency control and RoCof Control. Today experimentation is continuing with the creation of particular kind of Virtual Power Plants for the participation in balancing markets: in particular aggregator of the size of at least 1 MW of RESs, consumption units and storages will able to offer balancing and tertiary frequency control to the grid (these aggregators are called UVAM or Unità Virtuali Aggregate Miste [171]. Moreover The Italian TSO Terna [169] has recently started a new ancillary service for storage systems based on the provision of fast droop control. The resources to be gathered should reach at least 200 MW of resources.

As for now, the US, China, Japan, and the Republic of Korea host most of the stationary electrochemical storage [143]. However last European Union energy directives are moving towards an effective integration and regulation of storage systems Firstly, in 2017 System operation guidelines (SOGL) [38] accounted for the presence of energy storages providing FCR (Frequency Containment Reserves) and in Article 156 point 11, ordered Continental Europe and Nordic Europe synchrnous areas's TSOs to propose a cost benefit analysis in order to evaluate the best time period for which LER must remain available while providing full activation of the FCR. Moreover in 2019, Electricity Directive [138] states that energy storage facilities management should be "market-based and competitive" and explicitly integrated in new market designs. System operators could own and operate storages to provide network security and reliability, but they cannot be used for balancing or congestion management.

Chapter 3

Literature review on frequency coontrol

Section 3.1 present the methodology followed to organize the literature review. This review critically discuss what is present in literature, categorizing the works in a original way taking into consideration the scope of the analysis (open loop, closed loop and normal operations) and main relevant areas of research. Papers are critically compared in terms of models, methodologies and results obtained and are grouped when possible by similarity of topic and approach. From this work, it was possible for me to grasp the current trends of the existing literature and the topics of the case studies built in the next chapters. Results and author opinion on the analyzed works are gathered at the Conclusion chapter of this thesis

3.1 methodology

As real implementations continues to increase, the scientific studies concerning BESSs fast frequency control services and performances is increasing.

For this chapter I mainly (but not excusively) restricted my review to papers referring to the use of BESSs or EVs for fast frequency control services. While it is possible for these storages to participate to all frequency services, we will concentrate on PFC and Rocof control as BESSs are particularly suited and this service is especially remunerative.

I have identified three main typologies of studies in the literature depending on how the electric grid is modelled and what impact or aspect of the BESSs system is analyzed:

Open loop studies . In these studies BESSs contribution to the frequency stability is not considered. The grid is therefore is not topologically modelled,

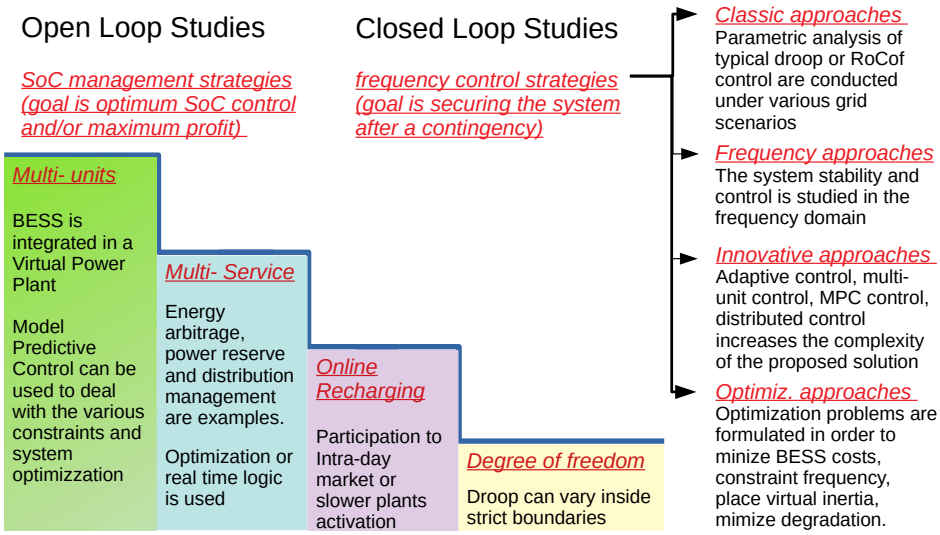

Figure 3.1: families of strategies and approaches used in the analized works

but it is present in the form of input data to the BESS controller and management system (for example, frequency error dynamics, price signal, dispatching orders etc...). These studies usually focus on the the BESS techno-economic operations, multi services provision, degradation of the cell etc. Usually several days of normal operations frequency profiles are used.

Closed loop studies for Contingency Analysis . In this case a contingency in the grid is usually modelled and simulated. The BESS or the other resources are used to fast intervene and assure frequency stability in the grid. The goal of the study can be to quantify how much BESSs are needed to stabilize the grid, what is the impact of PFC or RoCof control for the frequency stability and what is the stress sustained by BESSs.

Open loop studies for Normal Operations In these last group, we gather all the studies which are concerned with the impact of BESSs on grid frequency signal during normal operations. The main difficulty of these studies is to reconstruct a realistic frequency signal . The potentiality of this typology of study is to at the same time quantify the BESSs impact on the grid signal and on the BESS itself.

Some scheme summarizing the three categories are presented in 3.1 and xxx.

Secondly, while less important and more difficult to divide, it is possible to separate the works considering the level of details of the models considered. For what concern the electric grid system we can use simplified frequency response

dynamic models or complete dynamic models. For BESSs we have several families of dynamic models usually adopted in power system studies [40] :

Electrochemical Models they take into in account all the electro-chemical dynamic phenomena happening inside the cells (oxidation-reduction processes of anode-cathode elements of the cells). These models are white heavy and makes use of complete coupled partial differential equations [86] to be solved for time and spatial dimensions and describe both macroscopic (voltages and currents) and microscopic quantities like local distribution of charge, materials concentration, current, temperature etc.

Electrical It makes use of Equivalent circuit components to model the various BESS and cell parts. Usually voltage sources and passive elements are implemented through the use of look-up tables based obtained through repetitive testing of the batteries cells [14]. Models are usually quite accurate (1-5 % range of error) but are valid only for tested condition and extrapolation is often not advisable. The electric model can be also extended to take into account SOC runtime computation, degradation and temperature dynamics.Technique such as impedance spectroscopy tests could also be used. [153]

Mathematical Models they are usually the most computational light ones based on analytical or stochastic approaches. They completely neglect a physical description of the cell, but they provide BESS parameters like State of Charge (SOC) levels and power production based on simplified or numerical models. Usually current and voltages informations are neglected.

it is not only important but also fundamental to consider the presence of converters interfacing the unit to the grid. The converter unit is responsible of converting the DC current produced by the storage device to AC current. The converter does not interact naturally with the grid but it operations depend exclusively on its control algorithm [116]. Its velocity is actually what assures the provision of fast services (fastest times are in the order of few milliseconds), but on the other hand the storage devices behind it should be able avoid voltage instability problems on the DC capacitance connecting the storage device and the converter. If the storage source behind the DC-link is not sufficiently fast and if strange interaction with fast grid lines dynamics are created, the Converter unit is slowed down [166]

the use of electrochemical models is usually limited to detailed studies of BESSs technologies with little applications to power systems, while electrical and mathematical models have wide applications.

3.2 Papers groups

3.2.1 Open Loop papers

These studies could be categorized starting from three main features of interest:

- the strategy used to provide frequency control to the grid and at the same time to manage the SOC of the BESS to assure continuity of the service.
- Secondly the model of the BESS used and the possible quantification of BESS degradation due to service provision.
- Finally a third interesting aspect is to look at what kind of input data are used and outputs are computed from the models: often specific rules and real data are used in order to produce realistic (even if case-specific) results. Economic index are often used to quantify investment viability in BESSs systems. the main economic output are classical indexes such Return on investement (ROI), Net Present Value (NPV) and related BESS degradation when quantified. This part will not be investigated in this chapter.

SoC managment. To perform SoC management, the answer of a BESS providing PFC can be divided in two components:

$$P_{\text{BESS}} = P_{\text{PFC}} + P_{\text{SOC}} \tag{3.1}$$

where P_{PFC} follows the usual linear droop frequency control with a certain droop $\frac{\sigma=\Delta f/f_n}{\Delta P/P_n}$ usually going from 2 to 5% (reference needed). This part should be always assured in order to better cope with contingency or faults during grid operations. Even if frequency control can be considered a zero-mean energy service (due to the symmetry of the frequency signal), due to the internal BESS losses or long over or under-frequency periods in the grid, BESS energy content can be depleted or reach 100 % un-enabling the possibility to perform PFC. For this reason P_{SOC} is constructed in order to stabilize the SOC. Note that in these works, as the grid is not explicitly modelled, is not possible to quantify the impact of this component (and also of the classical droop control) on the grid, which is clearly a limitation. The various techniques can be group in several families:

First approaches. Scheduled recharging or dead-band recharging are first simple approaches used in early experimentation or researches. in [97] a pilot project is presented for a battery providing frequency control for the islanded system of West-Berlin. The BESS is recharged during low load hours and clearly in those times cannot provide PFC endangering the grid. The presence

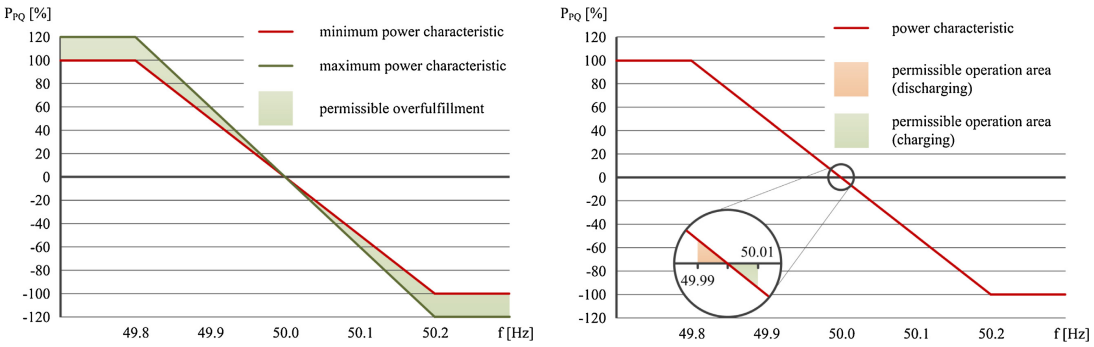

Figure 3.2: Degree of freedom in PFC in Central Europe for BESS [64]

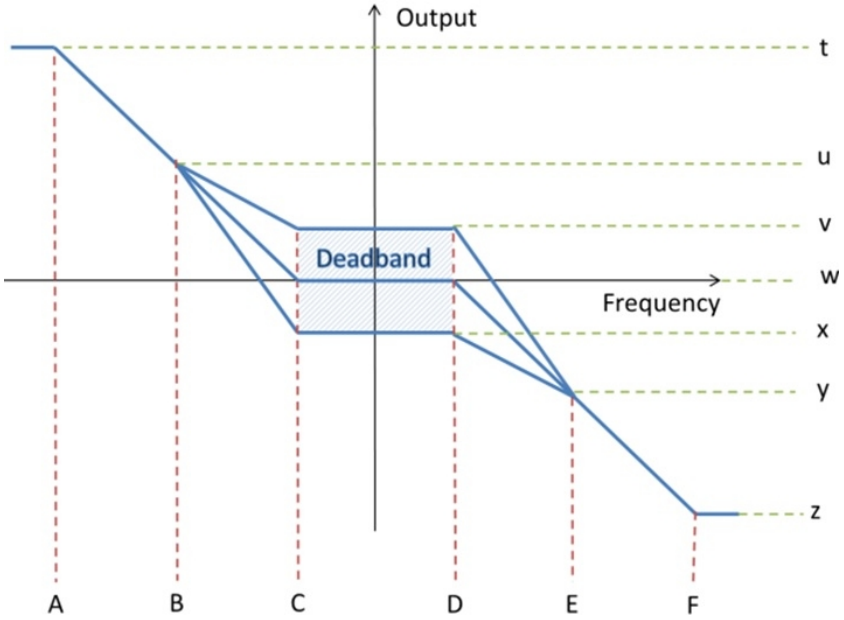

Figure 3.3: UK enahnced frequency response envelope [196]

of the BESS at those early years is justified by the islanded topology of the West Berlin system. More recently in [135] and [112] one of the control techniques make use of the periods when the frequency error is located inside a narrow window around the nominal value (in Continetal Europe, ENTSO-E prescribe a value of 10 mHz around 50 Hz) by recharging or discharging the BESS with a certain rate equal to a small percentage of the nominal power. While a certain help to SOC control is given, no guarantee is given that the SOC goes to 0 or to 100 % after long over-frequency periods.Moreover if many BESS are allowed for dead-band control the grid frequency itself can

oscillate more.

Services degree of Freedom A group of studies are based on the analysis of BESS operating under the degrees of freedom which are allowed in the Central Europe and UK fast frequency markets. As described in [64] there are three degrees in German market (see Figure 3.2: exploitation of the deadband space, over-fulfilment in over or under frequency and scheduled transactions in the intra-day market. In [51] and [65] the same degrees of freedom are exploited with better battery models and optimization techniques. In UK, the BESS are allowed to operate inside an envelope whose borders depends on the sub-typology of the service offered (see Figure 3.3 with the generic shape of the envelope).

In [82] deadband, constant offset and variable droop strategies based on look up tables are used and results are compared in terms of SOC management. in [106] the problem of optimizing the behaviour of BESS sub-units is studied while at the same time applying the degree of freedom given by the Central Europe Market: as every unit possess is own non linear efficiency curve, at partial load it is necessary to consider a proper sharing between the units and a corresponding good SOC management to keep all sub-units charged and the system working at the highest efficiency possible.

Online Recharging. This strategies fundamentally works like a filter of the control provided by BESS: while responding to dangerous fast frequency error components the BESS, a second much slower components create an offset in the control used for SOC management. In [110] and [23] technical and economical analysis to find the optimum Energy to power ratio for BESS performing primary frequency control is studied. The control technique is similar and consists on a P_{SOC} component computed as:

$$P_{\mathrm{SOCt+d}} = \frac{\sum_{j=t-a}^{t}(-P_{\mathrm{PFC}} + P_{\mathrm{loss}}(j)}{a} \tag{3.2}$$

where d is the delay period of the control, a is the averaging period and $P_{\mathrm{loss}}(j)$ is the estimated losses of the BESS due to stand-by losses and internal inefficiencies. In alternative is it also possible to activate slow ramps to restore SOC activating slower plants or buying energy from market. a faster P_{SOC} component means better SOC management and less need to over-dimension the BESS, on the other hand it can be more destabilizing for the grid. For this reason in In [110] three index are computed to quantify how much and often this offset is requested. In [105] and [118] Discrete Fourier Transfrom (DFT) is used to analyze the frequency signal. Different

energy storage technologies were dimensioned to address the the different harmonics of the frequency power spectrum. BESSs are very well suited for very fast oscillations (with mean zero and low energy content needed) while pumped hydro is more effective in case of slower oscillations.

MPC and multi-units. Model Predictive Control (MPC) is a type of control which can be positively used in the case of been able to predict input dynamics and been able to build a reliable system dynamic model. It performs multiple hours optimizations with a receding horizon of predictions which are able to increase efficiency and robustness in the solution proposed under uncertainty of real conditions. In our case it is often used when there is a need to coordinate not only BESS but a pool of different units. For example in [180] electric vehicles aggregator and traditional generators provide PFC as a group and MPC is used to optimize the use of the different resources considering their typical constraints. Instead in [91] an MPC controller for a BESS performing PFC is used in combination with a short term frequency predictor. Multi-units layouts are used also in [162]. In [18] a run of river hydro-electric generator is augmented with a BESS in order to continuously providing PFC independently from the primary source variability. While BESS is always faster, more precise and available, installing too much capacity can lead to economic losses depending on actual reserve prices.

Multi-services To guarantee multiple flows of incomes BESSs could provide more services at once. In this case SOC management is even more important as the single services must not limit or conflict with each other. a typical useful layout is the one of joining PFC with energy arbitrage in order for the BESS to enhance its profitability while trying to improve SOC [34]. A good example is in [24] where two fuzzy logic controller are used. the first inputs frequency error and SOC values in order to perform a variable droop strategy useful to contain SOC deviations. On the other hand the other controller inputs SoC and price levels (which is compared with a mean historical price). The BESS will try to buy or sell energy if signal prices suggests it is convenient but at the same time will try to not go against the SOC level of the BESS. In the study these two controllers makes SOC management very robust but gains from energy arbitrage are not high even when membership function of fuzzy controllers are adjusted. Participation in Energy and Power markets is studied in [88] and [87] where optimizations techniques and robust approaches to deal with uncertainties are used to make BESSs participate to three different services and increase profits. Finally in [123] the BESS is used to perform PFC and distribution grid management at the same time where day ahead optimization is followed by a real time

strategy used to assure that SOC and services are fulfilled under different real conditions.

BESS models. Finally various BESS models and degradation models were used in the studies. Simplest models is the constant charge and discharge efficiency with a fix power and energy characterization. On the other hand [82] presented the model developed in [24] through a series of experiments and laboratory trials. The model is composed of a series of resistance capacitance blocks. Each block is derived from a specific electro-chemical modelled phenomenon linked to the battery operation. Moreover The SOC is estimated from the voltage of a nonlinear capacitance, thereby addressing the intercalation of ions into the electrode structure. While this model is more realistic , it is much more complex and computational intensive: as shown in [82] using this model, simulations last 50 times more than simple models. A good solution could be the use of empirical efficiency models as used for example in [82] or [106]. This models uses a variable efficiency value for the BESS. this efficiency usually depends on SOC of the BESS and it is built starting from BESS empirical studies. In [145] a model of this kind is used starting from simple test experiments. A 2 dimensional look-up table is built where besides the SOC even the power level request to the BESS is used an input of the tests. This is useful in order to incorporate the auxiliary power losses of the BESS. As a matter of fact these systems are always equipped with a cooling and power management systems which should be taken into account. The results gives error with respect to real data of less than 5% in line with electrical equivalent models, which however are much more computational expensive. Therefore this approach presents good advantages and the challenge is to incorporate degradation of parameter over time (for now it is necessary to repeat tests at periodical time differences).

Battery degradation. For battery degradation the studies use a great variety of approaches and models. The approach used to account for degradation is even more important of the BESS modelling itself for studies which perform techno-economical analysis. This is because degradation is an important capital loss for the investment both in term of length of the investment and performance of the BESSs during its useful life. The simplest way to take into account degradation of BESSs is to evaluate the total energy cycled by the BESS and then obtain the equivalent number of cycle of energy by dividing it for the energy capacity of the BESS [82]. Another simple method could be to compute the average Depth of discharge [28] or C-rate during operations. In [110] a penality factor for battery cycles which goes over 85% or under 15 %. This approaches are simple and can

be operated also thanks to the data provided by BESS constructors which performs BESS tests at fix Depth of discharge and compute the maximum number of cycles performed by the BESS. In the actual operations (especially in the case of FCR provision) cycles are not easily recognizable an quantifiable. Moreover it is important for every cycle the explicit computation of the Depth of Discharge (DoD) and the average SOC during the discharge. In [51] and [188] to compute the cycles performed, a rainflow counting algorithm is used. Rainflow counting is a technique taken from the study of the mechanical fatigue of material which are subjected to stochastic load profiles. Moreover the models makes use of experimentation results to connect known chemical degradation processes (such as degradation of electrodes materials, electrolyte film formation etc.) to BESSs operational macro-variable (such as temperature, SOC, DOD of cycles etc.). In particular the degradation is composed by two main components: calendar ageing and cycle ageing. The first components quantify the BESS capacity loss over time and it is mainly correlated to the average SOC and temperature of the BESS during the years. The second component is instead linked to the actual operating condition and therefore depends on the accumulated losses each cycle causes and it is related to each cycle DoD, temperature and average SOC. Highly non linear expression considering power and exponential laws and the use of parametrized corrective factors have to be used to capture the complexities of the phenomena. In the case of PFC, in [51] it was computed that calendar aging is actual predominant to cycle ageing due to the shallow nature of BESSs cycles when providing the service. In [164] differet PFC and SoC managment strategies are compared in terms of capacity fade created during BESS operations.

3.2.2 Closed loop contigency papers

Both PFC and RoCof control are usually evaluated in these studies. The typical (but not exclusively) procedure is to model a contingency (e.g. a loss of a generator) in the grid at various inertia levels and assess the impact of different quantities of BESSs performing fast services on the grid frequency signal.

Different choices among the studies are made on different aspects of the problem. We can try to summarize the various points considering the models, methodologies, case studies and results used in the papers and trying to highlight most interesting points and/or differences:

Basic Modelling choices There is a fundamental choice to do when studying frequency control. In paricular works like [83, 174, 158, 27] are based on a low-order System Frequency Response Model (SFRM) [8] which make use of the Swing equation of the synchronous generators which simplifies the grids dynamics and the computational costs of running simulations. SFRMs have

been described in its basic components in the previous chapter . Further hypothesis On the other hand works like [129, 2, 144, 149, 25] makes use of complete dynamic models for all the relevant components of the grid. The SFRM and multi-machines full models are compared in [62] and especially in [160] even in the case of low inertia. SFRMs are based on certain restrictive hypothesis (rotor angle stability, voltage stability) and assume the power losses to be constant in the grid. These conditions are usually well found in the grid during contingency [149]. in SFRM all SG rotors dynamics are joined and the dynamic of the frequency signal (called the center of inertia frequency or f_{COI}) is unique. The comparison offers a pretty good matching between the simulated frequency dynamics. For the only purpose of studying frequency dynamics SFRMs offer a good and fast alternative to the use of complete models especially for assessment studies. In all papers considered the system inertia is considered to be one of the most important parameters of the grid [173] especially to limit the Rate of Change of Frequency (RoCoF) value in the first instants.

Note that with complete models we refer to a mathematical description of the grid based on algebraic-differential equations in which electrical, mechanical and magnetic phenomena are explicitly described. However a big number of equations and non-linearities can increase the computational burden of the simulations. So models have to be chosen accurately considering the problem at hand. As written in [114] time domain simulations is used for two reason: **(a)** assessing the electro-magnetic behaviour of power system devices or in our case **(b)** assessing the electro-mechanical response of the system after a disturbance.

For this reason generally there is no need to use EMT models or electro-magnetic transients solvers, instead fast or non linear phenomena (like switching gates of converters or hysteresis and magnetics flux dynamics in synchronous genrators) can be neglected and we can make use of phasor or dynamic phasors based model description [117]. For this reason model are usually constructed in the d-q axis and not in the abc time frame [96] in order to fasten simulations an appropriate numerical methods has to be chosen (for more information see [114]). Information lost (like quantification of harmonic distortion) is usually negligible for the studies under consideration. Typical softwares used in papers are Dig-silent, Eurostag, R-scad (typically used in the field of real time simulation [117]), PSSE and Dome which is a software based on python [113].

Objectives and methodologies adopted Many approaches can be recognized in literature.

Classic/Probabilistic control approaches. Basic approaches consider the loss of the biggest unit in the grid and the consequent intervention for BESSs in order to stabilize frequency providing droop and inertial control like in [37] where BESSs are added into the Korean system and their impact evaluated with respect to traditional reserves or in [127]. In [70] a probabilistic approach is adopted varying relevant grid and BESSs parameters in a wide but realistic range to quantify frequency recovery under all grid conditions. Several studies tries to quantify the real impact of BESSs systems providing PFC and RoCof control. For example in [92] the equivalent inertia provided by the BESSs H_{BESS} is computed considering BESSs delays and saturations. In [25] starting from simulations, output surfaces of f_{nadir} and other relevant quantities are built considering various delays values and BESSs installed capacities. In [5] a fleet of Electric Vehicles (EVs) providing PFC is simulated. A certain distribution of delays is applied to the population of vehicles to simulate the real operations of EVs fleet which will be operated from distribution grid. The contingency are characterized by strong wind changes under a very high penetration of wind sources. Also in [120] EVs are simulated while performing PFC. in this paper there is a great effort to simulate realistic presence of EVs in the grid by using different categories of EV and EV drivers which leads to different car uses and energy needs. Specific time and consumption of travels are extracted from specific probability distributions functions. EVs are also charged according to dumb or smart charging strategies which leaves just part of the battery to be used for PFC. Another important aspect is investigated in [130] where different typologies of measuring techniques and control strategies are used in order to evaluate the effect of energy storage after a fault in the grid. The control methods are based on the bus frequency direct measurement or the COI frequency or the voltage of the bus. Several scenarios are constructed based on different strategies, bus location and fault clearing time. A very high number of time domain simulations is performed and the percentage of unstable simulations is computed.

Frequency domain approaches In addition to explicit time domain simulations, also frequency domain analysis is used to investigate the BESS impact. In [27] and in [158] two slightly different SFRM models are analyzed for asymptotic stability checking the root locus of the system transfer function: the possibilities of instabilities are rare and connected to the presence of a negative zero in the governor response of generators which is usually present in certain kind of hydro-elettric plants or in the filters of Phase Locked Loop (PLL) devices in combination with RoCof control. Phase Locked loops devices are used to measure the grid frequency. However the derivative of a

signal amplifies noise errors, therefore caution must be used in designing the constants of the PLL loop control.

Innovative control approaches. In [22], the control strategy for BESSs and other resources presented in [23] is evaluated from the point of view of the effect on the grid frequency signal. Frequency control is provided by different storage technologies which are activated optimizing their intervention according to their possible ramp rate and energy content. While frequency control is provided as required by the grid operator, every unit participate for a specific part and frequency signal present minimal changes with respect to a classical droop approach. In a similar way in [21] the effect of recharge strategies of BESS on the post-fault frequency signal is evaluated. In [193] an adaptive droop control is used for BESSs providing FPC in islanded microgrid where regulation provided by BESS is fundamental in order to guarantee frequency control. In place of the classic fixed droop, droop can change depending on the available power margin of the battery and the need for better droop response. the technique guarantee better small signal stability (studied through the root locus) and better power sharing between BESSs without the need of communications. Other works like [132][129] simulates a fault lines due to a short circuit. In this case BESSs provide local frequency regulation in order to avoid the Synchrnous Generator (SG) loss of synchronism. In order to control the converter controller specific additional control techniques such as Proportional Integral control or H_{inf} control are used in the place of the classical droop, RoCof control. Robust H_{inf} based control is also used in [90] in a Microgrid system on order to deal with renewable and load noises and uncertainties. The MPC is also used in various studies [181] [180] as it is able to keep into account the different resources energy and power rate constraints when providing frequency control. in [177] the MPC control is improved By inserting a so-called Control Lyapunov Function (CLF) as a terminal cost term which can assure stability. BESSs is able to perform better but on the other hand it could work more and in an unpredictable way. Note that making use of a SFRM is possible to design the controller exploiting the time invariant linear system theory for which is more easy to achieve the complete control of the variables. Other approaches which are gathering some interests and providing new solutions is the study of distributed frequency control as opposed to today PFC (local control) and secondary frequency (centralized control) [102, 128]. These approaches are based on the devices making use of the same frequency signal (for example the COI signal [133]) for a coordinated area rather than a local one. Moreover distributed control can be used to gather distributed demand resources and attempt to study these aggregation are made by also making use of game

theory and multi-agent systems [44, 101].

Optimization approaches. Some approaches tries to explicitly optimize the BESSs presence and intervention in the grid by using different techniques. In [108] an optimization problem is formulated in order to minimize the cost of installing BESSs able to assure frequency recovery in the . A simplified frequency dynamics is used as part of the problem constraints in order to formulate a easy to solve problem with off the shelf solvers. BESSs installation cost is of quadratic form $C_{\text{inst}}(Pb) = aP_b^2 + bP_b$ where coefficients a and b reflect the real economies of scale [141]. Additionally since linear frequency approximation oversize the solution, an algorithm is used after the optimization to slightly adjust the solution in order to find the best possible outcome. In [62] 5 objectives functions are minimized by determining the best values of droop and inertia provided by energy storage together with the parameters of PID secondary frequency controllers. These objectives functions takes into account the frequency signal shape and the value of virtual inertia constant H. To take into account all these dimensions an elitist Pareto-based multi-objective evolutionary algorithm is used which is capable of finding and rank the best possible solutions. In [144] an optimization problem is formulated in order to avoid the activation of load shedding after a contingency by using BESSs. The problem is solved by using heuristic methods (BAT optimization algorithm) and tries to minimize the participation of BESS to PFC and their energy content while at the same time never overcoming the Load shedding threshold. Moreover BESS location is addressed by identifying the transmission system bus with the larger transient frequency deviation. The placement of virtual inertia is addressed also in [140] where considering a linear network reduced power system an optimization problem is formulated based on a quadratic performance index measured by the $\mathscr{H}_2$ norm. The solution is non-convex, but it is possible to easily provide local optimum solution to particular instances of the problem. Finally in [107] the inertia level provided by BESS during the simulation changes thanks to an adaptive control which optimize the BESS impact and at the same time the energy storage depletion. The paper makes use of the analytical study of system dynamics similar to the SFRM model of the other works and a Linear-Quadratic Regulator (LQR)-based optimization technique. The proposed controller is then verified through the use of detailed power system simulations.

Models Usually simple models for BESSs are used as more attention is given to the grid system and to perform numerous simulation. In general simple power and energy description with the adding of a pole to simulate unit dynamics is used in studies based on System Frequency Response Model (SFRM) as

there is no presence of electrical currents and voltages. in [25] the delay is modelled as a delay part when BESS does not respond plus a linear ramp part to reach the assigned power. BESSs models present even in this group a great variety and the typologies presented in the first group are also used here. In [129] a generalized linear model for an energy storage is presented in order to maintain a realistic approximation of the answer of the BESSs without modeling a computational heavy non-linear electrical equivalent system.

Great attention is also given into the modelling and simulation of the frequency signal and its derivative in order to evaluate fast intervention in the grid. As known the operation of derivative can lead more easily to numerical or physical instability of systems. The first problem is related to the software used and its numerical integration methods (used for solving differential equations), the second is instead related to the actual behaviour of the control in real-world operating scenarios. In the case of RoCoF control, the power variation should theoretically be immediate as inertia is a physical parameter of synchronous generators which instantaneously reacts to a change in the grid. However the computation of the frequency time derivative is not easy and requires the use of appropriate filtering, computation techniques and temporal windows studied in [148, 132, 149, 25, 46]. For what concern RoCoF control a minimum time window of 100 ms or more should be used to avoid too much measurement noise. Note that today in Ireland and UK a moving window of 500 ms is used in the anti-islanding relays [46]. Moreover a full response within at least 300 ms is needed to have a good impact on the frequency which should be reduced to 100 ms to achieve best control qualitatively similar to the rotating inertia of Conventional Generations (CGs). Note that in literature other control techniques such as virtual synchronous generators , self synchronizing synchroverters , matching control do not require explicit frequency derivative computation and can potentially be faster, but present other limitations and problems. The interested reader can refer to [116, 148].

The key elements for frequency measurements and frequency control of BESSs are the frequency measuring device and the converter control mode. Today the typical device used is the PLL or Phase Locked Loop and the typical control mode is the the *Grid-following mode* [166]. In this case the voltage phasor (in magnitude, phase and frequency) of the converter is imposed by other grid forming units (Synchronous Generator is a typical grid forming unit). The device is then able to injects the desired level of active and reactive power by regulating the current. The main challenges of this type of control resides in PLLs which can be sensitive to noise, delays and errors

under different scenarios [148] or in the DC-side dynamics which can be become unstable if AC-side are not slow enough or its capacitance value is not correctly designed. The first problem is usually sufficiently studied. For example a basic scheme and 5 possible implementations of PLLs are presented in [131]. The PLL is based on three parts (aggiungere figura): A Phase Detector to pass from $v_{abc}(t)$ to $v_q(t)$ in the dq reference frame, a Loop filter based on tracking controller like PI controllers which estimates the bus frequency deviation and finally the Voltage-controlled oscillator which provides the estimation of the voltage q-axis component [116]. Moreover especially in the case of RoCof, the signal can be filtered or computed over a discrete time moving window like in [25] in order to avoid numerical instabilities and filter out electro-magnetic transients in the signal. The dc-side voltage is instead always implicitly considered stiff or anyway with faster dynamics than AC operations. This means that the energy storage behind the converter should be fast enough to provide for power in case of fast service into the grid. Additionally in order to avoid unstable interaction with grid line dynamics, input power measurements high frequency components can be filtered. DC voltage source is actually the key of converter control in many new technique especially the ones which makes the converter work as a grid forming unit. In this case the Converter exhibits SG capabilities such as black-start capabilities, load sharing, frequency and voltage regulation. The principle is the opposite of the grid-following unit: the converter devices imposes and substain the voltage levels of the power systems. For this reason a stiff DC source is needed to adjust the active power produced. The families of possibles controllers in this case are [166]: droop control, virtual synchronous generators [152], matching control [77], virtual oscillator, self-synchronized synchroverters [195] and ICT based techniques. In particular matching control exploits the duality existent between the DC link voltage and the SG rotor angular frequency. Virtual synchronous generators on the other hand can have both functionalities as grid-forming or grid-following units [16].

The generic scheme of converter modelling can be viewed in fig 7 of milano reivew. Every block (plus the energy storage model) needs to be modelled according to different assumptions and level of depth desired. A possible basic scheme is to use current and voltage reference controllers in the form of PI controllers to make the unit follow a certain power schedule [139] without explicitly modelling the converter phenomena dynamics. More complex approaches can be found in studies like [43]. A complete derivation of the converter equations from switching gates in time domain to an averaged dq frame reference model can be found in [115]

Indices In general after a contingency frequency drops/increase very fast and

then stabilize after reserves are activated. To have an idea of the frequency deviations typical variables compared in the papers are initial RoCof of the frequency, the lowest frequency point and corresponding time $f_{\text{nadir}}$and t_{nadir} and regime frequency value and time f_{reg} and t_{reg}. In [158] and [62] also frequency integral error and the integral error multiplied by time are used computes as:

$$\int_0^t t|\Delta f|dt \tag{3.3}$$

These last two indexes are able to better follow the variability and oscillation of the frequency signal. Finally in [37] the equivalent BESS inertia is evaluated considering a scenario where RESs are introduced into the grid in the place of synchronous generators increasing the initial rocof of the grid after a contigency. Equivalent Inertia is the BESS inertia value for which the initial RoCof is obtained in the simulations. In the same way the primary frequency response effective factor is computed considering the ratio between the classical frequency reserves substituted over the installed capacity of BESSs which obtain the same nadir frequency.

Results Papers usually confirms the usefulness of BESSs in providing frequency control. In [25] the optimum delays of BESS to maximize impact is computed as less than 10 ms considering pure delay and ramp. However very good results can be reached already under 100 ms, which is already well within today BESSs systems capabilitiess [15]. In [70] the effect of small delays in RoCof control produces in the first instants a small hook shape indicative of possible dangerous transients with respect to classical inertia. Nevertheless stability of BESSs response is considered positively in this work as in the other papers.

3.2.3 Closed Loop Normal Operations

In this group of studies the impact of BESS is measured in longer time frame and under normal deviations of the frequency signal caused by the power swings of loads, RES and conventional generation present into the grid. The key questions in this group of studies are (1) how the impact of BESS is quantified and (2) how frequency signal is reproduced in this closed system. both points are fundamental to build a meaningful case study and obtain sound results.

Impact of fast resources

we divide the analyzed studied in three groups for what concern BESS impact:

classic primary frequency control impact A part of the studies deals with secondary frequency control [33, 193, 35] in which BESS impact is compared with CG. Another group deal with PFC, with a even smaller portion discussing also the role of Inertia or RoCof control during normal operations. In [163] the impact of a ESS on a small power system is evaluated in field tests by changing the primary frequency control parameters and estimating the change in frequency deviation when the BESS is open or close. The decrease in the frequency signal is estimated by looking at the grid frequency deviation. In [85], the frequency signal of Korean system is reproduced and a specific control algorithm taking into account droop control and SOC management for the ESS is implemented. Its effect on the time domain frequency signal is simulated without making use of a specific index to quantify this intervention. In [111] ESSs are used to provide PFC and the effect on the frequency PDF is assessed considering different controller parameters.

filtering frequency signal techniques. In [29] the effects of wind fluctuations on the grid are simulated. BESSs and a supercapacitor is used to increase frequency stability. For this purpose a fuzzy-logic controller is used. The frequency error is filtered into three different ranges and the SoC of the storages are taken into account in order to chose the power to be produced or consumed. Finally an heuristic differential evolution algorithm is used to minimize the cost of installed storages while at the same time avoiding big grid frequency deviations. The approach to divide frequency signal in its frequency components is also used in [118] where Discrete Fourier transform is used to analyze the power imbalance and divide between its high frequency and low frequency components. Different components can be dimensioned to address the specific components of the frequency oscillation.

inertia impact. In [99] the ESS performs enhanced frequency control in UK grid and it is able to decrease the frequency standard deviation of the UK frequency signal. In [183], the Fokker-Planck equation is used to determine the probability density function of the system frequency under a variety of inertia levels, droop characteristics and generators deadbands. In the last two works cited, it was found that inertia (and similarly RoCoF control) do not apparently have a big impact on frequency deviations. Note that in these works the UK frequency recording were used with a sampling of 1 Hz. This represent a somewhat too low sampling rate for a signal like RoCoF which dynamics of interest starts well under the second.

Frequency signal reconstruction

In normal grid conditions a correct modelling of the frequency signal is essential for the realistic evaluation of the new frequency services. Many studies have noticed a certain complexity of phenomena causing the normal frequency deviations in today's power systems.

- In [150], the nature of frequency signal is studied. The area control error (ACE) of the American electric grid provided by PJM grid operator is analysed using the DFT to highlight the dynamic property of the signal. Distinct peaks in the power spectrum were observed at specific times (5,7.5,10,12,15 and 30 min). Reasons for this phenomenon was found in the market energy operations. The study was performed to create standardized duty-cycle for batteries performing ancillary services into the grid which served in [151] to offer a standard test to evaluate battery system performances of different technologies.

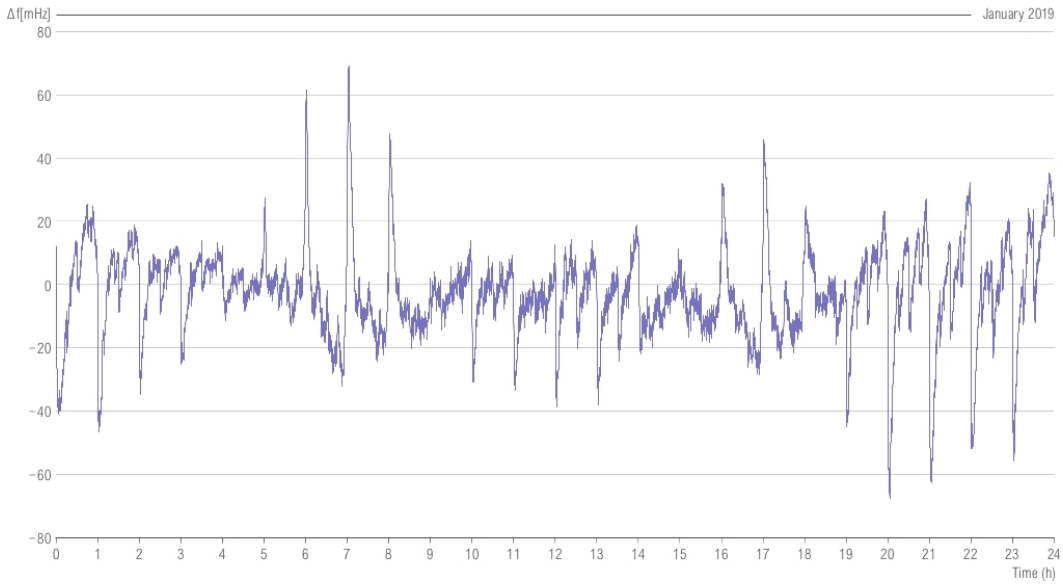

Figure 3.4: Monthly average of frequency signal in Europe [52]

- In [59, 52], the nature of frequency oscillation is studied for Europe. The liberalization of markets led to a worsening of frequency oscillations especially at hour intervals. two typologies of deviations exist: (i) stochastic frequency deviations due to the fast variations of loads and renewable sources, (ii) deterministic frequency deviations caused by the ramps of CG following their market scheduling. CG undergoes an hourly or sub-hourly unit commitment,

which leads to a long term mismatch with respect to the net load. In Figure 3.4 note how at the change of the hour, frequency is constantly away from its nominal value. The SGs follows in fact an hour or possibly a quarterly hour time production schedule built under the market mechanism of the grid which does not compensate the continuously changing power profiles of the loads. Moreover as explained in [52], generators are usually allowed to change their set-point at the maximum ramp possible and ,while rare, ACE error measurements can cause the prolonged and large deviation of the frequency signal during normal operations. The effect of these deterministic frequency deviatios is that the frequency signal distribution tends to not be gaussian, but it present heavy tails and possibly high Kurtosis values [154]. To minimize these deviations, it was suggested to pass to quarterly hour energy, balancing and ancillary service market, limit the SGs ramp rate and assure redundancy and ACE measurement verification. The implementation of new rules and actions lead to a lower need and activation of primary and secondary frequency control reserves and therefore less ancillary services costs for consumers as evaluated for the German market in [146, 187]

In order to reproduce a realistic signal it is necessary to simulate both typologies of frequency deviations and verify the resulting variability of the frequency signal with real-world data. However usually only stochastic processes are reproduced, for example in [33, 193, 35] recorded load demand and photovoltaic power plant measurements data are used, while the power exchanged at the tie lines and frequency reserves are estimated. In [29] wind historical data are used. In [111] and [183] instead of real data, power variations are modelled as a Ornstein-Uhlenbeck stochastic process. In [99] the swing equation of the system is inverted to compute the system demand profile which causes the frequency deviations. This last approach is promising, but for the way it was formulated, it still cannot divide between power deviations caused by net load dynamics or by CG primary/secondary frequency control responses, producing wrong future scenarios and misleading parameters evaluation. Note that, except for [111], all of these works make use of a SFRM. This model is expected to behave well in terms of reproducing frequency dynamics, because all assumptions upon which the model is constructed holds even more under normal grid dynamic conditions, characterized by a series of continuous small disturbances into the grid.

It's important to point out that the numbers of studies which concentrates on this particular group is evidently lower than the previous groups. It is author opinion that this is not due to the lower interest or utility in the objectives these studies propose but on the actual difficulty to model frequency deviations and its root causes.

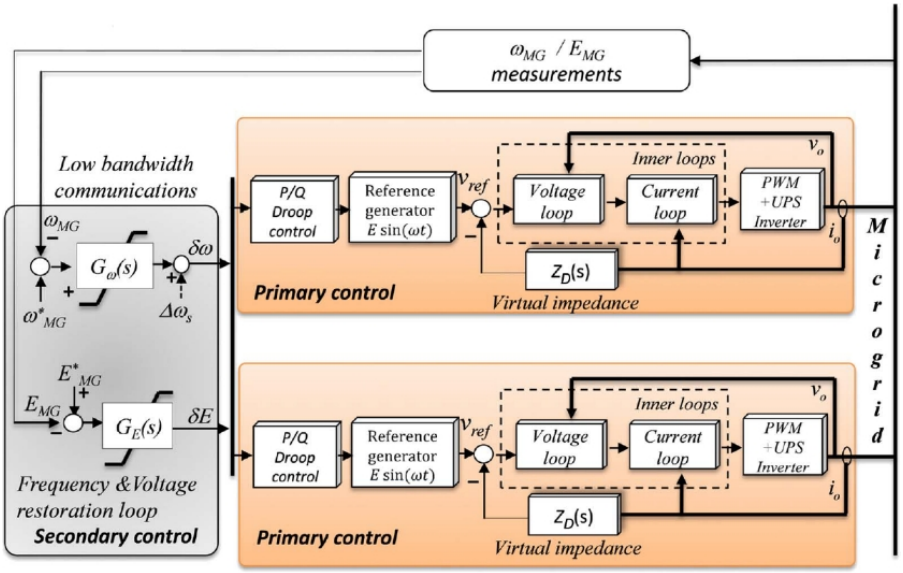

(a) Secondary and primary control of inverter-based microgrids [71]

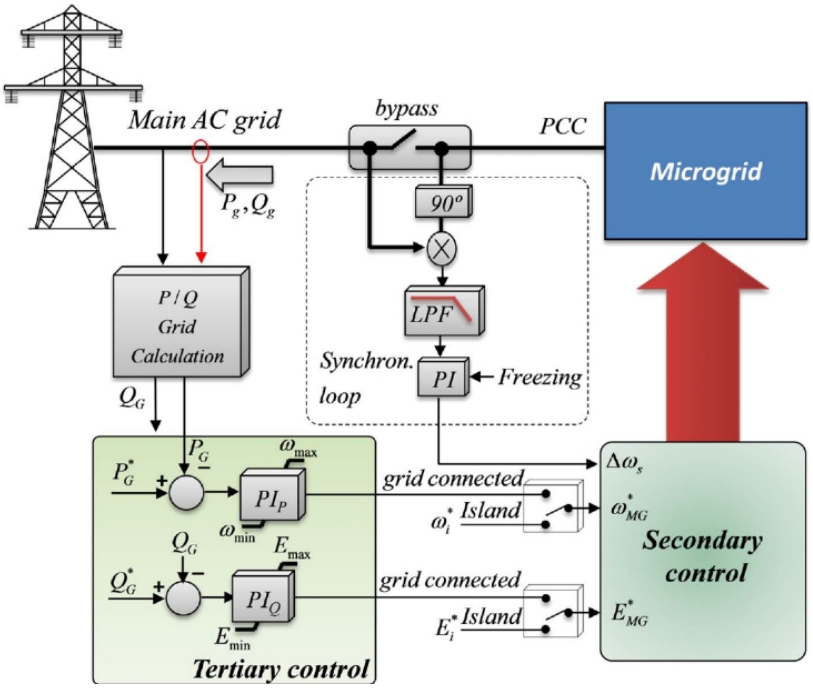

(b) Tertiary and grid connection control of microgrid

Figure 3.5: Degree of freedom in PFC in Central Europe for BESS [71]

3.2.4 Notes on Zero Inertia systems

When there is no synchronous generator present in the grid as in the case of Microgrid or isolated distribution grid with only converter connected resources there is a need to implement a parallel operation of converters. Different possibilities exists [71]:

Droop based This family of techniques mimick the typical droop concept in today's regulation control schemes based on changing the P and Q production by measuring local frequency and voltage magnitude. On the contrary of the synchronous generator case, in the case of only converters, frequency and voltage are imposed by the converter as the consequence of the measured ΔP and ΔQ on the grid. In this way we minimize the need for communication and we have plug and play feature for the converters [161]. Droop can be conventional (P-f, Q-v), inverted (P-v, Q-f) or mixed, depending on the nature of lines and presence of Voltage Output Virtual Impedance used to improve operations of the microgrid. To improve stability and to assure proper connection with the grid, Secondary and Tertiary Control is needed. In secondary control, two additional signal $\delta\omega$ and δE are sent to some converters (usually the bigger ones) with hypothetically similar or slightly faster rate of Today's main grid Secondary Control unit. Tertiary control will instead sends some signals to the Secondary Controller (reasonably from the TSO Energy management system to the DSO management system) about P and Q rated values that the distribution system should produce. Moreover, synchronization with the main grid must be assured through proper communication and procedures. This TSO and DSO flow does not need a very high bandwidth communication and therefore is quite robust (See Figure 3.5a and 3.5b). Droop techniques are the first to appear in 1990's in order to promote the parallel operation of converter exploiting the possibility for converters to be grid forming units. They represent the first step of the more general virtual synchronous generators techniques. However due to their simplicity are not characterized by the numerical instabilities which can be present in the more complex controls due to the presence of differential equations.

Communication based techniques Usually every converter has to be connected to the communication line and therefore they are actually used for small to medium Micro-grids [73] (for example Uninterruptible Power Supply systems or ship-system). Data rate should be as reliable as possible. Applications on large-scaled distribution grid are very difficult and theoretical. 3 typologies are of control are possible:

- master/slave: A master unit will set the voltage level of the principal

bus and sends its current to other units; in case of deviation, other slave units will change their output current accordingly. The slaves can also track the voltage of the principal bus to synchronize their voltages. Usually the Master will be the highest Power rated Converter to be able to deal with the transient.

- concentrated control [124]: it is usually used in the UPS. The total load current is measured and transmitted to a central controller. Then, based on each DER unit characteristics, the contribution of each unit is determined and output current reference set points are sent back to the units; an outer loop simultaneously controls the voltages of the system. This method results in fast mitigation of transient; however, communication is crucial in this scheme and its failure will lead to a system collapse. Two fundamental communicated signals are needed: current sharing signal and voltage signal (usually used for synchronization with the grid).
- distributed control: There is no Master and no central control, but it still needs communication lines for sharing current reference and also a signal (that can be local) for synchronization (frequency). But it in general needs less communication bandwidth and moreover it permits plug and play of converters easily (any converter can connect and disconnect from the grid without causing major stability problems).

DC control techniques As no SG is present, one possibility can be directly connect and run the system in Direct Current as to save the transformation losses of solar energy and DC loads. For DC grids, application still refer to small Microgrid systems and most of the work is still theoretical [79]. The stability problems refers to assure in normal operation, small and big contingency that voltage level are respected in every node to deliver the desired amount of power. The most used and stable scheme is very similar to the hierarchy control used in droop techniques for AC systems. It is based on a droop technique which assure stability and power sharing between the sources and on to three levels of control. Rationale and communication needs resemble the equivalent case for AC grids except for that that values to be communicated are just one and not two.

Chapter 4

Impact of BESS fast frequency control after a contingency

in this chapter, I present two case studies quantifying the impact of fast primary frequency control and rocof control from BESSs. These two case studies are based on the SFRM model of the grid and they are part of the classical approaches papers in the group of closed loop contingency studies as seen from previous chapters. The two case studies are based on different grids and analyze the impact of classical control frequency loops and are presented in [174, 119].

4.1 First case study: a 2 area frequency model

4.1.1 System set-up

The first work aims to highlight the impact of BESSs in low inertia power systems, when a proper combination of PFC and RoCof control is used. The study is conducted by considering two-area power system SFRM model (see Figure 4.1. With respect to the one presented in 2 this system consider the presence of two equivalent generators swinging in a coordinated system. The two generators represents two equivalent power system areas transmitting power at the tie lines. In general this power can be expressed as [58]:

$$P_{\text{ik}} = \frac{E_i E_k}{X_L} \sin(\delta_i - \delta_k) \tag{4.1}$$

where E_i and E_k are the voltage magnitudes at the two terminals of the tie-line, X_L is the tie-line reactance, and δ_i and δ_k are the voltage angles at the two terminals. Note that, if ΔP_{ik} (power flowing between areas i and k) is positive for one area, it will be negative for the other area. Linearizing about an initial

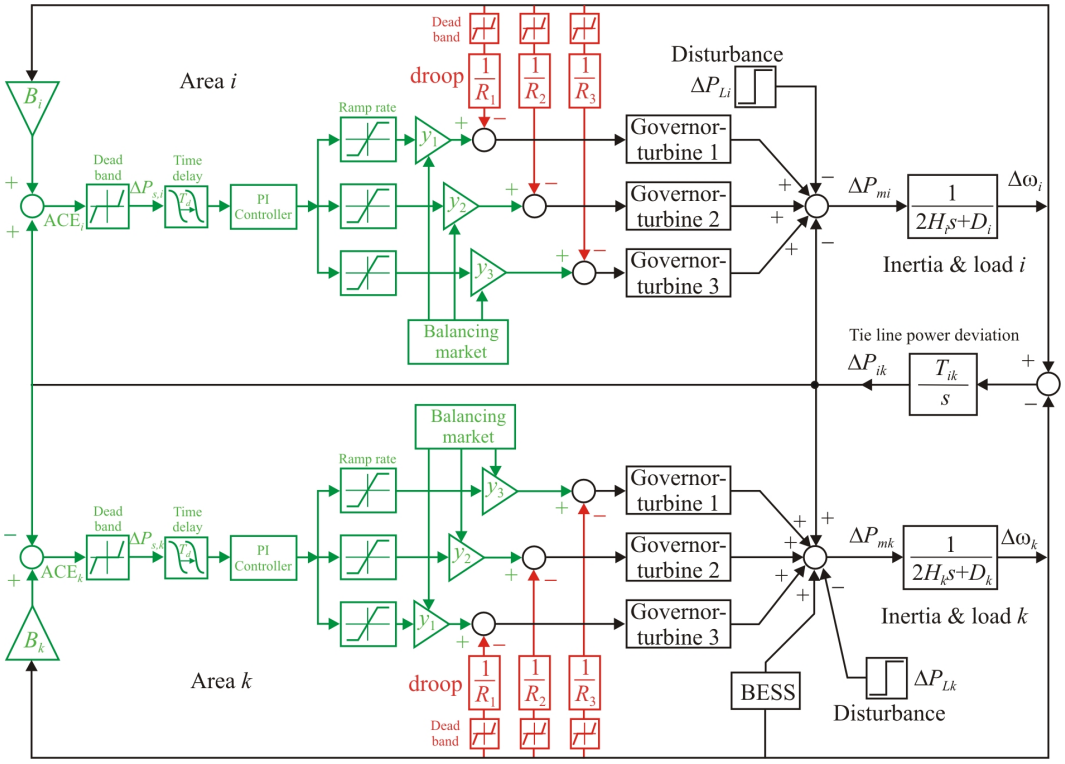

Figure 4.1: Power system model used for the study

operating point represented by $\delta_i = \delta_{i0}$ and $\delta_k = \delta_{k0}$, one can obtain the active power variation on the interconnection line:

$$\Delta P_{\mathrm{ik}} = T_{\mathrm{ik}} \Delta \delta_{ik} \tag{4.2}$$

where $\Delta\delta_{ik}$, and T_{ik} is the synchronizing torque coefficient between the two power systems, that is:

$$T_{\mathrm{ik}} = \frac{E_i E_k}{X_L} \cos(\delta_{\mathrm{i0}} - \delta_{k0}) \tag{4.3}$$

The governors systems model of steam and hydro unit is different depending on the actual primary sources and typical control scheme of power plants (transfer function are of second or third order and are taken from [96]). In figure 4.2 , typical power response of different technologies after a contingency are shown: BESSs are by far the fastest, while hydro power plants usually are characterized by opposite initial response due to the sudden decrease in duct pressure when gate valves moves. Steam power power plant profile usually depends on the presence of reheat units. In fact while steam increase almost immediately its flow in the first high pressure turbine, producing more power, a certain time is needed for the steam to pass though the reheat units and in the second mid-low pressure turbine systems.

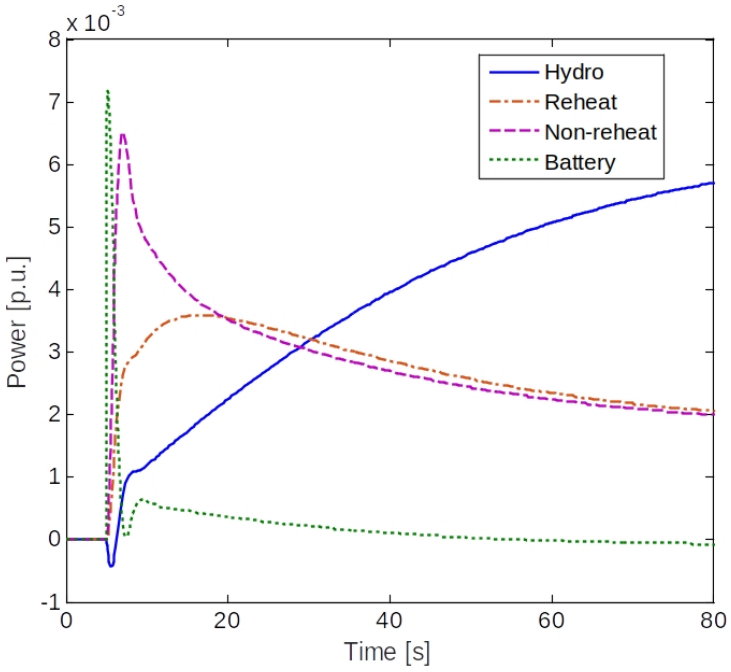

Figure 4.2: power plant response after a contingency

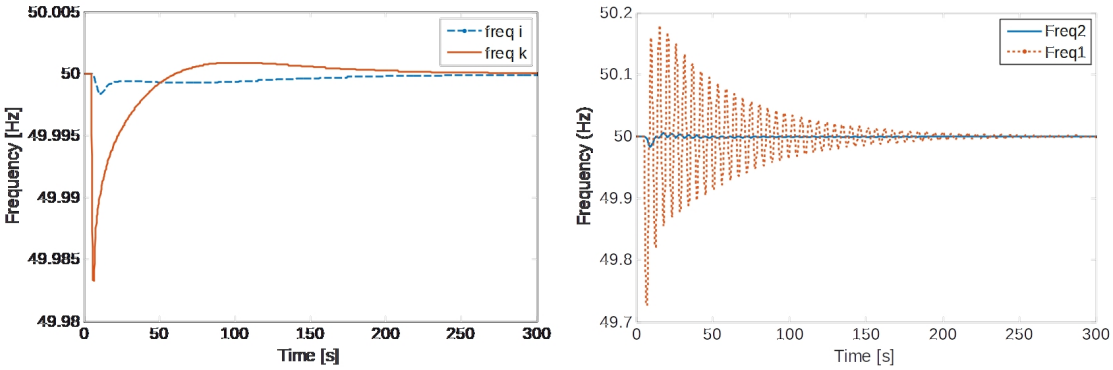

Figure 4.3: frequency response after a contingency

Moreover depending on its typology of control (boiler following, turbine following or coordinated control [61]) different dynamics are to be expected (typically an integrated system control is used which guarantee power plant stability and enough response reactivity).

The BESS control is based on a pole constant to model delays and ramp time and two different adjustable coefficients (K_1 and K_2) to simulate different proportions of primary and rocof control (see figure 4.4. In this way we are able to accurately grasp the different impact of primary and rocof control on the grid.

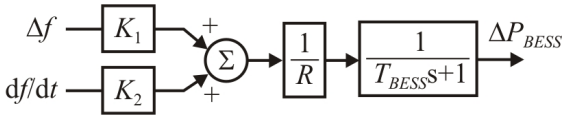

Figure 4.4: BESS model used for simulations

PFC follows a typical droop control. Moroever Secondary frequency control is implemented. An Area Control Error (ACE) is calculated for each area, using the following formulas:

$$ACE_i = \Delta P_{\text{ik}} + B_i \Delta\omega_i \tag{4.4}$$

$$ACE_k = \Delta P_{\text{ki}} + B_k \Delta\omega_k \tag{4.5}$$

where B is the bias factor and it correspond to the regulating energy of each area. The ACE is followed by a PI controller which forces the area with the disturbance to balance its own power mismatch at steady state, while both areas contributes to frequency control during the the transient condition of the system.

The electric grid is modelled through the Load damping D and the inertia H of the system. In the base case a typical value of $6.5s = 2H$ was chosen; a future scenarios was considered where all synchronous generators excepts hydro power plants are shut off and the inertia is decreased to $2H = 3s$. The system is dimensioned in per unit quantities and the contingency represents 10 % of the model base power power. Without BESSs, in the future scenarios frequency is jeopardized by the lower frequency reserves and by the unstable behaviour of hydric power plants which can enhance power/frequency oscillations through the power tie-lines . As seen in figure 4.3 , the frequency can oscillates a lot in case of low inertia. The contingency is localized in area k, which is also a smaller area and suffers more the frequency oscillations (the effect in our study is also increased to show the differences)

4.1.2 BESS sensitivity analysis

Three sensitivities are simulated. The first on the value of the weights for PFC and rocof control. The two coefficients range between 0.2 (low weight) to 0.8 (high weight) to initially study the controller response. As further hypothesis, unlimited power is available in the battery for frequency control. Time response $T_{\text{BESS}} = 0.1s$ s was considered and moreover virtual inertia term follows the BESS natural dynamics. Figure 4.5a shows the frequency response when using different weighting factors for the input signals to BESS. The simulations show that a

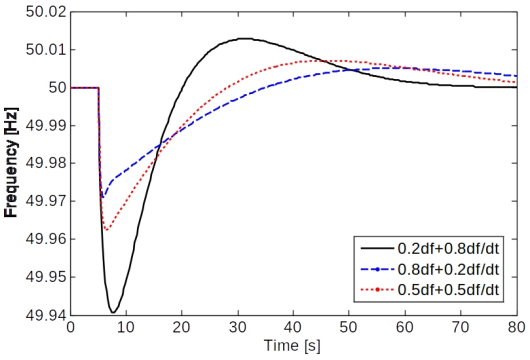

(a) Frequency response in low inertia power system by contribution of BESS (the case of unlimited power reserve)

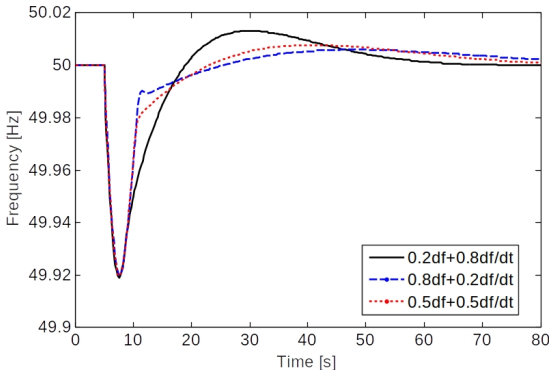

(b) Frequency response for battery having reserve limits.

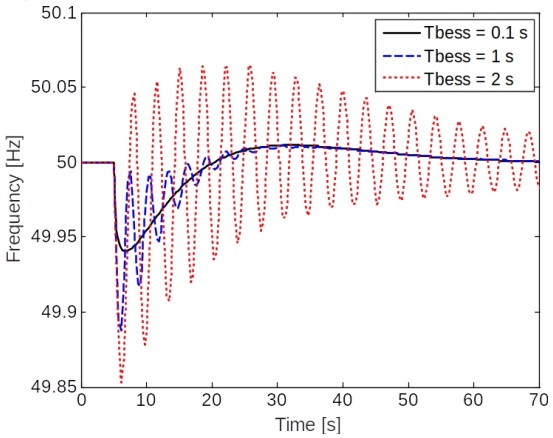

(c) Influence of the BESS time response on the frequency stability

Figure 4.5: BESS parametric sensitivity analysis on the 2 area system

larger weighting factor assigned to the frequency variation reduce the frequency sag, whereas a larger weighting factor assigned to the RoCof component provide a smoother behavior in terms of frequency oscillations damping.

in figure 4.5b the same weights are simulated while the reserve available for control was reduced. The BESS control band was set to $P_{\max} = 0.005pu$ and $P_{\min} = -0.005pu$, values smaller than the unbalance. The frequency signal reach the same f_{nadir} in all the same cases as the BESS reserves are saturated for whatever weights are used. The value it self is much lower with respect to the infinite reserve case. However steady state is reached within a similar time frame. This fact shows that, even if the size of the deployed reserve is very important to limit the frequency sag, the limited reserve does not affect the frequency stabilization and that rocof

control can smooth the frequency signal post-contingency.

Finally last simulation evaluates the effect of different T_{BESS} constants. The input signal of the BESS has been set to $0.2\Delta f + 0.8df/dt$, and three different time constant for the BESS have been analyzed in figure 4.5c. The figure shows that, in low inertia power systems, for time reactions of the BESS greater than 1 second, the frequency oscillations become unacceptable. The oscillations are caused by the slow intervention of BESS (the figure shows only the frequency of the area k). 0.1 seconds are an acceptable time pole for BESSs to provide fast frequency services.

4.2 Second case study: the sardinian insular system

In this second case study, the objective was to provide a quantitative analysis and effects of the possible installation of BESS and Synchronous compensator in the sardinian Insular case. The differences with the previous case study are:

- a single area SFRM model was implemented to model Sardinia which can be considered a synchronous area connected to the mainland through the use of HVDC systems. Also real frequency protection schemes are added. Real presence of conventional Synchronous generations is modelled and a validation on a real event is performed.
- Reference incident was dimensioned according to historical dispatching of the island, considering the tripping of the biggest plant or off the HVDC lines connecting the island to the mainland.
- An equivalent saturation logic is used to tune in a meaningful way the control parameters of the BESS fast control. In this way Rocof and PFC intervention are dimensioned following the typical layout and capabilities of synchronous generators plants.

4.2.1 Models used

The SFRM model used in this study is depicted in figure 4.6. the various blocks are set as:

- the total inertia of the system is expressed in $MW \cdot s$ and is computed as $E_{\text{k,aya}} = H_{sys} \cdot S_{\text{tot}}$ where $H_{\text{sys}} = \frac{\sum_{i=1}^{N} D_i \cdot H_i}{S-\text{tot}}$ where S_i is the rated power of the generator i [MW], H_i is the inertia constant of the generator i and N is the number of synchronous generators. $S_{\text{tot}} = \sum_{i=1}^{N} S_i$.

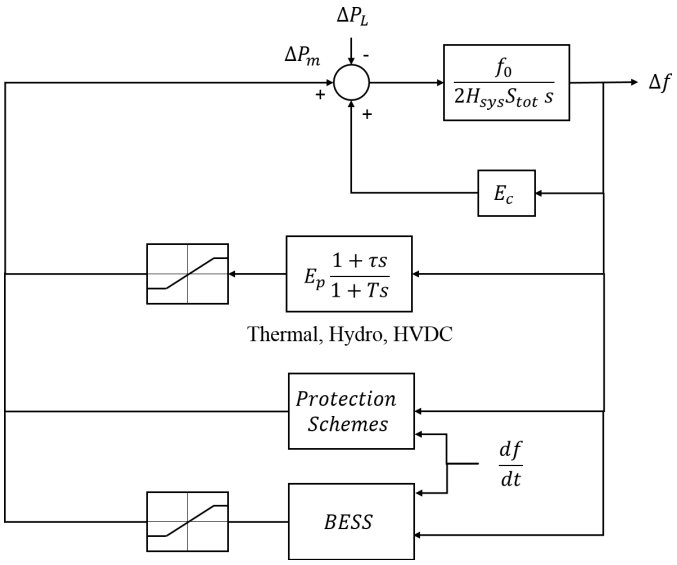

Figure 4.6: One area equivalent model

- The load regulating energy $E_c = D_L S_L$ computed as [MW/Hz]. D_L is the damping coefficient of the load and it represents the percentage change load to a frequency deviation.

Table 4.1: dynamic data of resources

Resource	Zero const. τ	Pole const. T	Droop [%]	Band [MW]
Thermal	3	10	5%	$0.1P_n$
Hydro	-1	6	4%	$0.1P_n$
HVDC	3.3	10	5%	$P_{\max}$

- The regulating energy of the single generator is computed as $E_b = \frac{S_i}{f_o \sigma_i}$ where σ_p is the equivalent droop of the generator, f_o is the nominal frequency and S_n is the nominal power of the machine. Thermal , Hydro, HVDC resources are represented by an equivalent transfer block whichs sums together power capacity and droop intervention. Every typology is then characterized by a different pole-zero constants to represent its peculiar plant dynamics. The values are reported in table 4.1. No secondary frequency control is modelled as we are interested in first few seconds after a contingency where secondary control does not intervene. Moreover secondary scheme in Sardinia operations are typically not automatic, but manually dispatched. HVDC response was modelled following the typical answer of real systems in Sardinia.

- The real protection schemes and thresholds are based on the ones adopted by ENTSO-E [54], with different shedding shares of load and generation depending on frequency values: (a) Wind shedding, starting from 50.6 Hz. (b) Hydro shedding, activated at 51 Hz. (c) Pump shedding, starting from 49.5 Hz. (d) Interruptible load shedding, at 49.3 Hz. (e) Automatic load shedding, for extreme situations from 48.8 Hz.
- model of BESS is a simple fast pole dynamics model like in previous case study (see 4.7). Power saturations are added to the total power output and also to the single control channels. As a matter of fact the two services have two different objectives and in principle TSOs could ask the BESS owner to assure a certain band for pfc and another for rocof control.

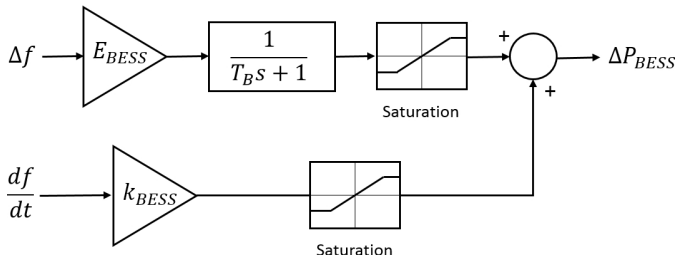

Figure 4.7: BESS model used in the simulations

4.2.2 Equivalent saturation logic

The services implemented by the ESS are RoCoF control and Primary Frequency Control (PFC). In order to give a reasonable value for the virtual inertia K_{BESS} and regulating energy E_{BESS} we try to mimick the behaviour of CG. For what concern PFC, E_{ESS} is computed such that the saturation of the available power band happens at the same $\Delta f_{\max}$ where the CGs saturate their PFC bands. In general the regulating energy [pu(MW)/pu(Hz)] of a resource is equal to:

$$E_{\text{CG,pu}} = \left| -\frac{f_{\text{nom}}}{\Delta f_{\max}} \cdot \frac{PFC_{\text{band}}^{\text{CG}}}{1} \right| , \tag{4.6}$$

$$E_{\text{BESS,pu}} = \left| -\frac{f_{\text{nom}}}{\Delta f_{\max}} \cdot \frac{PFC_{\text{band}}^{\text{BESS}}}{1} \right| , \tag{4.7}$$

where PFC_{band} represents the regulator band in pu. Taking $\Delta f_{\max}$ equal for both resources and dividing equation (4.6) by (4.7), we obtain the relationship which

correlates both the regulating energies:

$$E_{\mathrm{BESS,pu}} = E_{\mathrm{CG,pu}} \cdot \frac{PFC^{\mathrm{BESS}}_{\mathrm{band}}}{PFC^{\mathrm{CG}}_{\mathrm{band}}} \ . \tag{4.8}$$

For each value of the CG regulating energy (which can be evaluated using the droop value used in table 4.1) one obtains a corresponding ESS values which saturates its regulation band at the same frequency deviation of the CG resources. From equation 4.8 E_{BESS} is easily computed as:

$$E_{\mathrm{BESS}} = -E_{\mathrm{BESS,pu}} \cdot \frac{P_{\mathrm{BESS}}}{f_0} \tag{4.9}$$

For RoCoF control case, an extreme RoCoF value, df/dt_{max} is set as a limit value which activates all the power band reserved to this service. Grid codes usually fix this maximum admissible value during operations of the system (typical about 1 Hz/s). Starting from this value, it is possible to compute H_{ess} as:

$$H_{\mathrm{BESS}} = \frac{f_{\mathrm{nom}} \cdot RC^{\mathrm{BESS}}_{\mathrm{band}}}{2 \cdot |\frac{df}{dt}|_{\mathrm{max}}} \tag{4.10}$$

where $RC^{\mathrm{ESS}}_{\mathrm{band}}$ is the power of the ESS to be used by RoCoF control. From H_{BESS} it is straightforward to compute K_{BESS} .In general the power bands for PFC and RoCoF control go from 0 to 1. In this study their sum is fixed to 1 to avoid the two services sharing part of the power band.

4.2.3 Case study and results

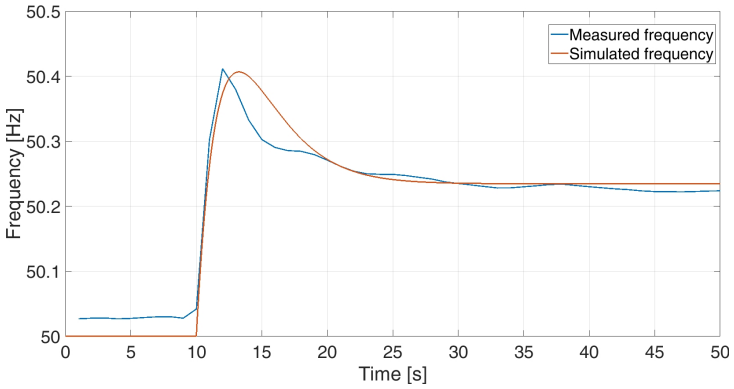

Figure 4.8: comparison of 1 area model with real system

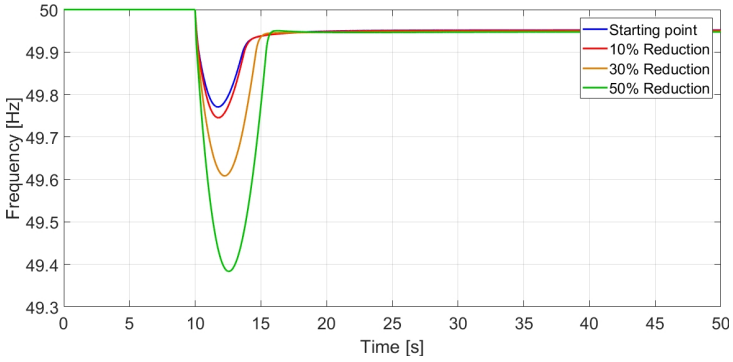

Figure 4.9: Impact of worst under-frequency contingency for the inertia scenarios considered

Table 4.2: Calibration Results

	Measured	Simulated
Zenith [Hz]	50.41	50.41
ROCOF [Hz/s]	0.36	0.37
T_{zenith} [s]	2	3.26
f_{reg} [Hz]	50.22	50.23

The Sardinian system has a maximum load of 1500 MW and it is connected to mainland through two HVDC lines (SACOI and SAPEI). The SFRM model is calibrated using a real events during an HVDC failure which lead to an over-frequency event. The two curves are depicted in figure 4.8 and table 4.2 and are pretty similar in terms of main frequency parameters (rocof, f_{zenith} and steady state). Another incidents is compared in the case of an under-frequency event and results are also similare ([119]). Starting from today scenarios, three scenarios were constructed with respectively 10,30 and 50 % of less inertia due to the actual closure of power plants. The chosen contingency represents the biggest thermal unit failure of Sardinia on the winter peak, the 17th january 2018 at hour 10:30 causing a under frequency event, which is also considered very critical because the HVDC SACOI was out of service. Fig 4.9 represents the frequency profile after the contingency at the various inertia levels. Similarly to previous study, BESS and synchrnous compensator are added to improve on the situation.

the table 4.3 present the 9 situations simulated with different amounts and parameters of BESS controls. Also other two additional situations were simulated with 6 and 10 synchronous compensator added. Every set of simulations is repeated for 3 inertia levels in the grid. The grid contingency is simulated and the relevant results are evaluated. A graph comparing the value of f_{nadir} for the 3

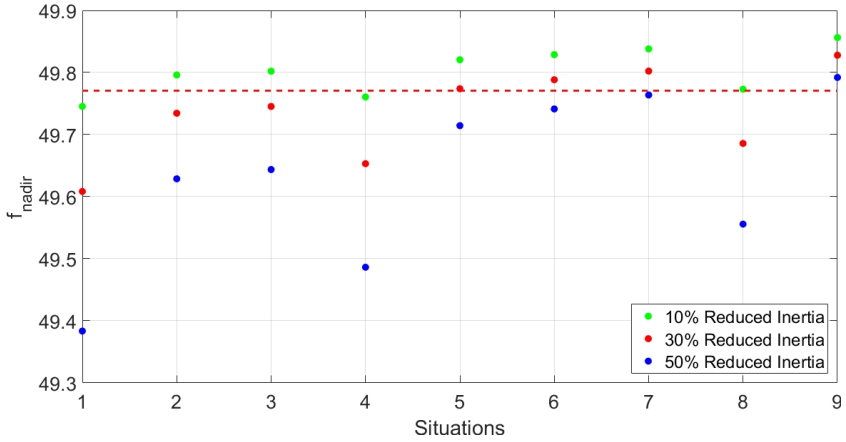

Figure 4.10: BESS impact on f_{nadir}

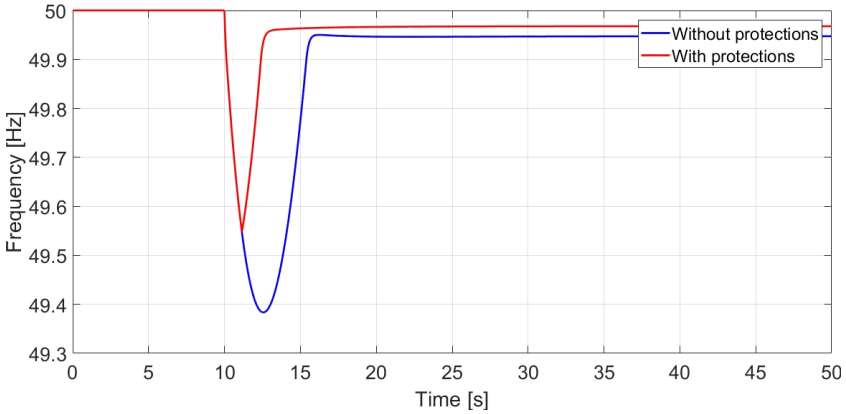

Figure 4.11: Frequency stability due to shedding of wind or load reosurces

Table 4.3: BESSs simulated scenarios

n	MW	T_B	$RC^{\text{BESS}}_{\text{band}}$
1	0	0	
2	50	0.3	0.5
3	50	0.1	0.5
4	50	0.3	1
5	50	0.3	0
6	100	0.3	0.5
7	100	0.1	0.5
8	100	0.3	1
9	100	0.3	0

Table 4.4: Results of under-frequency scenario with 50% reduced scenario

n	$f_{\text{nadir}}[Hz]$	RoCof [Hz/s]	$T_{\text{nadir}}[s]$	$T_{\text{reg}}[s]$	f_{reg}
No BESS addition					
1	49.383	1.066	2.57	5.78	49.947
Addition of Synchronous Compensator					
6	49.52	0.787	2.57	5.78	49.947
10	49.60	0.623	2.72	6.11	49.947
Addition of BESS					
2	49.63	0.946	1.85	9.07	49.949
3	49.64	0.946	1.85	9.02	49.949
4	49.49	0.850	2.63	5.90	49.947
5	49.71	1.066	1.11	9.80	49.950
6	49.74	0.850	1.23	9.73	49.950
7	49.76	0.850	1.26	9.66	49.950
8	49.56	0.707	2.68	6.02	49.947
9	49.79	1.066	0.72	9.97	49.952

inertia levels scenarios is shown in For brevity, the table 4.4 present the results in the case of 50 % reduction of inertia. This is the most dangerous case and the rocof value is dangerously over the 1 Hz/s threshold. 50% is also the only scenarios when load or wind shedding is triggered by the severe frequency dynamics (see figure 4.11. When BESS or Synchronous Compensator are added, shedding is disactivated to properly quantify the BESS impact and be comparable with other

scenarios. Synchronous compensator and BESS rocof control avoid to overcome 1 Hz/s while pfc is able to improve the f_{nadir} and t_{nadir} more than rocof. However too much fast t_{nadir} can also be dangerous for SG equilibrium and therefore it is better to keep 50 % rocof and 50 % droop control. A negligible difference is observed when passing from a T_b pole constant of 0.3 to 0.1 seconds. In the case of 50 % inertia reduction it seems clear how at least 50 MW are necessary for Sardinia to overcome a contingency. Also another contingency is considered, i.e. the failure of SAPEI HVDC line. The line is exporting at the time of interest and therefore causes a an over-frequency event. Similar results to the underfrequency-event are reported. For whole set of tables, refer to [119]. Also in simulation

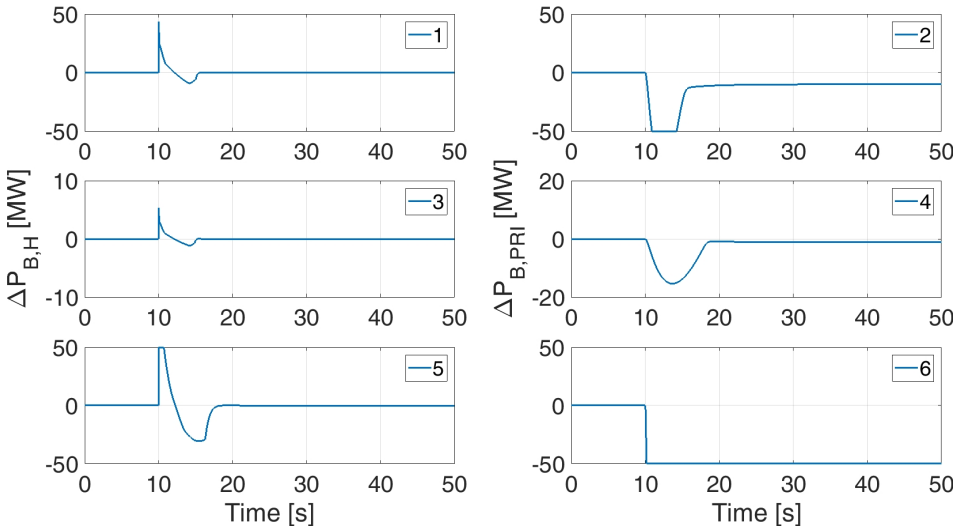

Figure 4.12: Comparisons of the inertial and primary BESS delivered with different control parameters

ESL comparison

ESL is one of the logic that can be used for dimensioning BESS reserves. For example in [4] H_{BESS} varies in the range 0.01 to 500. To show the effects of different weights a sereis of simulations were performed with the ten times lower or bigger values for K_{BESS} and H_{BESS}. The overfrequency simulation with BESS situation number 6 was used for this parametric analysis on BESS intervention. Figure 4.12 reports the inertial and primary shares of the BESS delivered power in the ESL case (1, 2), lower (3, 4) and higher (5, 6) values cases. With lower values, the BESS support is not exploited enough, whereas with higher values the saturation of the BESS is reached with possible concerns for the BESS stress. It is evident that the ESL shows the best compromise in terms of BESS saturation and performance.

Chapter 5

Impact of BESSs in normal grid conditions: a System frequency response model approach

In section 5.1 I present the two parts of the model (FORWARD AND REVERSE) used to reproduce whole days of frequency oscillation. The procedure of frequency reproduction is explained and few notes on a possible new BESSs model to be used in future simulations is presented. The model will be used to asses the potential of PFC and RoCof control by BESS during normal operations of the grid. In section 5.2 the case study based on the Irish grid is introduced, simulated an discussed. An alternative frequency domain approach to evaluate BESS impact is also described. Finally in section 5.3 the irish frequency signal is described in its peculiarities and the initial approach to study its main characteristics is introduced.

5.1 The model construction

The model presented in the previous chapter in section 4.2 was expanded in order to be used for normal operations analysis. The model was developed in the Simulink software. First of all the ΔP_m produced by regulating resources in the grid was augmented considering the three frequency services which are current used in ENTSO-E continental system:

- Frequency Containment Reserve (FCR also called PFC) which represent a proportional power control based on the frequency error Δf which is able to contain the frequency deviation;
- Frequency Restoration Reserve (FRR) (also called Secondary frequency control (SFC)) based on an integral controller on the frequency error, which

aims to restore the frequency signal as introduced in 4.1 ;

- Replacement Reserve (RR) (called also Tertiary Reserve) manually activated by the TSOs in case FRR Band is saturated, and aiming to restore the FRR.

During normal operations, the term ΔP_e represents the global change in active power consumed due to the short and medium term variability of the load and the variation in non-dispatchable renewable sources due to the stochastic behaviour of primary sources (like wind velocity and sun radiation) with respect to dispatchable generation. These changes could be more or less fast and cause the frequency continuous perturbation. Moreover, ΔP_e could also consider the eventual mismatch between load and generation due to an incident (for example the trip of a generator producing 500 $[MW]$ will cause a $\Delta P_e = +500$).

In literature, deterministic frequency oscillations are introduced to explain frequency unbalance at the changing hour due to the market scheme (such as Energy or balancing markets) as explained in literature review chapter. This phenomenon is caused by the mismatch between Net load and the dispatchable generators which ramps to reach new set points. For convenience in our study this component is also associated in the ΔP_e component . Finally we will also consider the frequency dependency of the load with a certain Load Damping coefficients. To sum up we can write all the terms forming ΔP_m and ΔP_e, in particular we have:

$$\Delta P_m = \Delta P_{PFC} + \Delta P_{SFC} + \Delta P_{TFC} \tag{5.1}$$
$$\Delta P_e = \Delta P_{mis} + \Delta P_{Load}(f) + \Delta P_{contingency} \tag{5.2}$$
$$\Delta P_{mis} = \Delta P_{Load} - \Delta P_{CG} - \Delta P_{Rene} \tag{5.3}$$

5.1.1 the FORWARD model

The forward model implements all the components described in equations (5.1)(5.2)(5.3) and it is represented in figure 5.1. The model is composed by:

- A unique equivalent power plant for every typology (Hydro,Steam etc. ...) in the grid is modelled which is used to represent the sum of all the plants of that typology. Specific flags let the user decide what frequency services should be performed by each plant and decide how much of the power band is used for that service as a percentage of the P_{max}.

- ΔP_{FCR} is computed by using a customizable and time changing regulating energy and a dead-band for every plant typology, by simulating the dynamics of the plant with a simple but effective zero-pole dynamics. Even HVDC

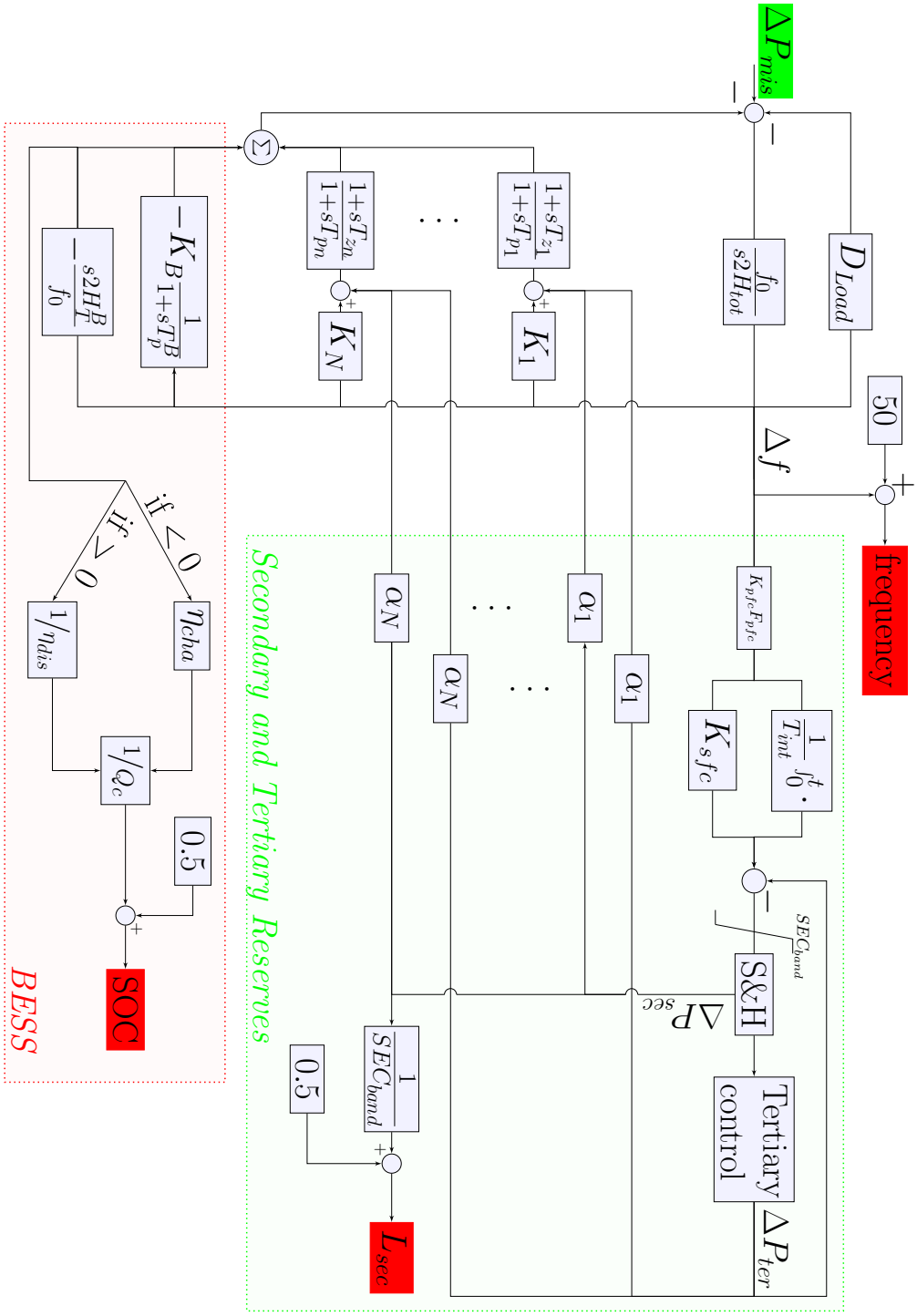

Figure 5.1: The FORWARD model

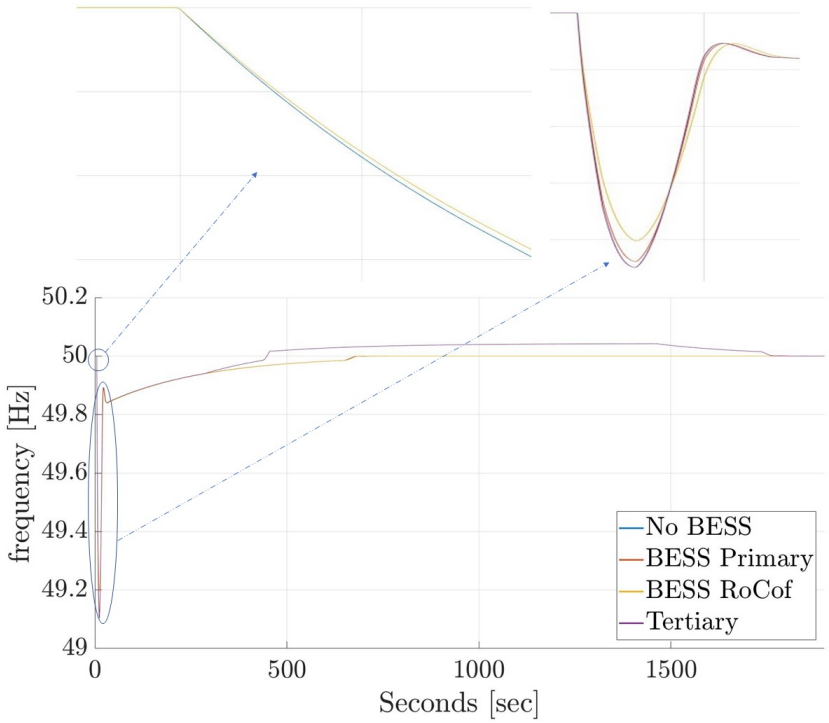

Figure 5.2: Simulation of a contingency at time=5sec in the FORWARD model.

lines which connect two asynchronous AC grids could be considered to provide PFC. The PFC service is performed up to some saturation point of the respective plant topology production which can change during the day dependign on $P_{\max}$.

- ΔP_{SFR} is computed by taking the integral frequency error and by considering a certain secondary band. The equivalent power plants will participate in providing this band proportionally to their respective percentage of production through the use of coefficients α. the sum of all α coefficients is 1. Generally each plant can have its own α value depending on TSO's dispatching orders and rules. $S\&H$ represent the Sample and Hold function which models the typical process of TSO computing the secondary level and sending a new value every two to four seconds. The secondary level is computed as:

$$L_{sec} = L_{INI} - \frac{{}^{1}/_{T_{SEC}} \cdot \int_0^t \Delta f dt}{2 \cdot Band_{SEC}}, \qquad [pu(MW)] \tag{5.4}$$

where L_{INI} in the Secondary initial level (usually 0.5), T_{SEC} is the integral

constant (usually between 90 and 200), $Band_{SEC}$ is the power Band of the power system dedicated to secondary control.

- Finally Tertiary frequency control is used to de-saturate the Secondary reserves. In real power systems, Tertiary reserves are manually dispatched optimizing their costs; however in this model tertiary reserves are not the focus of the work and they can be automatically activated when needed to free Secondary Automatic Reserves without considering costs constraints. The amount of tertiary used will reflect real needs, but the dynamics of its activation can change depending on real TSO implementation and market design. The desaturation can happen in two ways:

  - the first one is done by producing a ΔP_{TFC} opposite in sign to the one coming from the secondary controller. This power level will last for a certain extended period of time (30 min or 1 hour) and will unbalance the frequency signal in order to re unbalance the L_{sec}. In practice, this is what happens when Tertiary reserves are directly activated without coordination with Secondary Reserves. The frequency signal results unbalanced and forcibly free Secondary reserves. Tertiary reserves are activated when the $|L_{sec} - L_{sec}^{rif}| > L_{threshold}$ and create a linear power increase which last for a certain time t or until $L_{sec} \approx 0.5$. The final power reached depends on the SEC_{band} value to be desaturated.
  - Another way is to directly act on the ΔP_{sec} signal by decreasing it due to the activation of tertiary reserves (ΔP_{ter}) which is caused by the ramp of some CG power plants (that could belong to all typologies). This is the type of action that happens when there is perfect coordination between secondary and tertiary reserves, so that ΔP_{sec} decrease/increase at the exact same time when ΔP_{ter} changes value and frequency signal is "virtually" not affected (perfect coordination is impossible in reality!). In the figure 5.1,however, the second is the solution that is implemented because it works flawlessly with the REVERSE model (see next section). For the objective to have a sense of how much and when tertiary reserve is needed, this hypothesis seems reasonable.

- A new resource (that could be considered as a simple model of a BESS) performing new grid services such as PFC considering very fast dynamics due to internal chemical processes activation and RoCof control which can act almost immediatelyy thanks to the power electronic interface. Energy constraints are considered using simple efficiency coefficients when charging or discharging. An automatic recharging of the BESS could be considered in

case SOC is too low. The real charge profile will actually depend on market prices and regulations.

The "Forward" model simulations will have as input the ΔP_{mis}(see equation (5.3)) and will compute the resulting frequency error considering the frequency reserves and the system parameters. As an example in Figure 5.2 an unexpected loss of generation is simulated in the FORWARD model and the resulting frequency signal and reserve activations are plotted (the contingency is simulated as a step input of value $500MW$ and the grid parameters refers to a specific day of the Irish dataset presented at the end of this chapter). At first instants, frequency decreases, slowed down by the inertia of the grid. In a brief period of time (under 50 seconds) FCR manages to stabilize the grid. after SFC brings back the frequency up to 50 Hz, but it soon saturates (reaching a level close to 1) and the RR is automatically called. This service activates a certain ΔP_{ter} for 30 minutes or less until L_SEC returns around 0.5 and it substitute exactly the secondary power band used. Note how BESS performing FPC are able to increase the frequency nadir, while on the other hand BESS performing rocof control are able to decrease initial RoCof of frequency of the system. Finally note the different approach for Tertiary Reserves. the first three simulations implements the second method where Tertiary intervention does not unbalance the grid, while the last line shows the use of the first method where the ΔP_{ter} unbalance the grid to lower the Secondary level. The frequency rose over 50 Hz for some time and secondary level is able to decrease returning around 0.5. The fast dynamics around f_n are due to the presence of the dead band of primary controllers.

5.1.2 the REVERSE model

REVERSE model rationale and scheme

So far, we used the FORWARD model starting from a $\Delta P_{mis}$and obtaining a certain δf. The contrary is also possible, and it is what the REVERSE model accomplishes. Rewriting equation (5.1) using equation (5.2) and (5.3) and the definition of ΔP_{mis}we get:

$$\Delta P_{mis} = \Delta P_m(f) + \Delta P_{LOAD}(f) - \frac{2H}{f_n} \cdot \frac{df}{dt}) \tag{5.5}$$

where $\Delta P_m(f)$ is the sum of the three frequency services. All the terms on the right depend on the frequency signal and its derivative. Therefore by knowing the frequency and its derivate we can compute ΔP_{mis}, which represent the power mismatch that will cause the corresponding frequency oscillation.

If we have real frequency samples of the grid, and we evaluate the derivative, we could use the REVERSE model to compute the $\Delta P_{mis}$and then apply it to

the FORWARD model to get the same frequency signal. At this point we could change the frequency reserves parameters (for example reserves quantities, time constants, inertia etc.) and see its effects on the grid frequency signal and other variables.

Theoretically, there is no strict requirement that grid parameters and real frequency measurements refer to the same grid. Even using "invented" data will play the trick being the two models mathematical abstract representation of the grid balance. However The more consistency we have between data sources, the more the resulting ΔP_{mis}, L_{SEC} and the other state variables of the system will be realistic. It is important to note that the models parameters could change during the simulation (like production mix, reserves bands and characteristics etc.) as customized by the user.

5.1.3 Methodology Validation

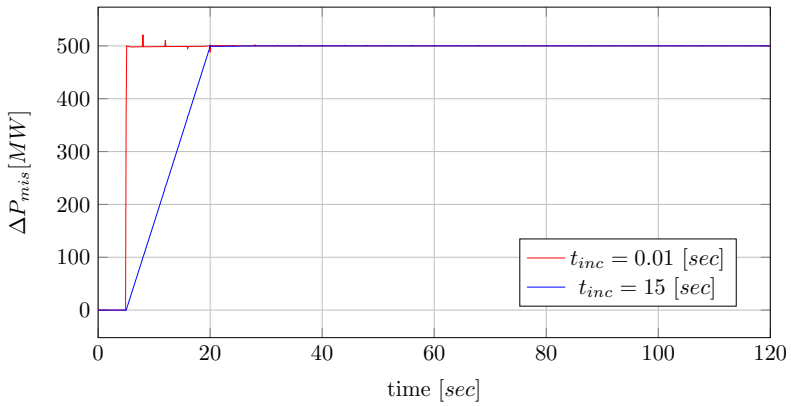

Figure 5.3: ΔP_{mis}signal evaluation by the REVERSE model using the same grid parameters of the FORWARD case

Step Incident: to validate the model we use the same contingency used in the previous paragraph. In this case we take the resulting frequency signal coming from the "NO BESS" simulation and we try to recover the ΔP_{mis}which caused the unbalance (a step input with a value of $500MW$). First we compute the numeric derivative of the frequency signal and then we input these two signal in our REVERSE model. The resulting ΔP_{mis}signal is show in figure 5.3 The $500MW$ step input is recovered, except for small "imperfections" just after the step due to the difficulty for the Simulink solver to maintain perfect numerical stability using a signal with such a steep rise of its value (remember that the derivative of the

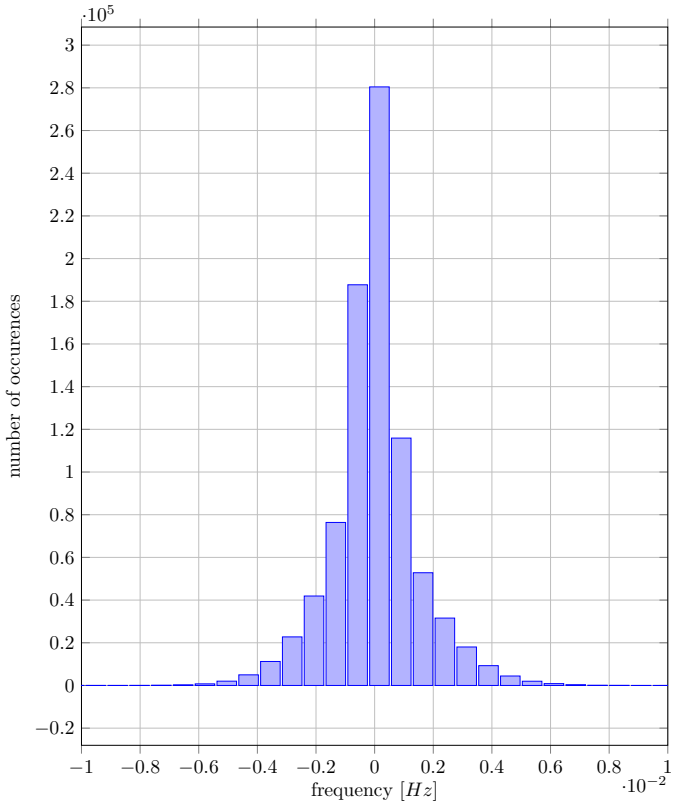

Figure 5.4: The histogram representing the distribution of the error between simulated and real frequency for a day of simulation

frequency signal was computed with a finite step and a simple Euler formula). To prove this, we tried to reconstruct an Incident with a slower time duration (15 seconds) and the REVERSE model is able to reconstruct the values without the small errors of the first case. Anyway the differences are negligible and the step incident is well reconstructed in both case.

Whole day: Using the same methodology we have reproduced one real day of frequency using the same day of Irish data used for the simulations. Using the REVERSE model and then the FORWARD model we can always reproduce the frequency signal with an error always less than 0.01 $[Hz]$ for every point of the time series length. (see Figure 5.4 where the error is computed as $\Delta f_{sim}(t) - \Delta f_{real}(t)$, where $\Delta f_{real} = f_{real}(t) - f_n$ and $\Delta f_{sim} = f_{sim}(t) - f_n$. The signal in total is composed by 864000 samples). All the errors are well under 0.01 Hz (the value of the governor typical dead-band) and therefore they are negligible with respect to the frequency signal itself. The error are still related to the numerical methods

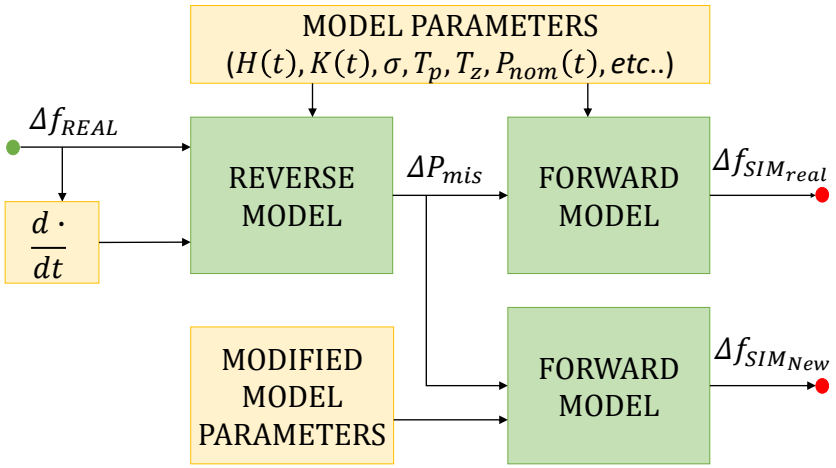

Figure 5.5: Time domain approach scheme

the solver use to integrate differential equations.

We can now modify the FORWARD model parameters and repeat simulations to see the effect on the frequency signal. For example, we could reduce the value of inertia or increase the regulating energy by adding BESS or other new resources of the grid (see figure 5.5 with a summary scheme) Reproducing the real frequency signal is fundamental for having realistic results because in today power systems, frequency oscillations are caused by stochastic phenomena (like wind and load fluctuations) and deterministic ones (due to the hourly energy market). Impact of changes (like adding BESSs) will strictly depend on the type of frequency signal which characterize the grid: fast changes or slow changes makes a great difference. Our reproduced signal retains those properties and therefore the impact of new resources will be realistic.

5.1.4 BESS model further insights

As for now we have used a simple BESS model based on power, energy and efficiency BESS model characterization. As we have seen in the literature review chapter, this simple model is actually enough if our objective is principally to evaluate grid improvements. Instead in case we need a better appreciation of battery degradation or market strategies can be interesting to adopt an equivalent electrical model. Running such a model (as described in [82] in chapter 3) is much computationally heavy. A possibility to maintain low computational power requirements and simulate closed loop analysis with a detailed BESS model is to use a SFRM model for the grid and make use of san electrical equivalent description

for the BESS cell based on the characterization of the open circuit voltage V_{OC} and an at least a resistance-capacitance group. To connect this circuit to grid, first is necessary to multiply the electrical quantities for the number of cell in parallel or in series (under the hypothesis that the cell racks equally share the produced or stored power). Secondly the converter which connects the battery to the grid can be modelled simply as in figure XXXX: A pole dynamics which represents the small delays due to Converter control connected to a dc link capacitance. In the place of a typical voltage-current converter control, a simple model can be used which produce a power balance over the dc link capacitance. Voltage and current information are not utilizable in the case of SFRM. With this approach we can compute detailed cycle and SoC behaviour for the BESS better taking into consideration the non linearities of the BESS models.

5.2 Irish case study

The model presented in the previous section was used to study the impact of pfc and rocof control by BESSs in the Irish power system. Secondary and tertiary reserves are not implemented as they are not present in the Irish grid as automatic frequency services. Irish power system and frequency data used for the REVERSE models are presented in subsection 5.2.2. Beyond a time domain analysis, A preliminary study on normal grid dynamic conditions and ESS impact considering a linear SFRM. The study is performed in the frequency domain by computing the bode plots of the system and the power spectrum of the real power variations. This study help us explaining why and how primary and RoCoF control impact the frequency stability and is presented in subsection 5.2.1. Time domain analysis are presented in subsection 5.2.3. Finally results are showed in 5.2.4

5.2.1 Frequency Domain Approach

It is possible to obtain additional information on our problem by using classical frequency analysis tools such as the Bode magnitude plots or the Parseval theorem. In order to do this a linearized version of the Irish SFRM system is studied without deadbands or saturation and considering time invariant parameters. While quantitative results will be obtained with the time domain approach, this study help us understand better the role and impact of new frequency services. The logic scheme of the approach is presented in Fig. 5.6. In general in a linear time invariant FORWARD model with a certain transfer function $TF(\omega)$, input ΔP_{mis} and output Δf, we can write $|\Delta f(\omega)| = |\Delta P_{\text{mis}}(\omega)| \cdot |TF(\omega)|$. By using this correlation and making use of the Parceval theorem, the $\Delta f(t)$ can be written by using its power spectrum values in the frequency domain:

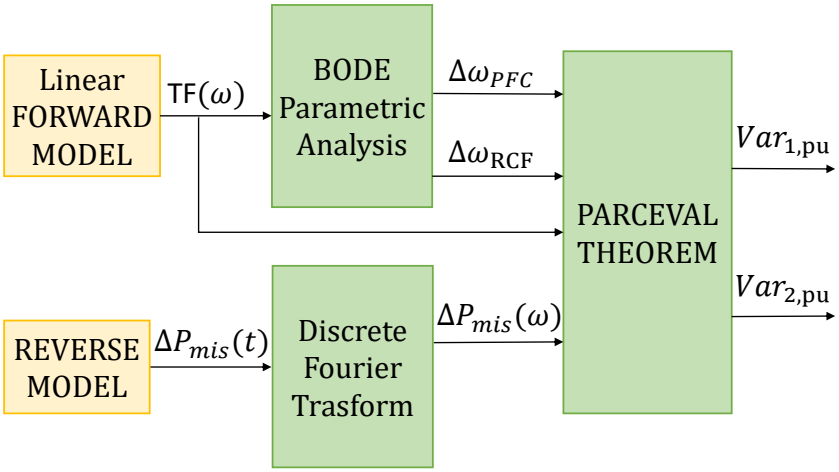

Figure 5.6: Frequency domain approach scheme

$$Var(\Delta f(t)) = 2 \cdot \sum_{i=1}^{N/2} |\Delta P_{\text{mis}}(\omega)|^2 \cdot |TF(\omega)|^2 \ , \tag{5.6}$$

where Var is the variance of the signal and N is the number of the harmonics of the signal. Normalizing Equ. 5.6 and dividing the sum at certain specific harmonic, say N_x, we can write:

$$\begin{aligned} 1 &= Var_{1,\text{pu}} + Var_{2,\text{pu}} \text{ with} \\ Var_{1,\text{pu}} &= \frac{2 \cdot \sum_{i=1}^{N_x} |\Delta P_{\text{mis}}(\omega)|^2 \cdot |TF(\omega)|^2}{Var(\Delta f(t))} \ , \\ Var_{2,\text{pu}} &= \frac{2 \cdot \sum_{N_x}^{N/2-N_x} |\Delta P_{\text{mis}}(\omega)|^2 \cdot |TF(\omega)|^2}{Var(\Delta f(t))} \ . \end{aligned} \tag{5.7}$$

It is possible to set a specific N_x by a qualitative study of the Bode plots of our FORWARD model. In particular by changing the FORWARD model parameters into realistic ranges it is possible to study what harmonics are more influenced by RoCoF control and by PFC values. The two harmonic ranges thus identified $\Delta\omega_{\text{PRI}}$ and $\Delta\omega_{\text{rocof}}$ are used to set a specific N_x and compute $Var_{1,\text{pu}}$ and $Var_{2,\text{pu}}$. These two terms are computed for every day of real frequency measurements at our disposal and they gives us a qualitatively weight on the importance of RoCoF control and PFC on the frequency signal.

5.2.2 Irish data and power system parameters

The case study is based on about 300 days of frequency signal measurements made in University College of Dublin in the year from 2015 to 2016 with a sampling of 10 Hz. In order to compute the grid time varying parameters the data about the consumption and generation of the Irish grid for those days were provided by the Irish TSO Eirgrid divided between wind production and CG generation P_{CG}. The time variant inertia H is computed using Equ. 5.8:

$$H = \frac{\sum_i H_i \cdot S_i}{\sum_i S_i} \ , \tag{5.8}$$

In this formula, a typical mean inertia value H_{CG} for every generator inertia H_i and a certain instantaneous capacity factor $c_f = \frac{\sum_i S_i}{P_{\mathrm{CG}}} = \frac{S_{\mathrm{CG}}}{P_{\mathrm{CG}}}$ in order to compute the nominal power present in the system during the day. K_{CG} is computed as $K_{\mathrm{CG}} = K_{\mathrm{CG,pu}} \cdot \frac{S_{\mathrm{CG}}}{f_{\mathrm{nom}}}$. c_f and other important parameters (H_i, time pole dynamics, etc.) are chosen considering typical values and the Irish grid code (note that Irish grid has almost no hydro resources so that the PFC CG dynamics shown in figure 5.1 is consistent with a Steam Generator. In this way the reconstructed inertia levels and regulating energies present realistic changes during the day considering the real operating conditions of the grid. The constant parameters used in the time domain simulations are shown in Tab. 5.1. Some parameters were kept constant (see Tab. 5.1) to represent a meaningful average system representation. A parametric analysis was performed in order to study the $TF(\omega)$ of the system. The changing values are shown in Tab. 5.2 where the values are obtained by multiplying the base value (bv) for the corresponding ranges. In compliance with our frequency data sampling ω goes from $10^{-}5$ to 10. In general the delay of the ESS be represented by summing a pure delay part (approximated by a Padè polynomial) and a ramp part (approximated by fast pole) depending on the actual system. The parameters changed are related to BESS or to frequency control by CGs.

Table 5.1: Constant parameters for time domain simulations

H_{ESS} [MWs]	c_f $[pu(MW)]$	$K_{\mathrm{CG,pu}}$	D [%]	τ [s]	T_p [s]	T_g [s]	T_c [s]	$PFC^{\mathrm{CG}}_{\mathrm{band}}$ $[pu(MW)]$	T_{ESS} [s]
6	0.7 [1]	20	1	3	10	0.225	0.35	0.10	0.1

[1] This number was chosen by considering typical values of generators in todays grid in absence of very precise data. In particular using [17] it is possible to reconstruct 15 real capacity factors

Table 5.2: Parameters for frequency domain analysis

Parameter	bv	Range	Parameter	bv	range
Inertia $[pu(MWs)]$	6	$0.1 \div 2$	τ $[s]$	2	$0 \div 2$
K_{ESS}	250	$0 \div 4$	T_p $[s]$	8	$0.5 \div 1.5$
δ_{ESS} $[s]$	0	$0 \div 0.1$	τ_{ESS}[s]	0	$0 \div 0.1$
$\delta_{\text{ESS}}^{PFC}$ $[s]$	0	$0 \div 0.25$	τ_{ESS}^{PFC}[s]	0	$0 \div 0.25$

Table 5.3: ESS parameters simulations

	1	2	3	4	5	6	7
σ_i $[Hz]$	0.0290	0.0372	0.0455				
μ_i $[Hz]$							
$c_{\text{f,CG}}$ $[pu(MW)]$	0.25	0.50	0.75				
$c_{\text{f,ESS}}$ $[pu(MW)]$	0	0.35	0.7	1	1.35	1.7	2
$S_{\text{ESS}}^{\text{PFC}}$ $[pu(MW)]$	0	0.25	0.50	0.75	1	$1^{\star}$	

5.2.3 Scenarios and case study indexes

For time domain simulations BESS are added into the system by considering several scenarios and quantities. ESL used in the previous chapter is used here to dimension PFC (parameter K_B) and RoCof control (parameter H_T^B). saturation to both control channels are applied. CG presence is decreased in future scenarios and ΔP_{mis} is kept fixed. The three elements composing ΔP_{mis} (see Equ. 5.3) depends on several factors such as renewable and load growth, market structure, auto-consumption of renewable energy, power variability smoothing due to increased installed capacity and new grid requirements, interconnections etc.. Moreover it is not easy to model and parameterize the single components as they represent the global mismatch caused by the power perturbations of hundreds of elements in the grid. In order to avoid unnecessary complications, the ΔP_{mis} time series was left equal while instead CG capacity was decreased, consequently reducing the inertia and regulating energy present in the grid which represents the most important factor influencing the frequency signal. To create comparable scenarios, as ESS capacity is introduced into the grid, CG capacity is decreased by a constant amount along the day, which is computed as a percentage of the mean CG present in that day. ESS installed into the grid is computed as:

of the UK grid. The average is 0.69, a little lower during the night and higher during the day

$$P_{\mathrm{ESS,i}} = c_{\mathrm{f,ESS}} \cdot (1 - c_{\mathrm{f,CG}}) \cdot \mathbb{E}[P^{CG}_{\mathrm{nom}}(t)_i] \cdot PFC^{\mathrm{CG}}_{\mathrm{band}} \tag{5.9}$$

where i represent a generic day and $c_{\mathrm{f,CG}}$ defines the percentage of CG to be reduced. The mean CG production $\mathbb{E}[P^{CG}_{\mathrm{nom}}(t)_i]$ is multiplied by the PFC band. In such a way ESS added capacity results proportionally to the the lost amount of regulating energy in the grid due to shutting of CG capacity. Three days are simulated representing low, medium and high standard deviation (σ_i) scenarios. For what concern ESS regulation strategy we will try out different complementary PFC and RoCoF control bands such that $S^{\mathrm{PFC}}_{\mathrm{ESS}} + S^{\mathrm{RoCoF}}_{\mathrm{ESS}} = 1$. A last strategy consider both $S^{\mathrm{PFC}}_{\mathrm{ESS}}andS^{\mathrm{RoCoF}}_{\mathrm{ESS}}$equal to 1. We consider 3 days σ_i , 3 CG coefficient capacities $c_{\mathrm{f,CG}}$, 7 BESS coefficients $c_{\mathrm{f,ESS}}$ and 6 different sets of values for the ESS band assigned to PFC and RoCoF control ($S^{\mathrm{PFC}}_{\mathrm{ESS}}$and $S^{\mathrm{RoCoF}}_{\mathrm{ESS}}$), for a total of 378 simulations. All the parameters of the simulations are summarized in Tab. 5.3 ($S^{\mathrm{RoCoF}}_{\mathrm{ESS}}$ is always equal to $1 - S^{\mathrm{PFC}}_{\mathrm{ESS}}$ except in the case when $S^{\mathrm{PFC}}_{\mathrm{ESS}} = 1^{\star}$ which corresponds to $S^{\mathrm{RoCoF}}_{\mathrm{ESS}} = 1$, so that both services are assigned the full band).

Two simple indexes can help us investigate the impact of BESS In the grid. In particular we can define the i index.This index provides a measure of the relative improvement to the dynamics response due to the ESSs. It is defined as:

$$h_{\mathrm{ESS}} = 1 - \frac{\sigma_{\mathrm{ESS}}}{\sigma_o} \ , \tag{5.10}$$

where σ_{ESS} is the standard deviation of the frequency of the system with inclusion of ESSs and σ_o is the standard deviation of the frequency for the same scenario but without BESS.The index can therefore go from 0 (no improvement) to 1 (no frequency deviations). Similarly in the place of σ_o we can use σ_{CG}, the standard deviation of the system considering the original presence of CG. In this way it is possible to quantify the amount of ESS reserve needed to substitute the original CG reserves $S^{PFC}_{\mathrm{CG,o}}$. In a more explicit way, we can compute this quantity in the point where $\sigma_{CG} = \sigma_{ESS}$ and define a new index k:

$$k = 1 - \frac{P_{\mathrm{ESS}}}{P^{PFC}_{\mathrm{CG,o}}} \tag{5.11}$$

this index can be < 0 in case ESSs are less efficient of original reserves and inertia in limiting frequency excursions, and tend to 1 in case of optimal performance.

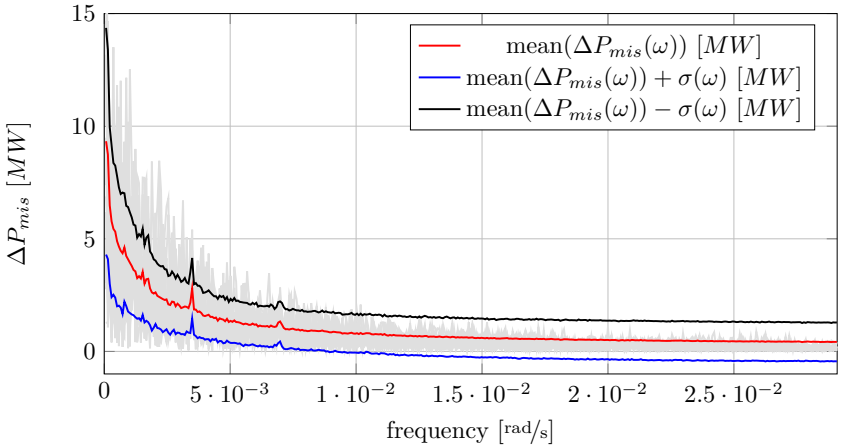

Figure 5.7: ΔP_{mis} Fourier amplitudes.

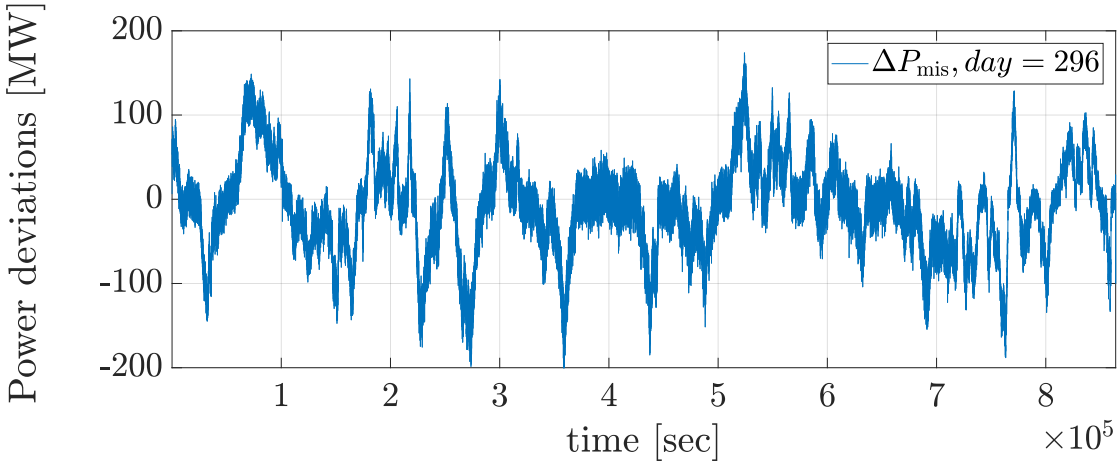

Figure 5.8: ΔP_{mis} profile example for one day

5.2.4 Results

Frequency domain results

In figure 5.10 is shown the magnitude of the system transfer function obtained by changing the values of selected parameters. For brevity only 5 relevant parameters for PFC and 3 for RoCoF control are shown (the delay parameter δ is modelled by using a Padè polynomial approximation of the fifth order) both for BESS and CG resources. The figures suggest that the impact of PFC and RoCoF control can be roughly divided in two areas: while PFC has a great influence on harmonics up to 1 rad/sec , inertia and therefore RoCoF control is limited to fast frequency harmonics starting from 0.5 rad/sec. This is expected as RoCoF control

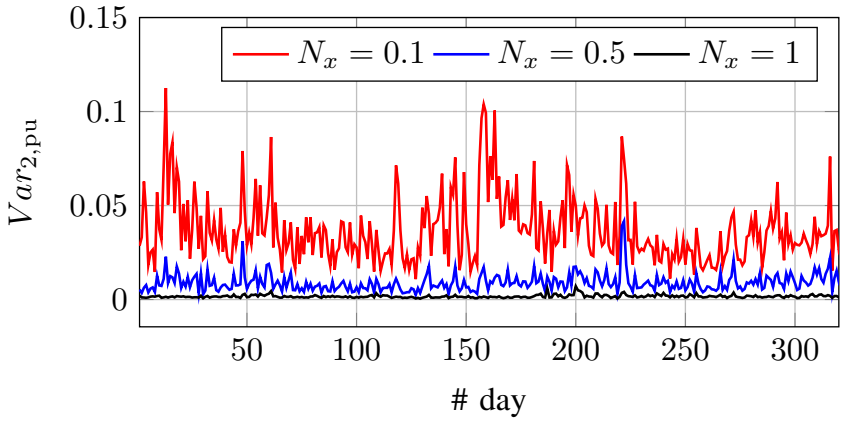

Figure 5.9: $Var_{2,\mathrm{pu}}$ results for all the days considered

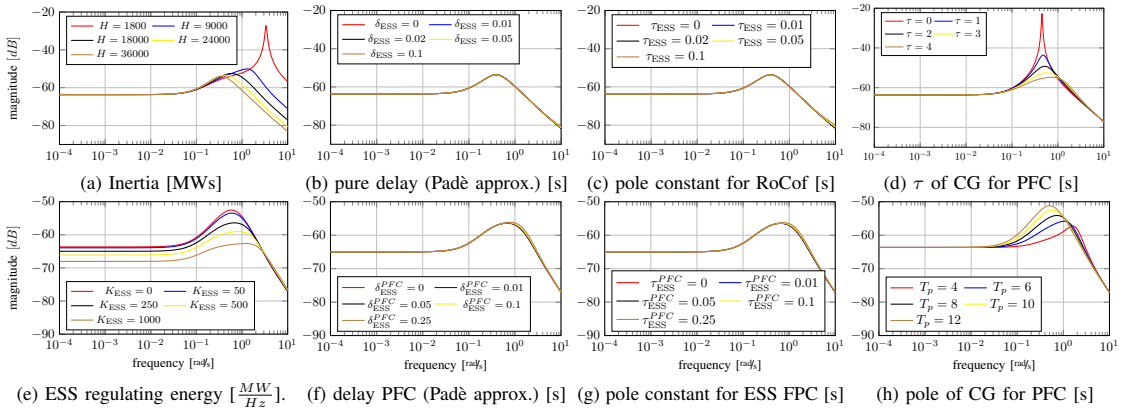

(a) Inertia [MWs] (b) pure delay (Padè approx.) [s] (c) pole constant for RoCof [s] (d) τ of CG for PFC [s]

(e) ESS regulating energy [$\frac{MW}{Hz}$]. (f) delay PFC (Padè approx.) [s] (g) pole constant for ESS FPC [s] (h) pole of CG for PFC [s]

Figure 5.10: Bode magnitude plots of the system transfer function changing various parameters. Parameters description and unit of measurements are located under the singles figures.

mimick physical rotating inertia, which smooth fast torque changes while slightly opposing slow changes. Eventual delays of rocof and primary control can worse the system response but only for big values which are already outside the technology capability. Both poles and delay dynamics were analyzed as in general the answer of a BESS can be modelled with both components. Note that for fast PFC CG control dynamics, we have a lower resonance peak in the transfer function (with τ having more importance than T_p). Finally it is important to highlight that even without BESS and with lower inertia from CG, high frequencies inputs are usually well damped expect for very low values of inertia (less than 10 % with respect to average todays values). From the analysis above we have thus identified three possible values for the N_x corresponding to 0.1,0.5,1 rad/sec frequency harmonics.

ΔP_{mis} times series are computed for more than 300 days considering the approach proposed in the previous section. Every day has a different time profile. In figure 5.8 an example of time profile for one day is obtained, while in Fig. 5.7 the Discrete Fourier Transform is applied to each day and the first 400 harmonics amplitudes are shown. In the frequency domain, the days are quite similar to each other and the first harmonics present much higher values than the last ones. The ΔP_{mis} is therefore a slow signal characterized by large high period harmonics.

Finally by using equation 5.7 we compute the $Var_{1,\text{pu}}$ related to PFC for each day and N_x vonsidered. $Var_{2,\text{pu}}$ is just the complementary of the $Var_{1,\text{pu}}$ value obtained. In figure 5.9 the results are shown. It is clear how frequencies more subject to the intervention of RoCoF control represent on average a very small part of the signal. In the case of $N_x = 0.1 rad/sec$ this is well under 10% and in the case $N_x = 1\ rad/sec$ even lower than 1% . This is for two reasons: ΔP_{mis} is a slow signal and therefore interest slow frequencies which are more influenced by PFC. Moreover the transfer function magnitude plots reveal that the system naturally (even for low inertia values) behaves like a low pass filter such that, high frequencies components are well damped.

From these results we expect that in normal operations fast primary frequency control will have much bigger impact with respect to RoCoF control- This qualitatively analysis will be followed by time domain simulations to validate this thesis.

Time domain results

ESSs clearly help the containing of frequency (see Fig. 5.11 as an example). The results of h_{ESS} for day 3 and $c_{\text{f,CG}} = 0.25$ is shown in Fig. 5.12. The dotted line represents the simulations with both RoCoF and PFC control while the green line represent the case with only RoCoF control by BESS. As it is clearly depicted, the RoCoF control action has very little impact on the frequency signal standard deviation. The index h_{ESS} has the same behaviour also for the others days and $c_{\text{f,CG}}$ values. In Tab. 5.4 the average of h_{ESS} values considering all strategies (excluding the one with only RoCoF control) and capacities installed is shown. simulations with lower $c_{\text{f,CG}}$ values, days with higher standard deviation and when there is a large ESS capacity installed, have on average, higher values of h_{ESS}. This is due to the presence of the deadband in the PFC controllers which make ESSs and CG work less or more when the frequency is more bounded or unstable. The index K was computed for all $c_{\text{f,CG}}$ and days for the best ESS strategy (the one with both full band used by PFC and rocof) in the case when $c_{\text{f,ESS}} = 1$. In these cases the regulating energy offered by BESSs is actually equal to the one lost by decreasing CG as can be verified by using Equations (4.8) (5.9) (5.11) (5.11). Nevertheless the index is near one (on average 0.975) meaning that in normal operations ESSs keeps the frequency bounded similarly to CG.

Table 5.4: index h_{ESS} averaged values

	$c_{\mathrm{f,CG}}$		
Day	0.25	0.50	0.75
1	0.40	0.23	0.10
2	0.46	0.25	0.12
3	0.46	0.27	0.13

The allmost zero value of h_{ESS} due to RoCoF control is due the nature of frequency oscillations in the grid. The oscillations are substantially "very slow" concentrated on 30 minutes or higher period harmonics. Therefore inertia has a low impact on the oscillations and also fast primary control from ESSs is not much more efficient than normal PFC from CG as evinced from the value of index K. For example in Fig 5.14, three frequency profiles profiles of the same day are shown in the condition where regulating energy from ESS is the same of the CG lost. As can be seen the difference between blue (original signal with CG) and orage/yellow is very small. Moreover, the difference between orange and yellow (where we have RoCoF control in addition to PFC) is allmost zero, except for a small difference in the deadzone zone of the primary controller where PFC does not act. The difference is nevertheless small because due to the dimensioning method for rocof control (see Equations (4.10) (5.9)) the inertia added to the grid is less than half of the one lost due to CG shutting off.

The low impact of inertia can also be seen in Fig 5.13 where different level of inertia were simulated by keeping PFC reserves equal to the base case scenario. Only at inertia levels less than 10% with respect to base case scenario the grid frequency starts to be more unstable with respect to the original case except.

5.2.5 Further Insights

From the simulations above, it is clear as inertia and RoCoF control have little value for frequency stability except in very low inertia scenarios On the contrary, Inertia is very important during first moments after a contingency. As a matter of fact, a contingency can be thought as a power step deviation applied to the power system which is decomposed in the frequency domain as a sum of all harmonics fast and slow. Therefore inertia as an important role in opposing

[1]Note that this conclusion refers only to frequency stability. Inertia could also influence rotor-angle and voltage stability [173] so that higher level or particular distribution of inertia are needed in the grid.

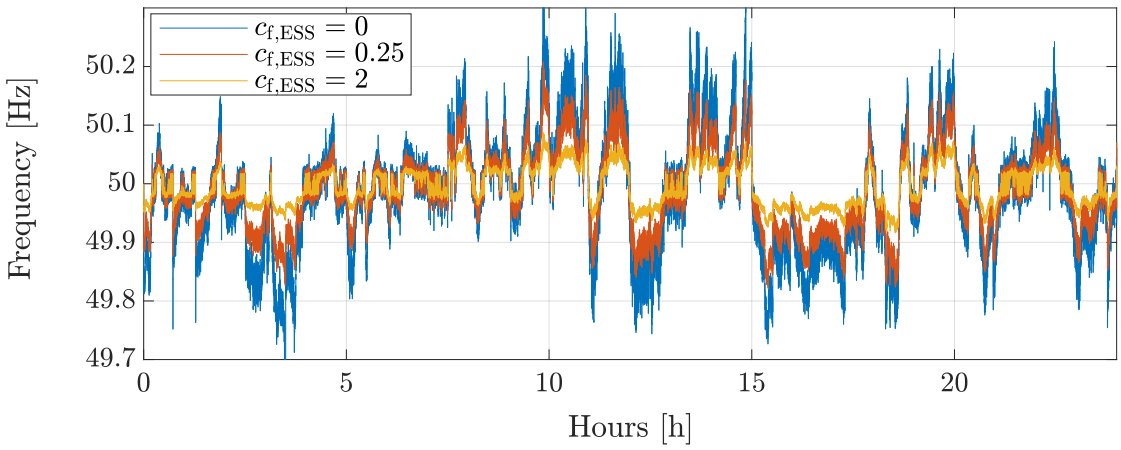

Figure 5.11: Frequency profiles examples for day 3 and

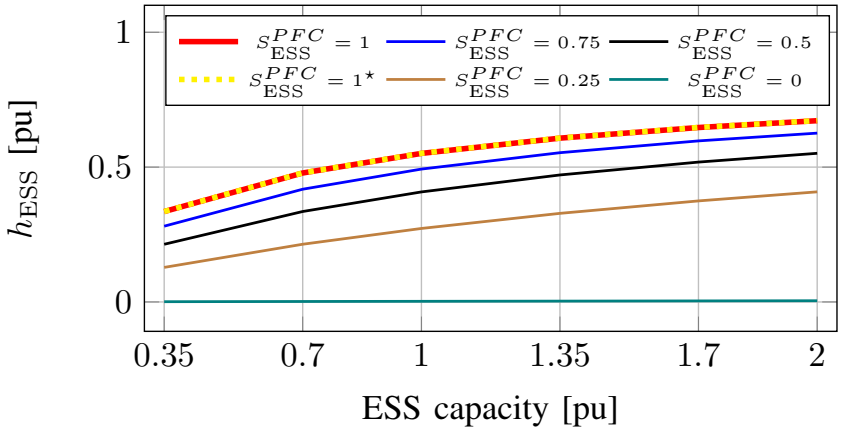

Figure 5.12: index h_{ESS} profiles for day 3 and $c_{f,CG} = 0.25$

the fast harmonic components and avoiding value of RoCof. Therefore knowing that during normal operations the RoCoF control is under-used, and primary is instead very important, we could think of keeping both services at the time with the full band to counteract the event of a contingency. This choice is not straightforward as during a contingency, it is possible to saturate both bands and have a worse control. For this reason, we have performed with the same aggregate model a certain number of simulation to study the frequency behaviour during a contingency.

Contingency Analysis

The goal is to study the behaviour of ESS control during a contingency in order to understand what is the best ESS strategy for the frequency containment. The

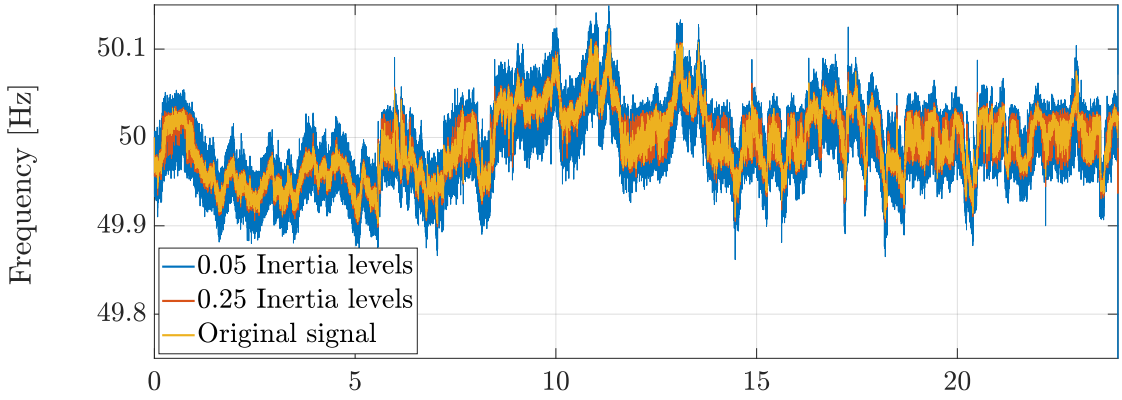

Figure 5.13: Frequency profiles examples fby changing only Inertia in the grid

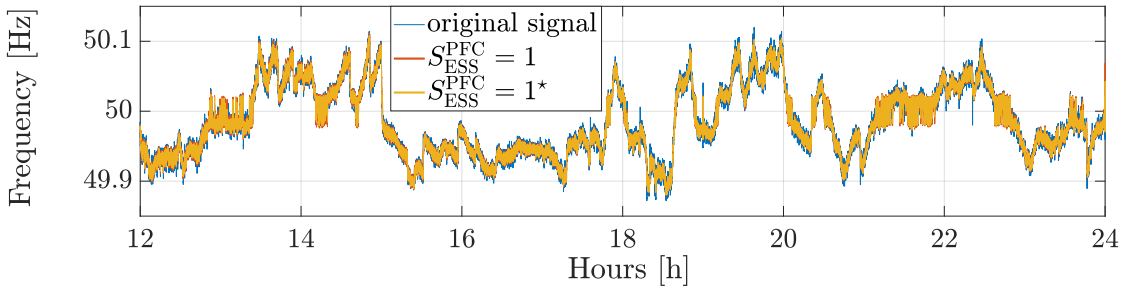

Figure 5.14: Frequency profiles examples for day 3 and $c_{\text{f,CG}} = 0.25$

ESSs band is divided between RoCoF and primary control as before. Moreover in the case of overlapping power bands, the ESS can easily saturate in case of big contingency. Without any aim of completeness, we restrict ourselves to a unique example scenario to show what happens during a contingency. the scenario chosen correspond to day 1,$c_{\text{f,CG}} = 0.25$, $c_{\text{f,ESS}} = 1$ and four different strategies. The first three ESS strategies used have complementary bands with $S_{\text{ESS}}^{\text{PFC}} = [0, 0.5, 1]$ and finally the fourth strategy has both bands equal to 1 (we refer to it using $S_{\text{ESS}}^{\text{PFC}} = 1^{\star}$. A big contingency is applied to the system and the frequency signal and ESS intervention is recorded and analyzed. The results of the frequency signal shows (see Fig 5.15) that the best choice for ESS control is the use at the same time of full RoCoF and PFC band. In Tab 5.5 the main parameters of frequency are shown: $\overline{P_{\text{ESS}}}$ represent the average power provided by the ESS during the simulation. This value is higher in the case with $S_{\text{ESS}}^{\text{PFC}} = 1^{\star}$. Using both full bands makes the ESS provide more power and therefore control in the grid even considering the potential presence of reaching bands saturation. Infact as can be seen in Fig 5.16, the two controls present different time ranges and characteristics during a contingency: on one one hand RoCoF control is needed in first instants after a contingency and it fade very fast to zero value, on the other hand PFC

starts outside the controller deadband after the RoCoF control is decreasing and reach a stable point different from zero. The overlapping between the two services is still present but it is limited even in the non represented case when the ESS output is saturated. Therefore to give full power band to both services is the best choice from the grid point of view.

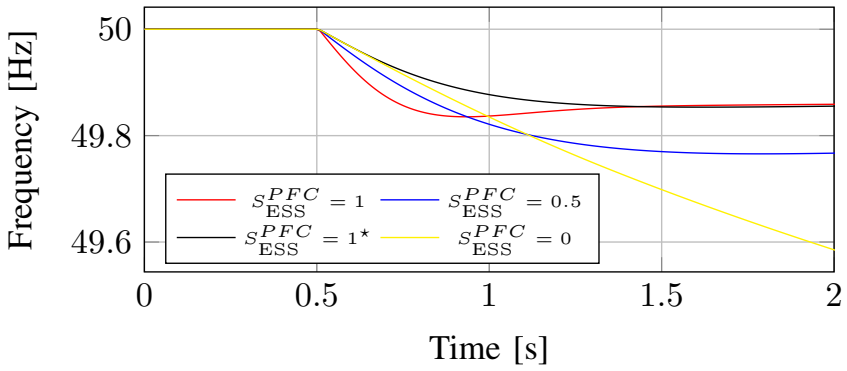

Figure 5.15: Example of frequency profiles after a contingency

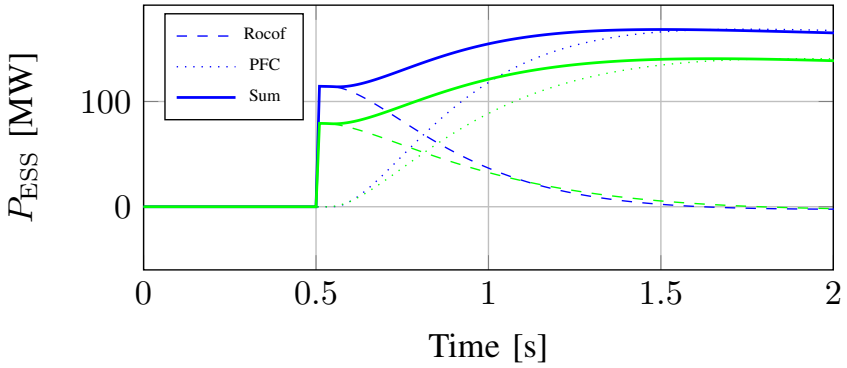

Figure 5.16: Example of ESS requested power profiles in the case with $S^{\text{PFC}}_{\text{ESS}} = 1^{\star}$ (blue) and $S^{\text{PFC}}_{\text{ESS}} = 0.5$ (green)

Note on SOC profiles

In our simulations we have considered BESS as it were a unique plant with a capacity equal to the installed capacity. Therefore we can study the effects that frequency control has on BESSs SOC and the consequent energy requirements a System operators should install or try to incentivize to assure frequency stability. During simulations we recorded SOC dynamics (assuming a certain battery capacity $Q_c = 4 \cdot P_{BESS}$).Note that talking about SoC or Energy is equivalent as they differ for just a constant in this framework.

Table 5.5: Frequency profile parameters results

$S_{\text{ESS}}^{\text{PFC}}$ $[pu(MW)]$	RoCof $[Hz/s]$	f_{nadir} $[Hz]$	f_{reg} $[Hz]$	T_{nadir} $[s]$	T_{reg} $[s]$	$\overline{P_{\text{ESS}}}$
0	0.80	49.83	49.88		32.1	
0.5	0.49	49.76	49.84		35.3	
1	0.35	48.77	49.77		32.9	
$1^{\star}$	0.35	49.85	49.88		57.5	

State of Charge dynamics. Clearly due to internal efficiencies we would expect the equivalent ESS SOC to decrease constantly in time. By looking at the final SOC value or the corresponding equivalent energy value we instead find that in day 1 SOC tends to increase. As seen in 5.3 the first day present an average frequency signal over 50 Hz. This creates a bias effect in the primary frequency controller of the BESSs which, going against internal inefficiencies, makes the SOC increase (in this analysis we momentarily leave RoCof control to zero as it has very little impact on SOC dynamics) . Another factor which we have to take into account is the already stated fact that the frequency is a slow oscillating signal. Therefore as a first hypothesis we could state that the energy losses/gaining of BESS performing frequency control are formed by three terms which depends on various variables:

$$\Delta E_{BESS} = \Delta E_{eta}(\eta_{cha}, \eta_{dis}) + \Delta E_{bias}(\mu_f) + \Delta E_{intraday}(f(t) - \mu_f). \quad (5.12)$$

or by normalizing the Energy with the battery capacity and introducing the ESS initial SOC:

$$\begin{aligned} SOC(t) - SOC_{ini} &= \Delta SOC(t) \\ &= \Delta SOC_{eta}(t) + \Delta SOC_{bias}(t) + \Delta SOC_{intraday}(t). \end{aligned} \quad (5.13)$$

In order to reasonably quantify these three parts we can simulate SOC dynamics with as input the $\eta_{cha} = 1$ and $\eta_{dis} = 1$ so that we could consider $\Delta E_{eta} = 0$ and obtain the $DeltaSOC_{bias}(t) + \Delta SOC_{intraday}(t)$ part. Than by subtracting the simulation with the original one we can quantify the ΔE_{eta} component (following equation 5.13). To separate the ΔSOC_{bias} and $\Delta SOC_{intraday}$ components we can simulate the BESS behaviour with $\eta_{cha} = 1$, $\eta_{dis} = 1$ and as input a new frequency error signal equal to $f_1 = f(t) - \mu_f$. In this way we obtain the $\Delta SOC_{intraday}$ part. By opportunely subtracting the previous component obtain we can finally compute the ΔSOC_{bias}. Due to the presence of dead bands and saturation on the BESS control, this methodology is very precise, but not exact.

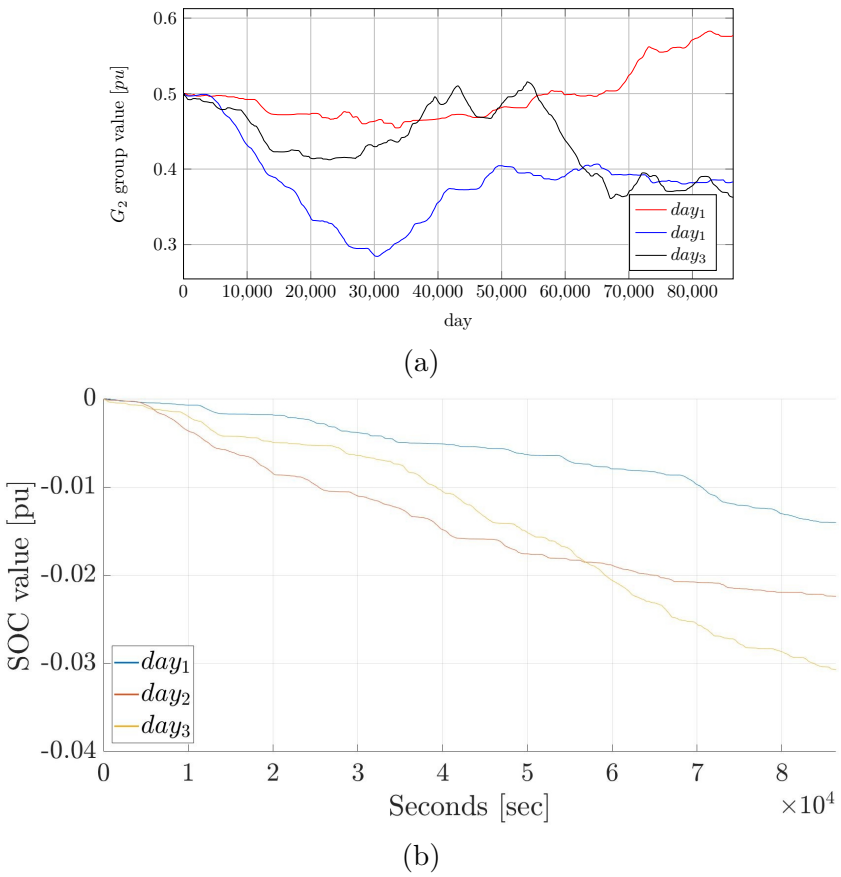

Figure 5.17: ΔSOC time profiles. (5.17a) represents the real SOC profile. (5.17b) represents the efficiency part.

Since these effects appear with primary control we just repeat the normal day simulations with $cf^{df}_{BESS} = 0$,$cf^{fpc}_{BESS} = 1$. Moreover we chose just one simulation per day, the ones corresponding to $cf_{CG} = 0.25$ and $cf_{BESS} = 1$ for an initial assessment of the SoC dynamics.

So for example in figure 5.18 we see the SOC time profiles of the three days decomposed in the different components. As expected, the efficiency components (figure 5.17a) decrease monotonically in time, while the bias factor is substantially linear (depending on the constant offset μ_f). Finally the intra day component stores all the different dynamics due to the oscillating cyclical nature of frequency while at the same time returning at the initial point. Note that, while the reconstruction made using equation 5.13 give very good results, the fact that intraday components does not return exactly to zero, or that the bias factor is not exactly linear, means that small deadband non linear effect are presents 5.13. It is clear just by visual inspection that the efficiency component, while is not negligible,

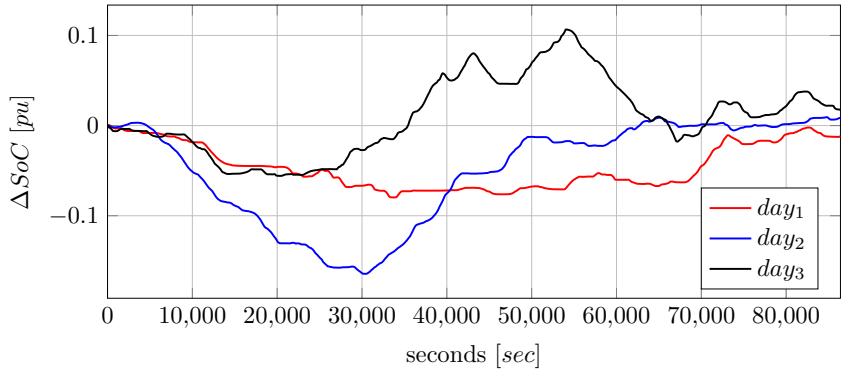

(a)

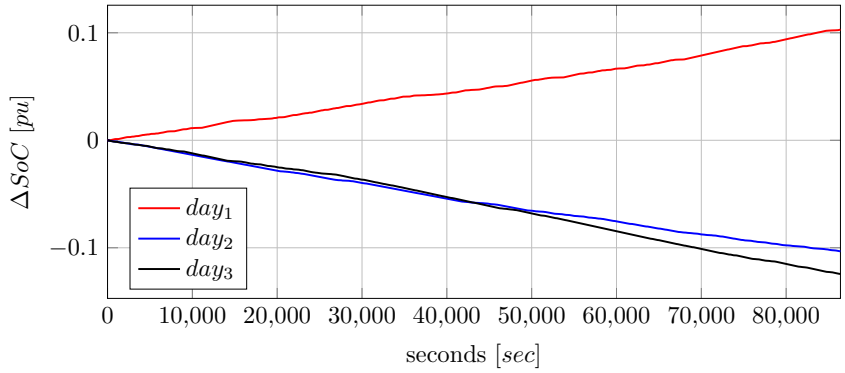

(b)

Figure 5.18: ΔSOC time profiles. figure (5.18a) represents the intra-day part. Finally, (5.18b) represents the bias component

poses less danger for BESS with respect to intra-day and bias components. Moreover as expected the efficiency part seems connected to the standard deviation of the signal. the more the BESS works, the more the internal efficiencies, make the SOC decrease. The bias factor is also as expected connected with the value of μ_f and finally the intra day part much depend on the the particular day considered.

The results are somewhat important: infact while the efficiency part causes SOC decrements from 1.5 to more than 3 % the bias factor can cause SOC change of more than 10 %. Note that as seen in table 5.3 while the μ_f value is not very big, its effect is quite important due to the fact that it last for 24 hours! Note that the effect of μ_f in the irish system is much more important with respect to for example continental Europe where mean is nearer 50 Hz. Note that in this case the battery capacity is equal to $P_{BESS} \cdot 4$, which is a reasonable, but somewhat big energy/power ratio for today ESS installations! In case we would have used smaller ratios as 3,2,1, the problem identified by these analysis would be much

more visible and potentially more dangerous for the continuous operation of these systems.For example efficiency losses could be as high as 12 % per day, bias factor and intra day could reach ΔSOC as high as 40 % each. Considering that a certain percentage of SoC should be always maintained for technology issues and also in case of big grid contingency, this could make the necessity of frequent intra-daily recharges/discharge.

5.3 jump frequency study

ADD AT LEAST 2/3 PAGES

Chapter 6

Impact of BESSs on the irish system: A Fourier Transform Approach

In this chapter a second study on impact of BESS during normal operations is performed. A Fourier transform procedure is developed to synthetize a realistic frequency signal depicting all the phenomena causing the Irish grid to deviate from nominal value of 50 Hz. the Irish grid model was used with more than 1000 buses and hundreds of power plants. Every load, RES and SG produces power oscillations such that the grid frequency changes as a whole in function of time. Finally BESS are added performing PFC control and their impact is compared with CG sources. Subsection 6.1.1 presents models of the resources present in the grid, 6.1.2 present the fourier transform based methodology to obtain an average frequency signal starting from real recorded data. Finally in section 6.2, case study and results are presented

6.1 methodology

6.1.1 Resource models

The models of the various resources are as simple as possible, considering that we are not interested in the single load/power plant description, but on their overall contributions to grid frequency deviations.

Conventional Generation

As already used in previous chapters, the conventional generation model is based on a zero-pole dynamic description and on the provision of PFC based on

a constant droop law and dead-band presence. The model is detailed enough for transient stability studies, where frequency variations remain well bounded and the focus is the overall response of the system. The power level set point can be user-defined. As explained later in subsection 6.1.2 the conventional generation is subject to user defined ramps ranging from few minutes up to one hour in order to mimic the power variations yielded by net load following dispatching. An example of such fluctuations is shown in Fig. 6.2.

Load

Load models are assumed to be voltage-dependent, i.e., exponential or ZIP models, and either static or dynamic voltage recovery [114]. The reference power consumption of a load, say p_{load}, is defined as the sum of two components:

$$p_{\text{load}} = p_{\text{det}} + p_{\text{sto}} \ , \tag{6.1}$$

p_{det} varies linearly between used defined values in a given period, e.g. 15 minutes, and represent the aggregated slow changes of power consumption; p_{sto} is a stochastic fluctuation thatm models volatility. p_{sto} is defined as a Gaussian distribution with a given standard deviation σ_{Load}in a given period Δt_i. Fig. 6.3 shows an example of load profiles.

Wind Generation

Wind generators are modelled as doubly-fed induction generators (Type C). The turbine is fed by wind speed time series, which are defined as the sum of two components: wind speed stochastic component $w_{\text{s,sto}}$ $[m/s]$ and $w_{\text{s,ramp}}$ $[m/s]$ component modelled as linear wind speed ramps with a certain time period. The stochastic component is modelled as a set of Stochastic Differential Equations (SDEs) based on the Ornstein-Uhlenbeck Process [191], also known as mean-reverting process. The equations for the wind speed ω_s can be written as follows:

$$w_s = w_{\text{s,ramp}} + w_{\text{s,sto}} \ , \tag{6.2}$$

$$\dot{w}_{\text{s,sto}} = \alpha(\mu_w - w_{\text{s,sto}}) + b_w(\sigma_w)\xi_w \ , \tag{6.3}$$

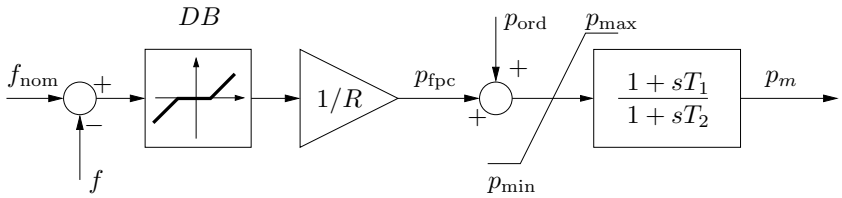

Figure 6.1: simplified model of the primary frequency control and turbine of conventional power plants. Note that all quantities in the figure are in pu.

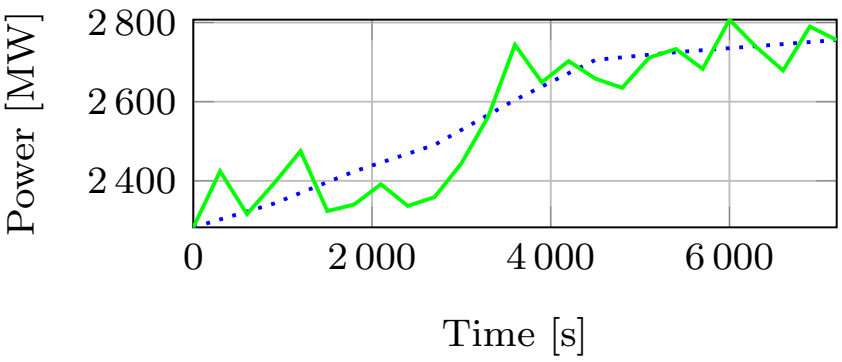

Figure 6.2: example of noise that reproduces slow fluctuations. The blue dotted line represents the net load, while the green solid line represents the net load plus CG fluctuations.

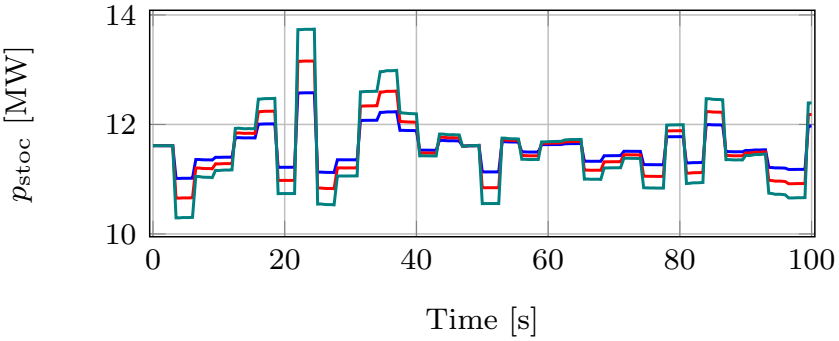

Figure 6.3: examples of p_{sto} profiles using $\Delta t_i = 3$ s and various standard deviations, namely 2.5, 4 and 5.5%.

α is the mean reversion speed that dictates how quickly the $w_{\text{s,sto}}$ tends to the given mean value μ_w (in our case 0). ξ_w is the white noise, formally defined as the time derivative of the Wiener process. This process is controlled by adjusting α and the standard deviation σ_w of the wind stochastic part which affects the b_w component. Fig. 6.4 shows three sample wind stochastic profiles obtained by changing the σ_w and α parameter.

ESS control strategy

The bess model in this study, is defined in [115] where the power produce by the BESS is transferred into the grid by a current source converter, opportunely controlled by a Proportional integral controller in order to set active and reactive power in less than one seconds in whatever initial BESS or grid condition. The BESS control strategies used are two: one is the usual fixed droop strategy (FDS),

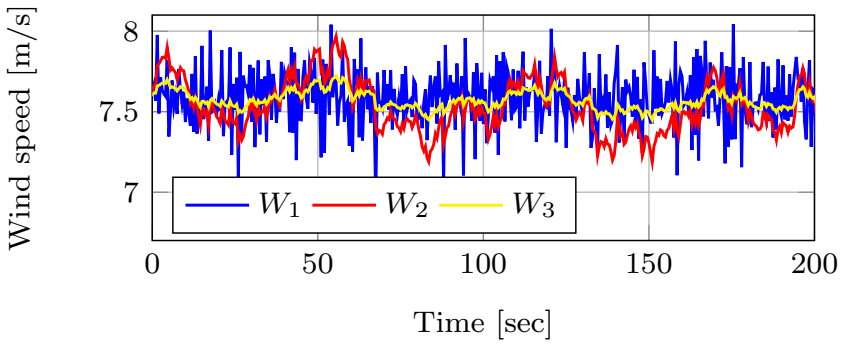

Figure 6.4: $w_{\mathrm{s,sto}}$ profiles. W_1 ($\alpha = 10,\ \sigma_w = 0.17$); W_2 ($\alpha = 0.1,\ \sigma_w = 0.17$); W_3 ($\alpha = 0.1,\ \sigma_w = 0.06$).

while the second is based on a variable droop strategy (VDS), built in order to help SOC management along the provision of PFC.

FD is computed in the same way of the previous chapters. For every typical CG droop R_{CG} value we can compute an equivalent BESS droop R_{BESS} for which the BESS saturate its reserves at the same frequency error level. The formula used is:

$$R_{\mathrm{BESS}} = R_{\mathrm{CG}} \cdot \frac{PFC^{\mathrm{CG}}_{\mathrm{band}}}{PFC^{\mathrm{BESS}}_{\mathrm{band}}} = R_{\mathrm{CG}} \cdot 0.1\ . \tag{6.4}$$

where in this study in accordance to typical Irish parameters we set $PFC^{\mathrm{CG}}_{\mathrm{band}} = 0.1$ pu(MW) and $PFC^{\mathrm{BESS}}_{\mathrm{band}} = 1$ pu(MW).

During normal operations frequency will change around the nominal frequency value. As seen from previous chapter mean-day and intra-day deviations of frequency can lead the BESS to work over or underfrequency for long period endangering the SOC profile depending on the particular frequency signal. Finally even if frequency were to behave as fast stochastic noise, oscillating around f_{nom}, the internal inefficiences of the BESS will lead the SOC to be gradually lead to 0. In the Variable Droop Strategy (VDS), the droop is left to vary in a certain range between two extreme values, namely R_{max} and R_{min}. These values are limited by system stability and resources technical considerations. Usually TSOs can request droop values between 2 and 8% [168] to attached resources, typical values are 4 and 5%. The droop can change in order for the BESS to avoid extreme SOC conditions. Depending on instantaneous SOC and frequency error, the droop will vary from the linear curve in order to discharge or charge the BESS accordingly to its needs.

The VD is implemented through the use of a two dimensional lookup table, where the droop value depends on the instantaneous frequency error $\Delta \mathrm{f_e} = \mathrm{f_{nom}} - \mathrm{f}$

and the State of Charge (SOC). The droop values are divided in five different areas (see Fig. 6.6): (i) in the red areas the values are close to $R_{\max}$, (ii) in the blue areas the values are close to $R_{\min}$ and (iii) in the green area (which correspond to a column vector) the droop values are all equal to the average droop R_{ave}, at half distance between $R_{\max}$ and $R_{\min}$. The values of the table are therefore constructed symmetrically in such a way that the BESS is expected to avoid excess discharge or charge keeping its SOC close to SOC_{ave} level. As an example, if SOC is high and Δf_e is positive then the BESS discharges with a low droop to reach SOC_{ave}, whereas if Δf_e is negative it charges with a high droop to slow down the SOC increase.

Note that, in order to regulate the SOC the best choice would be to set the droop values equal to $R_{\max}$ in red areas and $R_{\min}$ in blue areas. However, to avoid sudden droop changes and less effective frequency regulation, droop values gradually approach $R_{\max}$ and $R_{\min}$.

A better SOC regulation is achieved by setting the SOC_i values close to SOC_{ave} and taking small values of $\Delta f_{e,j}$. Better SOC management is also expected if the distance between the maximum and minimum droop $R_{\max}$ and $R_{\min}$ is large.

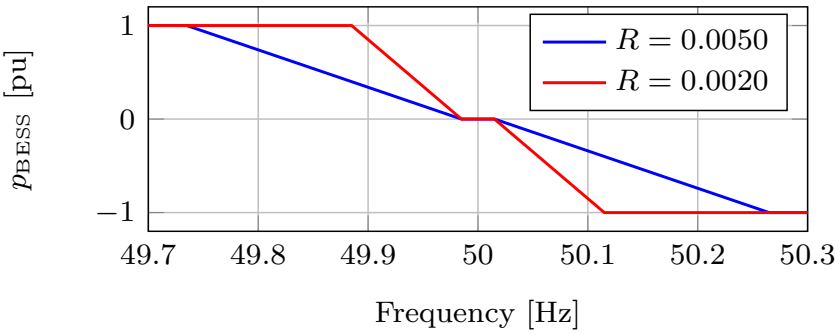

Figure 6.5: Power limits example for the VD frequency control.

6.1.2 Fourier transform Approach

basic idea

frequency signal can be regarded as a stochastic generic variable. To describe its behaviour classic parameters the mean, the standard deviation and the probability distribution function (PDF) of the signal. While these properties tell us a lot about a signal they cannot provide information on the "velocity" of the signal itself. A simple example to visualize this concept is shown in figure 6.7; the two simple signals have same mean, standard deviation and PDF. A tool to identify this time domain property of the signal is the Discrete Fourier Transform.

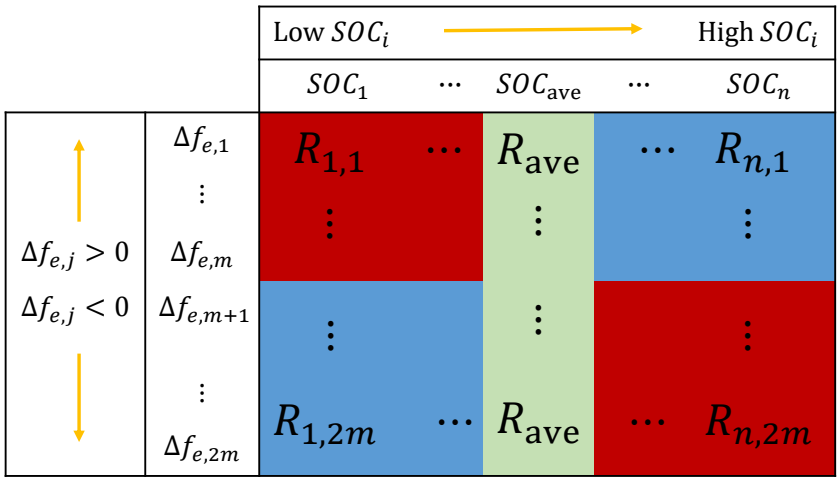

Figure 6.6: VD lookup table scheme.

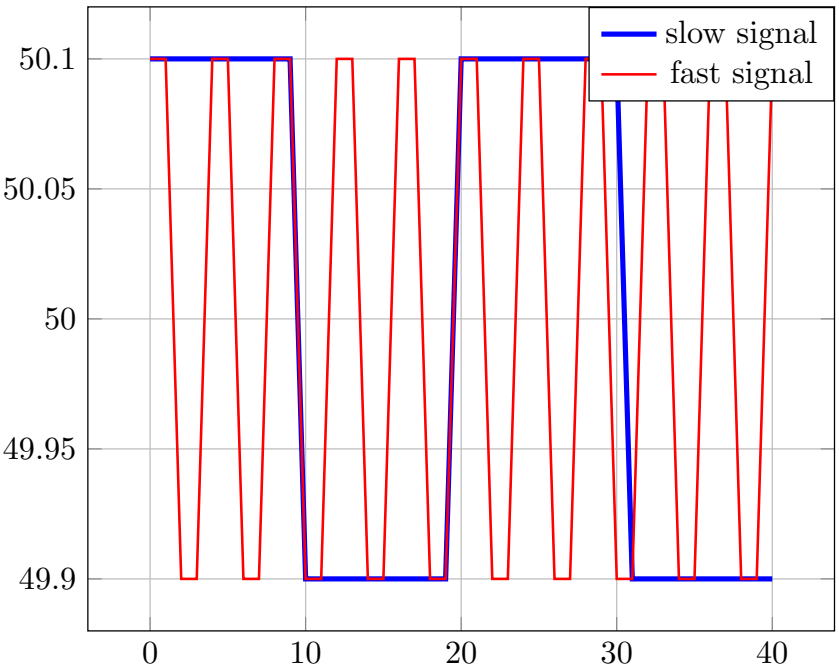

Figure 1: two signals examples

Figure 6.7: two signals with equal mean; σ and PDF

The DFT converts a finite list of equally-spaced samples into a list of complex coefficients of a finite combination of sinusoids, ordered by their frequencies (also called harmonics). The sampled function from its original time domain is moved

to the frequency domain. Given a generic input time series of the form $\chi = [x_1, x_2, \ldots, x_m]$, applying the DFT, after some manipulation we can write:

$$x_\nu = \frac{1}{N} \sum_{k=0}^{N-1} A_k \cos(\phi_k + k\omega_0 \nu) \tag{6.5}$$

with ν that goes from 0 to m. $\omega_0 = {}^{2\pi}/_{N}$ is called the *fundamental frequency* and N is the number of observations in the equally-spaced input time series χ. if now we multiply and divide ω_0 by the sample frequency f_s in Hz of the data, we can write:

$$x(t) = \frac{1}{N} \sum_{k=0}^{N-1} A_k \cos(\phi_k + \frac{k\omega_0 t}{f_s}) \tag{6.6}$$

and so at each harmonic k we can associate an angular frequency $\omega = \frac{k\omega_0}{f_s}$ and a corresponding period $T = \frac{2\pi}{\omega} = \frac{Nf_s}{k} = \frac{T_0}{k}$ with T_0 the length in seconds of our time series (see table 6.1 as an example. The phases of the harmonics gives frequency signal a specific time domain shape, but it is enough to reproduce the amplitudes of harmonics to reproduce the variability of the signal. So starting from our real frequency data of the Irish system, we want to reproduce the harmonic amplitudes of the real signal in order to obtain a realistic signal. In particular, the implemented procedure is valid to replicate the harmonic amplitudes of six hours of real frequency signal. Of all the thousands of harmonics computed through the DFT a for a six hour period, only the first 800 are considered, which represent more than the 98% of the variance of the signal for all the 300 days considered (as computed by applying Parseval's Theorem). This is because the irish frequency signal is quite a "slow" signal in which first harmonics with high periods hold much more weight than last harmonics. For example, in Fig. 6.8 we show the harmonic profiles related to the six hour period going from 6:00 to 12:00, the mean μ and the standard deviation σ of each harmonic for all days considered. All the profiles are similar. The grid frequency signal is therefore quite variable in time domain but much more similar in the harmonic content. Therefore, to reproduce similar harmonic amplitudes of the real data assures that the synthetic signal behaves realistically. Similar results hold for the other three time ranges (00:00-6:00, 12:00-18:00, 18:00-24:00).

procedure

In order to reproduce real data harmonics, we make use of power stochastic profiles from generation and consumption. These processes are divided in two groups following the taxonomy presented in the literature review, as follows:

Table 6.1: T_k values for the harmonics

k	T_k [s]
40	180
60	120
80	90
100	72
120	60

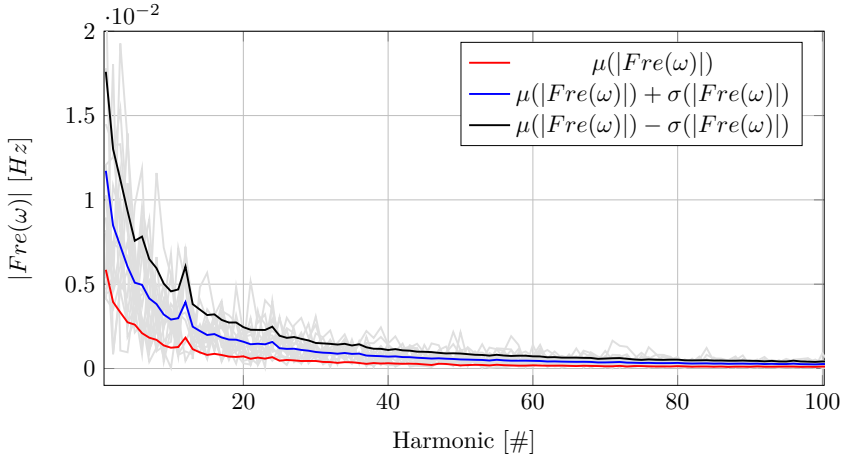

Figure 6.8: harmonics amplitudes related to the six hour period 6:00-12:00.

- *Fast Stochastic Processes (FSP).* The stochastic processes of load consumption and wind speed discussed in Section 6.1.1 are used to replicate the events that cause stochastic frequency fluctuations in the grid (typically with period lower than 2 minutes).

- *Slow Stochastic Processes (SSP).* Two noises are used to model deterministic frequency deviations: SSP1 which models wind and CG ramps and SSP2 which models the long term mismatch between net load and conventional generation due to the market structure of the system. SSP1 are noises up to 10 minutes, while SSP2 are up to one hour. We refer to these deviations as slow frequency variations.

To tune the parameters of each component of FSP and SSP, a precise mapping between stochastic processes and excited frequency harmonics is defined and stored in a database. This is obtained by varying the parameters values, simulating the grid and then computing and recording the resulting harmonic amplitude. To separate the effect of each stochastic process, one perturbation at a time is

considered, being null all other stochastic processes. The parameters used to variate the stochastic processes are the ones described in Section 6.1.1 and are a total of 7. The synoptic scheme that illustrates the procedure is shown in Fig. 6.9.

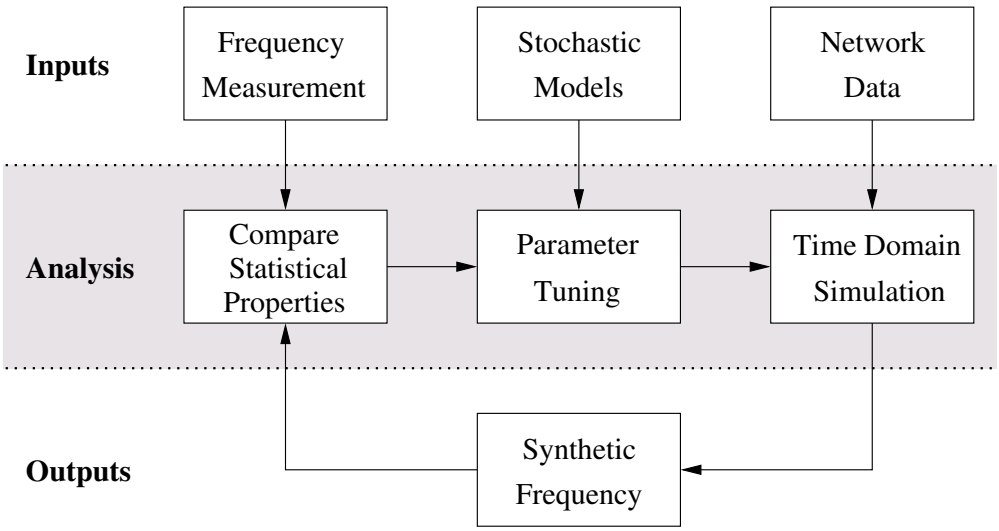

Figure 6.9: Procedure to generate realistic scenarios.

In particular, for the load model, a variety of time periods Δt_i (going from 0.5 to 2 seconds) and standard deviations σ_{Load} (going from 2 to 15%) values are considered. σ_w is the only parameter to be changed to vary the stochasticity of the wind component with α fixed to 0.1. For the SSP, time steps and power ramps are chosen from uniform distributions with specified limit values. In the case of SSP1, time steps Δt_{CG} go from 2 to 10 minutes, while for SSP2 the period goes from 13 to 60 minutes. In the case of power variations, requested ramps are both negative or positive, with a maximum $|\Delta p_{\max}|$ which goes from 10 MW up to 70 MW for both SSP noises.

Figures 6.10 and 6.11 show several harmonic profiles obtained from the simulation of FSP and SSP noises. As expected, The former noises excite short period harmonics, while the latter give rise exclusively to long period harmonics.

Finally, the stochastic processes of loads, wind speeds and CG power set points are summed together and the resulting profile, say p_{tot}, is thus identified by a given unique set of parameters that define the four stochastic processes.

From this point, if we could predict final global simulations harmonic values starting from single perturbations values, we could find analytically the combination which give us minimum difference with respect to the mean of real data.

As known DFT holds the important property of linearity. Given two time series $x_1[n]$ and $x_2[n]$ with Fourier complex coefficients $\chi_1[k]$ and $\chi_2[k]$ (where the

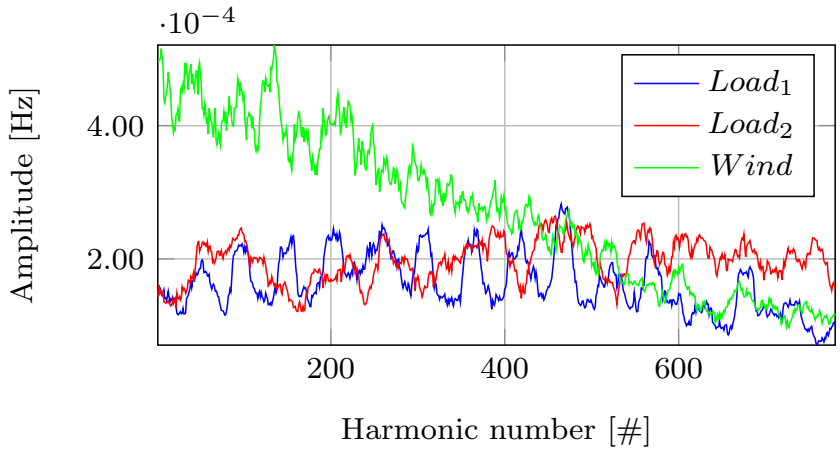

Figure 6.10: examples of harmonic obtained with load and wind stochastic processes. $Load_1$ ($\Delta t_i = 1s$, $\sigma_{\text{Load}} = 2\%$); $Load_2$ ($\Delta t_i = 0.5s$, $\sigma_{\text{Load}} = 2\%$); Wind ($\sigma_w = 3\%$).

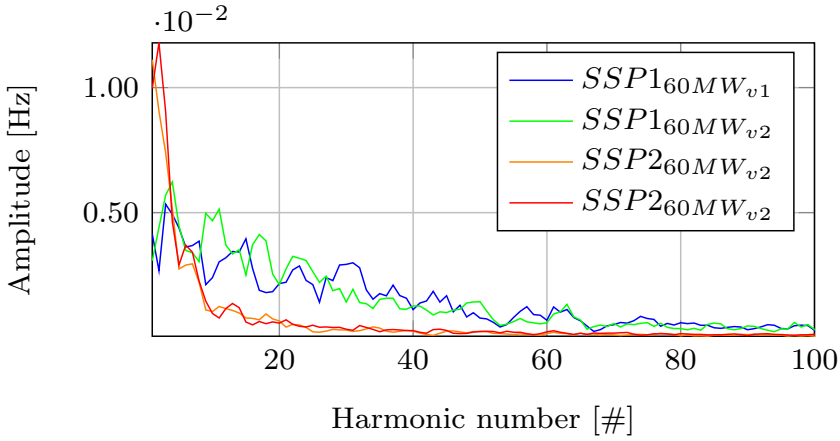

Figure 6.11: examples of harmonic groups obtained with the SSP1 and SSP2 noises. $v1$ and $v2$ refer to different noise profiles with equal $|\Delta p_{\max}|$ value. Δt_{CG} is equal to 3-7 minutes for SSP1 and 13-50 minutes for SSP2.

generic $\chi = a + ib$), where k is the harmonic number. Linearity means that if we have a third temporal sequence $x_3[n] = x_1[n] + x_2[n]$ then $\chi_3[k] = \chi_1[k] + \chi_2[k] = \Re(\chi_1) + \Re(\chi_2) + \Im(\chi_1) + \Im(\chi_2)$. In general, for a generic number of signals N we have:

$$|\chi_N[k]| = \sqrt{(\sum_{i=1}^{N} |\chi_i[k]|^2) + (\sum_{\substack{i,j=1 \\ i \neq j}}^{N} \Re(\chi_i)\Re(\chi_j) + \Im(\chi_i)\Im(\chi_j))} \tag{6.7}$$

In our case, linearity holds only if the frequency signal coming from combining the single simulations can be considered a linear sum of the 4 frequency signals (generically called $f(t)_i$) coming from the 4 different used noises. This means:

$$\Delta freq_{mix} = \Delta freq_{Load} + \Delta freq_{Wind} + \Delta freq_{\mathrm{SSP1}} + \Delta freq_{\mathrm{SSP2}} \tag{6.8}$$

where the generic $\Delta f_i = f(t)_i - 50[Hz]$, in this case the global simulation harmonic groups are a linear combination of the single perturbation harmonics. This equality is strictly true only for the random stochastic variables of the 4 noises: wind velocity v, sun radiation G, load set point P_{Load} and $\Delta P_{OFFSET2}$. In our case, non linearities can arise in the global simulation, due to saturation and dead-bands inside the components control laws and differential equations. The main non linearity in the simulations is the presence of the dead-band in the primary controller, which affects the linearity. However it gives us an hand to predict the final results and how to adjust noises parameters values and presence.

an error ϵ_f is used to compare the frequency harmonics created by the simulated p_{tot} with the real data, which is defined as follows:

$$\epsilon_i = \begin{cases} |(Y\mathrm{sim_i} - (\mathrm{Yreal_i} - \mathrm{std_i}))|, & \text{if } Y\mathrm{sim_i} < (\mathrm{Yreal_i} - \mathrm{std_i}), \\ (Y\mathrm{sim_i} - (\mathrm{Yreal_i} + \mathrm{std_i})), & \text{if } Y\mathrm{sim_i} > (\mathrm{Yreal_i} + \mathrm{std_i}), \\ 0, & \text{if } (Y\mathrm{real_i} - \mathrm{std_i}) < \mathrm{Ysim_i} < (\mathrm{Yreal_i} + \mathrm{std_i}) \end{cases} \tag{6.9}$$

$$\epsilon_f = \frac{\sum_{i=1}^{N_{\mathrm{harm}}} \epsilon_i}{\sum_{\mathrm{i=1}}^{\mathrm{N_{harm}}} \mathrm{Yreal_i}} \tag{6.10}$$

where ϵ_i is the error at the harmonic i; $Y\mathrm{sim_i}$ is the value of the simulated frequency data at the harmonic i; $Y\mathrm{real_i}$ is the mean of all real data at the harmonic i; std_i is the standard deviation of the real frequency data at the harmonic i; N_{harm} is the number of harmonic used.

If this error falls within the desired tolerance, the procedure ends, otherwise relevant noise parameters are increased or decreased according to their impact on the signal harmonics. In such a way the procedure creates a scenario in which frequency does not emulate a specific real day data, but it tries to recover the average variability of real measurements. The synoptic scheme that illustrates the procedure is shown in Fig. 6.9.

6.2 Case Study

6.2.1 Indexes

This section describes a variety of indexes that allow evaluating the impact of stochastic processes and the effectiveness of the PFC provided by ESSs and CG.

Impact of the stochastic processes on the system dynamic response

To quantify the contribution of each stochastic process to the overall frequency fluctuations, we consider the sum variance law of the frequency signal which defines the variance of a signal composed by N stochastic independent variables as:

$$\sigma^2_{\mathrm{TOT}} = \sum_{i=1}^{N} \sigma_i^2 \ . \tag{6.11}$$

To compare the impact of each process, it is convenient to consider a normalized variance per process, namely:

$$\sigma^2_{i,\mathrm{pu}} = \frac{\sigma_i^2}{\sigma^2_{\mathrm{TOT}}} \ , \tag{6.12}$$

in such a way, from Equ. (6.11), we can write:

$$1 = \sum_{i=1}^{N} \sigma^2_{i,\mathrm{pu}} \ . \tag{6.13}$$

Impact of ESSs on frequency fluctuations

This index provides a measure of the relative improvement to the dynamics response due to the ESSs. It is defined as:

$$h_{\mathrm{B}} = 1 - \frac{\sigma_{\mathrm{B}}}{\sigma_o} \ , \tag{6.14}$$

where σ_{B} is the standard deviation of the frequency of the system with inclusion of ESSs and σ_o is the standard deviation of the frequency for the same scenario but without ESSs.

Effectiveness of the PFC

This novel proposed index evaluates the effectiveness of the frequency control provided by any resource included in the system. Considering a resource k, the index is defined as:

$$e_k = \frac{E_k^+ + \left|E_k^-\right| - (E_{o,k}^+ + \left|E_{o,k}^-\right|)}{E_k^{\mathrm{ref}}} \ , \tag{6.15}$$

where

$$E_k^{\text{ref}} = \int_o^T \frac{P_{\text{nom,k}}}{R_k(r)} \left|\Delta f(r)\right| dr \ . \tag{6.16}$$

R_k [pu] is the droop of the resource which, for the ESS regulated with VD, is a time-dependent quantity, $P_{\text{nom,k}}$ [MW] is the nominal power of the resource and $|\Delta f(r)|$ [Hz] is the frequency error including the deadband. E_k^{ref} represents the integral of the exact real-time power profile requested by the PFC service in a given period T, E_k^+ represents the actual energy produced by the resources for $\Delta f > 0$, whereas E_k^- is the energy produced for $\Delta f < 0$ in the same period T. The condition $E_k^+ + E_k^- < E_k^{\text{ref}}$ generally holds as E_k^+ and E_k^- account for the delays of the primary frequency control dynamics. $E_{o,k}^+$ and $\left|E_{o,k}^-\right|$ represent the energy produced for $|\Delta f| < db$ where db is the deadband of the controller. These energies work against the PFC requirements and thus reduce the effectiveness of the frequency control.

According to the above definition, $e_k = 0$ if the resource does not participate to PFC, $e_k \ll 1$ if the resource is slow and not able to follow the PFC reference signal and $e_k = 1$ for an ideal frequency control with instantaneous time response.

Table 6.2: Main elements of the transmission system used

Network	#	Loads and Power Plants	#
AC Power Lines	796	Loads	346
Bus	1479	Conventional Generators	22
Transformers	1055	Wind power plants	472

Table 6.3: Parameters of primary and secondary frequency control

Primary Control	Reserve [MW]	Band [%]	Reserved [%]	Droop [mHz]	Deadband
S1	421	10	5	15	
S2 & S3	302	10	5	15	

Table 6.4: Parameters of the turbine governors of conventional generators

Time Constant	Steam	Hydro	Gas
T_1 [s]	10	2.5	0.5
T_2 [s]	3	0	0

Table 6.5: Stochastic noises parameters values used to create the scenarios

Scenario #	Load		Wind	SSP1		SSP2	
	Δt_i [s]	σ_{Load} [%]	σ_w [%]	Δt_{CG} [min]	$\Delta p_{\max}$ [MW]	Δt_{CG} [min]	$\Delta p_{\max}$ [MW]
S1 (6:00-12:00)	0.5	2.75	2.5	3-6	33	13-50	50
S1 (12:00-18:00)	0.5	3	5	4-7	38	15-50	47.5
S2 (6:00-18:00)	0.5	8.5	12.5	3.5-6.5	39	14-50	22.5
S3 (6:00-18:00)	0.5	16	25	4-7	20	14-50	10

This case study discusses the performance of the ESS PFC and its impact on various scenarios based on the procedure discussed before. With this aim, we make use of the Irish transmission system [49]. Table 6.2 in the appendix summarizes the main elements of the grid. The CG active installed capacity in S1 is 4347 MW while wind active installed capacity is 2123 MW. In S2 and S3 CG capacity is decreased by 25%.

document class latex All simulations are solved using Dome [113], a Python and C-software based tool that allows simulating large scale power systems modelled as a set of stochastic differential algebraic equations. Relevant components are modelled in detail such as a high voltage network topology, a 6-th order machine model of the synchronous generator, frequency and voltage regulators etc.

6.2.2 Scenarios Construction results

Three scenarios, S1, S2 and S3, are considered and the report of the static and dynamic parameters of the CG PFC is presented in Table 6.2 6.3 6.4.

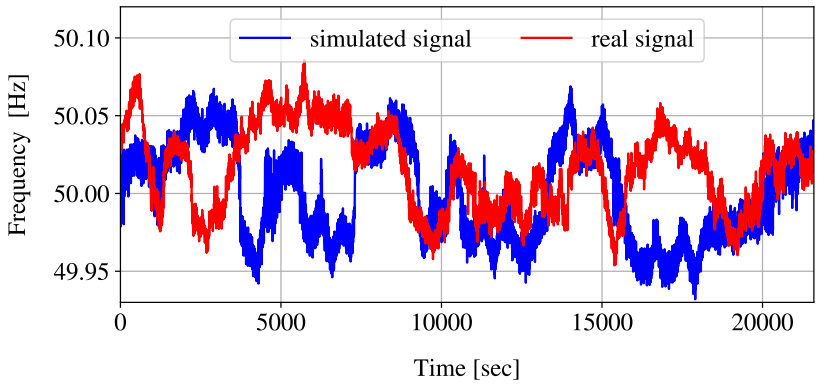

Figure 6.12: comparison between real and simulated (S1) frequency

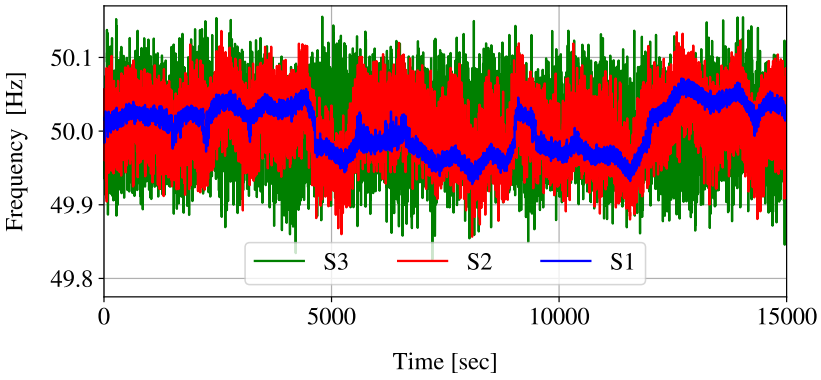

Figure 6.13: frequency profiles examples for the three considered scenarios.

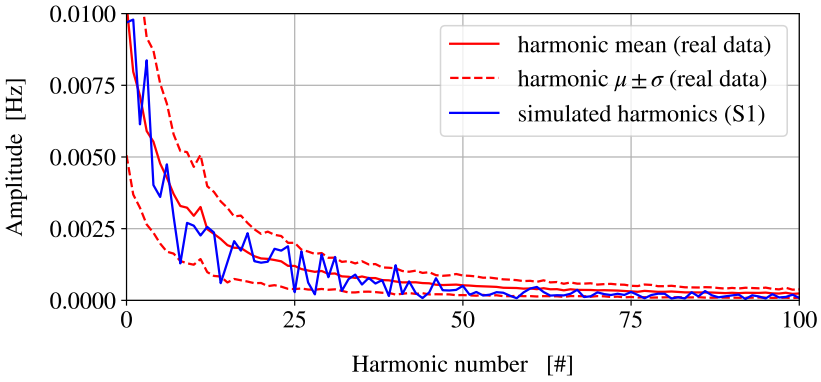

Figure 6.14: harmonic comparison between simulated and real data for the scenario S1, period 12:00 - 18:00.

The time horizon of the three scenarios is 12 hours, from 6:00 to 18:00. Load and wind linear slow power profiles are defined based on real-world data obtained by the Irish TSO Eirgrid, while the mismatch from the net load comes from the application of the 4 noises presented in Section 6.1.2.

Each scenario is first simulated without the BESSs. S1 represents the scenario that reproduces the measurement data obtained in the lab. S2 and S3 include higher level of noises and decreasing inertia levels, which lead to greater and faster frequency fluctuations. In particular, in S2 we increase the FSP noises and decrease the SSP2 noise, while in S3 the SSP noises are reduced almost to zero and FSP noises are highly increased.

One profile of scenario S1 and a real frequency time series are shown in Fig. 6.12. As expected, the synthetic frequency signal retains a similar variability with respect to the real data. Sample frequency fluctuations of the three scenarios are

shown in Fig. 6.13. Table 6.6 summarizes the standard deviation of the frequency of the system σ_f, the normalized variances $\sigma^2_{i,\text{pu}}$ of the four stochastic components and the two S1 errors ϵ_f evaluated by applying Equ. (6.10). In S1 (real-world scenario) the slow noises (SSP) represent almost 90% of the grid deviations with more than half coming from SSP2 noises. In S2 and S3, SSP2 noise goes towards zero. The noises parameters which were used to create the scenarios can be seen in Table 6.5. Note that in both this table and table 6.6 values of S2 ans S3 were computed as the average between the two six hours time periods.

In Fig. 6.8 the harmonics of real data and S1 scenario are compared and as expected from the definition of error ϵ_f, the simulated profile is well bounded by the real data harmonics standard deviation. Moreover the mean of the signal in the scenarios is set in accordance with the mean of the 330 real days. For this reason, frequency signal is slightly under 50 Hz for the first 6 hours and over 50 Hz for the period from 12:00 to 18:00. These frequency mean offsets are very important in order to capture day frequency dynamics which affect the ESS SOC profiles.

Table 6.6: normalized variances and frequency standard deviations for the three stochastic scenarios

Scenario #	σ_f [Hz]	μ_f [Hz]	$\sigma^2_{i,\text{pu}}$				ϵ_f [pu]
			Load	$Wind_{\text{sto}}$	SSP_1	SSP_2	
S1 (6:00-12:00)	0.0308	49.9996	0.09	0.02	0.34	0.55	0.032
S1 (12:00-18:00)	0.0302	50.0038	0.075	0.07	0.34	0.515	0.021
S2 (6:00-18:00)	0.0359	50.0028	0.22	0.12	0.37	0.29	-
S3 (6:00-18:00)	0.0431	50.0021	0.55	0.24	0.16	0.05	-

6.2.3 ESS Frequency Control

The simulations that include ESSs are divided in two groups: the first considers exclusively the dynamic behaviour of FD, the second compares FD and VD control strategies. For the first group, the three scenarios are simulated by considering four ESS capacities (100, 200, 300 and 400 MW) and three droop values ($R_{BESS} = 0.005, 0.004, 0.0035$). In the second group, S1 and S2 scenarios are simulated, with 100, 200 and 300 MW of ESSs characterized by two efficiencies ($\eta_{\text{BESS}} = 0.8, 0.9$) and by a power-energy ratio equal to 0.4.

With regard to the PFC, two FD droops (equal to 0.004 and 0.0035) are compared respectively to two VD strategies which are shown in Table 6.7: (i) “hard mode”, for which the droop varies in the range $R \in [0.002, 0.005]$, and (ii) “soft

mode", for which the droop varies in the range $R \in [0.003, 0.005]$. The tables have been built following the process described in Section **??** considering 4 SOC_i and 4 $\Delta f_e, j$ points. For both modes $SOC_{\text{ave}} = 60\%$, while R_{ave} is equal to 0.004 in the hard mode and 0.0035 in the soft mode which are the values used by the FD strategy. Both setups, especially hard mode, make the droop to vary significantly during the simulations in order to regulate the SOC as well as possible.

Table 6.7: lookup tables for VD "hard" and "soft" control modes. Note that droop is here expressed in % and not in pu to improve readability of values.

Hard mode					**Soft mode**				
Δf_e	SOC range				Δf_e	SOC range			
[Hz]	50%	55%	60%	70%	[Hz]	45%	50%	60%	75%
0.03	0.20	0.20	0.35	0.50	0.040	0.3	0.35	0.40	0.50
0.0175	0.20	0.25	0.35	0.50	0.020	0.35	0.375	0.40	0.50
-0.0175	0.50	0.45	0.35	0.20	-0.020	0.45	0.425	0.40	0.30
-0.03	0.50	0.50	0.35	0.20	-0.040	0.50	0.45	0.40	0.30

FD control strategy

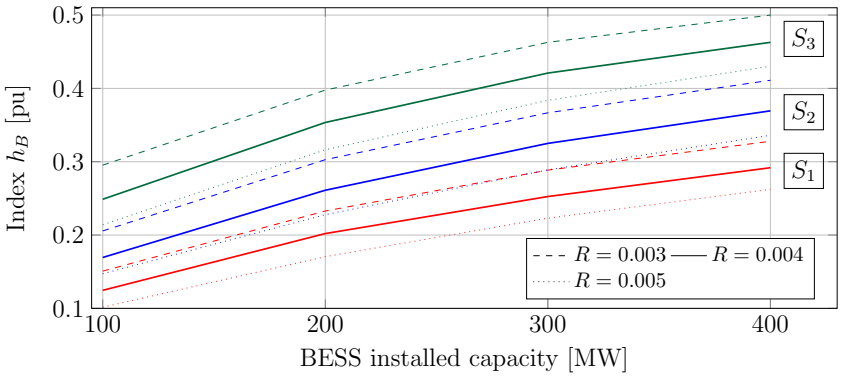

Figure 6.15: index h_{B} for the FD control strategy of the ESSs. The droop values is indicated by R. Different colors represents different scenarios.

Fig. 6.15 shows the index h_{B} for the various scenarios. The improvement of the frequency signal is more relevant for both scenarios S2 and S3 (see Fig. 6.16 for an example) than for S1. This has to be expected as, in S1, frequency has smaller standard deviation closer to the deadband value, which limits the impact

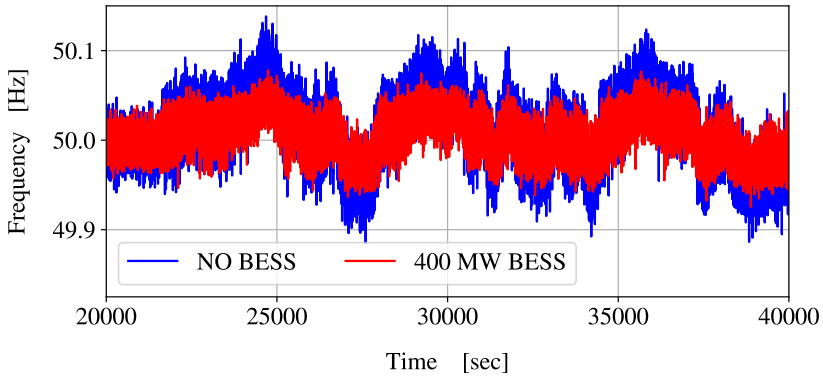

Figure 6.16: frequency profiles for scenario S2 without ESS and with ESS.

Table 6.8: index e_k for various scenarios and energy resources

Device	S1	S2	S3
BESS	0.99	0.99	0.97
Steam	0.92	0.78	0.31
Hydro	0.94	0.84	0.44
Gas	0.99	0.98	0.89

of BESSs. For similar reasons, as shown Fig. 6.15, the h_{B} index increments tend to decrease as BESS capacity increases.

Table 6.8 shows the index e_k for the available resources that provide PFC. In the table, only one value for each scenario and each resource is shown, as e_k is not greatly affected by the ESS installed capacity and its droop value. Two parameters mostly influence the index e_k:

- *The time response of the resource.* A fast time response of the resource improves its frequency regulation. As an example Fig. 6.17 shows the active power outputs of the ESS and of a conventional steam power plant. The blu dotted line is the reference PFC signal to be followed by the two resources. The fast response of the ESS leads to an almost perfect tracking of the reference signal.

- *The harmonic content of the frequency fluctuations.* The index e_k of the conventional power plants is higher in scenarios S1 and S2 than S3 in that the frequency signal is slower and easier to follow even for slower resources.

The result of the simulations is that in scenario S1, which represents the current situation, the performance of the ESSs is comparable with that of conventional

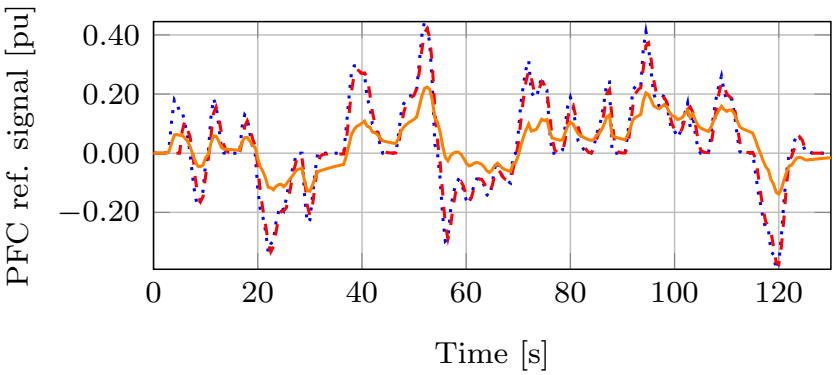

Figure 6.17: power production of the ESS (dashed red line) and of CG (solid orange line) following a PFC reference signal (dotted blue line).

power plants. In S2 and S3, which are characterized by faster frequency fluctuations, the regulation provided by ESSs have much more value than CG PFC service.

VD control strategy

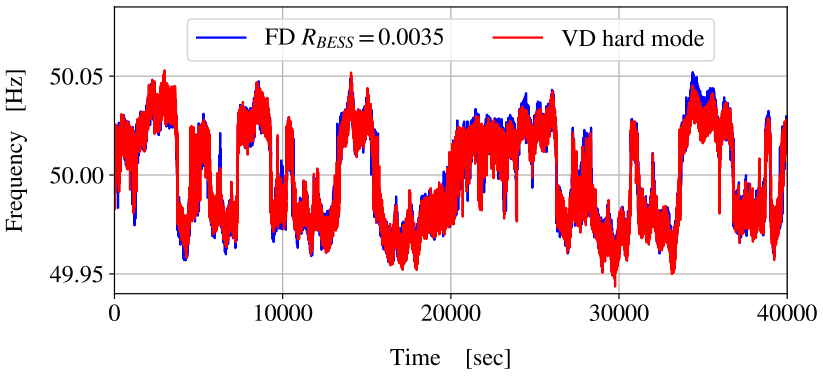

Figure 6.18: frequency profiles examples with FD and VD strategy ($\eta_{\text{BESS}} = 0.8$) adopted and 200 MW ESS installed.

In order to asses the impact of VD strategies, several standard statistical properties of the frequency signal are used. Note that only the results with $\eta_{\text{BESS}} = 0.8$ are shown. The cases with $\eta_{\text{BESS}} = 0.9$ provide similar results and thus are here neglected. In the case of VD strategies, the standard deviation of the frequency signal has a negligible difference in the order of 10^{-4} Hz with respect to the FD strategies. In Fig. 6.18 we can visualize the frequency signal of selected simulations which show great similarity. As shown in Table 6.9, VD strategies generally

Table 6.9: relevant parameters of simulations related to the case $\eta_{\text{BESS}} = 0.8$

Sim.	Par.	VD_{hard}	$FD_{0.35}$	VD_{soft}	$FD_{0.4}$
$S1_{200\text{MW}}$	$\sigma(fre)$	0.0239	0.02393	0.02444	0.02443
	Skew(fre)	-0.1004	-0.0662	-0.0821	-0.722
	$\mu(SOC)$	0.57	0.58	0.56	0.54
$S1_{300\text{MW}}$	$\sigma(fre)$	0.0223	0.02235	0.02285	0.02286
	Skew	-0.143	-0.118	-0.122	-0.12
	$\mu(SOC)$	0.59	0.61	0.59	0.62
$S2_{200\text{MW}}$	$\sigma(fre)$	0.02595	0.02581	0.02655	0.02648
	Skew	0.143	0.066	0.0938	0.0722
	$\mu(SOC)$	0.63	0.70	0.63	0.69
$S2_{300\text{MW}}$	$\sigma(fre)$	0.02349	0.02342	0.02418	0.02416
	Skew	0.142	0.04	0.131	0.042
	$\mu(SOC)$	0.63	0.66	0.63	0.64

enlarge skewness, creating small asymmetries in the frequency signal. If the initial skewness is negative, the VD strategies will further lower this value, while the opposite is true in case the initial skewness is positive. The difference is bigger in the case of hard mode with respect to soft mode and when ESS installed capacity is higher, except for the case $S1_{300\text{MW}}$. In general two compensating effects happen as ESS capacity increases: on one hand, as SOC diverges from the nominal SOC_{ave} value, the droop fluctuates around R_{ave}. This dynamic is responsible for creating the asymmetries in the frequency signal and increases its impact as more ESSs are used. On the other hand, the big ESS capacity makes the frequency less variable and closer to the deadband limiting the impact of VD strategies.

For these reasons the differences in the frequency signal remain small in the order of 10^{-1} [pu] and the values of skewness are still quite close to 0 and therefore do not represent a big distortion. Finally, in both scenarios, the kurtosis slightly increase in the order of 10^{-3} [pu].

It is therefore clear that little difference exist between VD and FD strategies even if a large BESS capacity is installed. Both strategies are enough to guarantee stability in the grid during normal dynamic conditions.

For what concerns SOC, in Table 6.9 the mean SOC value $\mu(SOC)$ of several simulations is shown. VD strategies, especially for S2, are able to keep the SOC statistically closer to SOC_{ave} with respect to FD strategies. Fig. 6.20 shows as an example two profiles related to the different strategies. As can be seen, the VD strategy is not able to perfectly regulate the SOC, but manages to decrease

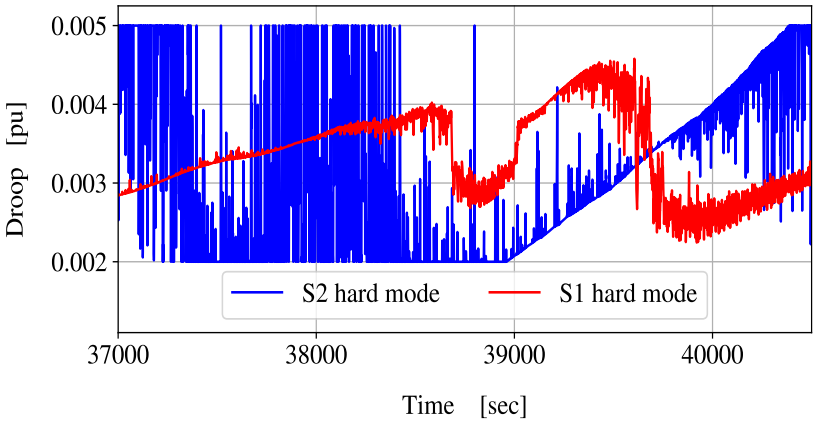

Figure 6.19: example of droop profiles in S2 with 100 MW of BESS installed and $\eta_{\text{BESS}} = 0.8$

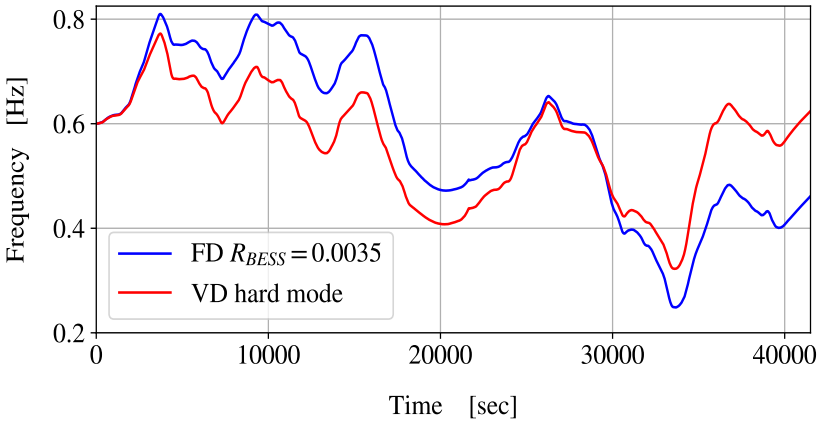

Figure 6.20: example of SOC profiles in the S1 scenario with 100 MW of BESS installed

its standard deviation with respect to the FD case avoiding too high or too low charge levels. Fig. 6.21 shows the SOC standard deviation for all the scenarios studied in the case $\eta_{BESS} = 0.8$. The decrease in standard deviation is slightly better in S2 where the alternation between over and under-frequency periods is faster, therefore the VD strategy changes values often (as shown in Fig. 6.19), reaching better performances. The possibility of using a bigger difference between R_{max} and R_{min} can further improve the SOC dynamics (e.g. $R_{\text{min}} = 0.002$ and $R_{\text{max}} = 0.008$), but its effect on the frequency must be carefully evaluated.

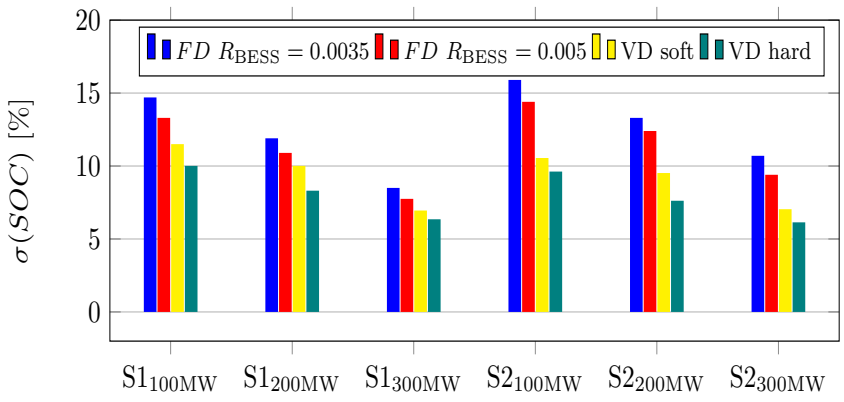

Figure 6.21: index $\sigma(SOC)$ for various ESS control strategies and capacities with $\eta_{\text{BESS}} = 0.8$.

Chapter 7

Electric Vehicles studies

Electric vehicles represent one of the most prominent new resources of the grid. EVs connect to the distribution grid in order to recharge after a road trip. Their presence in the grid is therefore not constant and can cause local problems. Due to their battery small size, they need to be aggregated for market coordination and service provision. Evaluate their possible impact into the grid performing frequency control is therefore quite complex and not straightforward. In section 7.1 we present all the elements which need to be taken into account in order to properly quantify the EVs potentiality to perform frequency control. Moreover a possible generic scheme to gather frequency reserves from EVs is presented. In section 7.2 and 7.3 we present two case studies developed in order to deal with two specific sub-aspect of the presented EV framework. These steps can be used as a basis to build the other elements of the problem formulation

7.1 Motivation and Framework

A great number of studies deals with the the provision of frequency reserves from EVs focusing on different aspects: for example on studies like [192, 75, 84] the focus is on the EV frequency control strategy and on the impact on frequency stability. Others [41, 74, 172] focuses on the economics of EVs providing frequency services considering at the same time recharge and availability of EVs. Finally some studies focuses on the presence of distribution grid constraints due to the energy management of EVs [67, 156], which anyway rarely consider the possibility of performing frequency control. The problem of evaluating EVs frequency reserves impact is actually a very complex one where many dimensions and levels should be taken into account at the same time in order to give a realistic quantification. The problem is summarized in figure 7.1 and considers all the main stakeholders:

Aggregator of EVs. Gathering more cars represents a solution to offer more reserves and decrease the expected stocasticity in EV availability. EVs can then more easily participate to power systems markets. In day ahead and intra-day market, aggregator buys the energy needed for recharging or adjust the power schedule in real time considering the real-behaviour of EVs. Moreover it needs to assure the dispatching of frequency reserves. Aggregator will use some form of control (centralized, distributed etc.) and an algorithm in order to recharge the available EVS from its fleet.

TSO . Considering a typical frequency regulation as performed in many European countries, frequency reserves are set in advance by TSOs dependign on system needs. Participation of resources can be compulsory or managed through the use of weekly or different time frame auctions. TSO expects the reserves are continuously operating and always available at the contracted nominal quantity.

DSO . It is the operator responsible for the medium and low voltage levels of the grid. In the case of possible grid congestions, it needs to assure the resolution of the problems as fast as possible. For this reason it could impose some restrictions in specific points of the grid

Note that not only EVs but also other new resources of the distribution grid (RES sources, smart buildings, water heaters, distributed storage etc..) could offer new services to the grid by being able to regulate their load. A stronger coordination between TSO and DSO should be designed to avoid that new resources destabilize the distribution grid itself. In [68], new TSO-DSO markets models are presented for various ancillary services and congestion management. Among others, frequency control presents a great opportunity [157], both for the new resources to increase profitability, and for the grid regulators to compensate the loss of controllable power generation, increase efficiency of the market and decrease prices, thanks to the higher number of competitors. An example of such coordination is shown in figure 7.2 and describe a possible market design to offer frequency reserves from resources at the distribution levels. In the figure it is shown the process to qualify the resources for the services over a certain time range (hourly, daily, weekly, etc.; usually the lower it is, the better for market efficiency). The trend today is to go for shorter time range periods. The single new resources offer a power band for frequency control (talking about primary or secondary does not create much differences). This offer possesses some level of elasticity. Higher prices payed correspond to bigger band offered in the market. A smart home management system could decide to sacrifice some comfort or discharge the home battery in order to have some economic benefits. Other resources, such as EV stations, have some level of flexibility as well. At the medium and high voltage

all the various offers from all the distribution grids are summed and DSO in this pre-qualification process could already decide to decrease or discard some of the resources offered due to grid security issues. The market is cleared and the accepted offers are communicated back at the MV and LV level, before a new market period starts. In this period, the winning resources will provide frequency control. As known from previous chapter, the worst situation is when the whole power band is requested due to a big frequency deviation. In this case local problems to distribution networks could emerge such as overvoltages, overcurrents, branch congestions etc.. therefore DSO after having analyzed the state of the grid considering also the possibility for full frequency control power band provision could deploy safety actions such as reactive compensation, adjust dispatching or block EVs perform PFC from certain positions.

The study of the potentiality and impact of EVs resources performing PFC is therefore nor easy or straight-forward. A series of intermediate steps are needed:

mporal description . The starting step to evaluate EVs behaviour in large scale scenarios is to give a realistic description of EVs energy requirements on different recharging points present in the distribution grid. Sizes of chargers are increasing in the course of the years (typical size is now around 22 KW) and therefore can represent a real threat for distribution systems. In section 7.2 an agent based modelling is constructed in order to simulate the behaviour of EVs over a simulated road and electric network and evaluate the impact of EVs on the grid using dumb charging.

charging algorithm an aggregator of EVs will have to optimize its cost of buying energy from the day ahead market based on needs prediction and at the same time respect the purchased profile in order to avoid any unbalance in real time. Different optimization framework exists in literature, in section 7.3 a simple priority based approach is used. The algorithm works and can be easily scalable for high number of vehicles. Moreover specific strategy to take into account the SOC losses and power Band for frequency control needs to be designed.

) real time control. Finally it is necessary to study the controls action the DSO could send to aggregators or other resources in order to keep distribution grid stable and secure. Firstly DSO should check the possible dangerous point in the grid in case the power band for frequency control is all activated in up or down direction. In the case (as typically happens today) DSO does not have a complete estimation of its own grid it could make use of probabilistic load flow to look for dangerous points. if not admissible points are found, different actions can be taken such as changing the networks layout and reactive power deployment. In extreme cases feedback orders to aggregators should be sent

and internal re-dispatch or stop in the frequency control provision could be issued.

Note that in this thesis I started working on first and second step. In the previous list and in the final subsection of chapter, hints and next steps to finish the work are described.

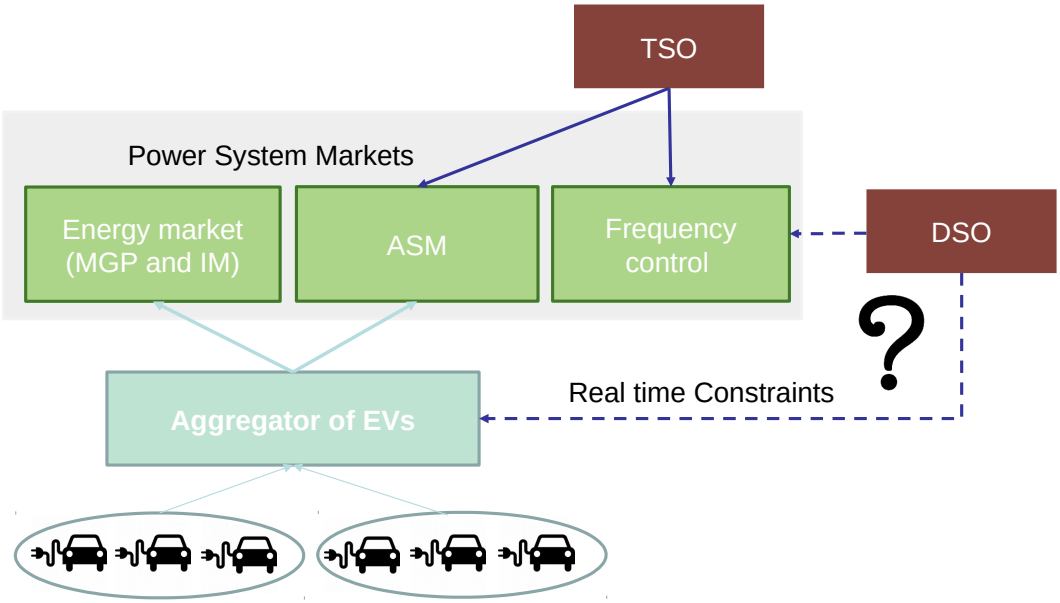

Figure 7.1: A scheme of the EVs interaction and stakeholders in the power systems

7.2 First application: agent based models

Typically real data data and/or probability distributions functions (for example, Gaussian and/or the Lognormal distribution or direclty empirical PDF computed from travel diaries) to decide the travel characteristics are used in works such as [41, 6, 194]. This approach is the most common and it is able to reproduce consistent single trips for EV cars, but it cannot model consistent travel schedule for an EVs, neglecting the expected correlations between travels characteristics and day schedules. It is also possible to build several archetypal driving patterns [190] starting from on-field measurements or car diaries. However also in these cases the trips of EVs are fixed and strictly depend on the location and surveys used. In order to reach a better description activity based models are used where the EVs schedule is a consequence of the actions performed by people using cars. A certain schedule for every EV users is constructed, based on less or more complex

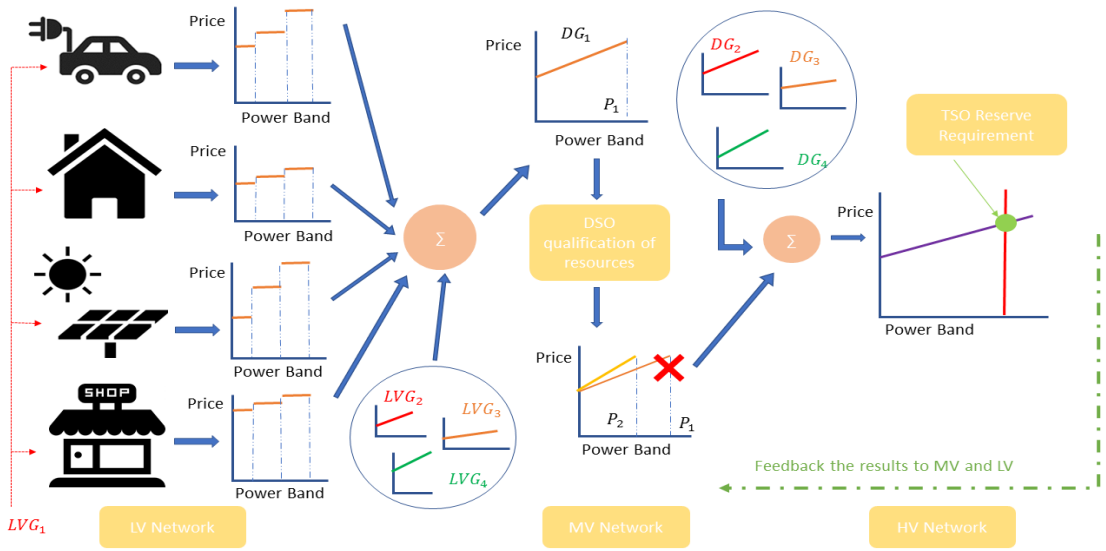

Figure 7.2: An example of DSO-TSO coordination for frequency control resources gathering

set of rules and relations [100, 109]. In pure transport studies [72, 76] activities schedules creation is a complex task based on a socio-demographic description of the population and on a stepwise approach that determines activities based on different time decisions levels. In this way, every driver makes realistic decisions for his/her schedule.

In order to built a realistic activity based models, in which EVs users activities can change and potentially be influenced by other users, we decided to model both the electric and traffic model grid and use an agent based model framework [103]. Notably only in one paper a tool with such a philosophy was developed ([186]). However this tool was more concentrated in policy decision and medium-long term horizon (days to week) more than on daily distribution system operations. Road and recharge points also assimilated in few equivalent points. Typically an agent based model is characterized by 5 typologies of components:

Agents a self-contained program capable of controlling the decision making of each individual, and able to influence or be influenced by the environment.

Environment It represents the space and dimensions where agents move and interact.

Object populates the environment along with agents.

Relationship links agents and objects.

Operations allows agents to perceive and transform objects.

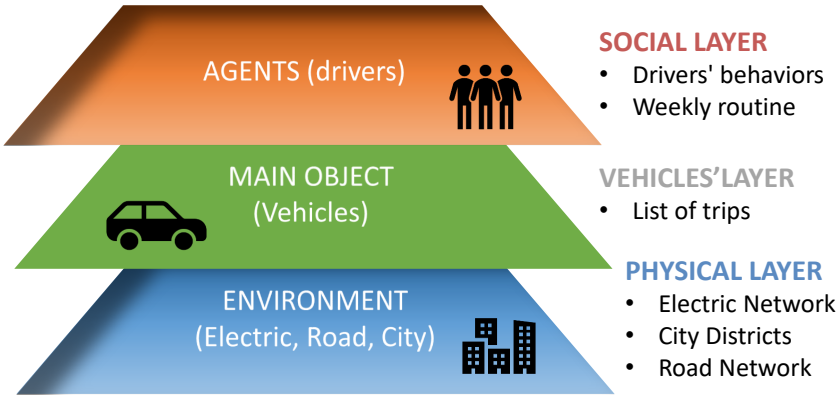

Figure 7.3: Layer structure of the model

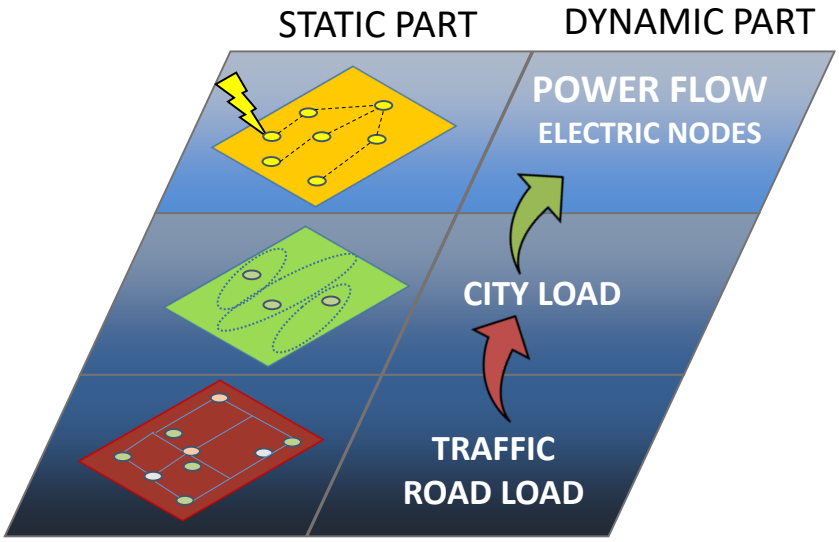

Figure 7.4: Environment layers details

7.2.1 Layers modelling

A three layers framework (see figure 7.3) was developed considering the presence of a time loop routine to keep consistency in the time line. The main agent is the drivers which makes use of a car, which can be electric or normal. The agent is characterized by a series of consistent set of parameters which defines its activity in space and in time. During travels, traffic is created when more agents need to reach the same destination influencing the time and energy spent in the travel itself. Finally EVs need to recharged as soon as they reach the destinations, influencing currents and voltages in the distribution network.

The Environments in which agent interact are actually 3: namely, the electrical

network, the road network, and the city structure (see figure 7.4). The networks have a static description in which the topology of the network is represented and a dynamic part which gathers the possible operations and methods agents and objects put in place during the day.

Static part

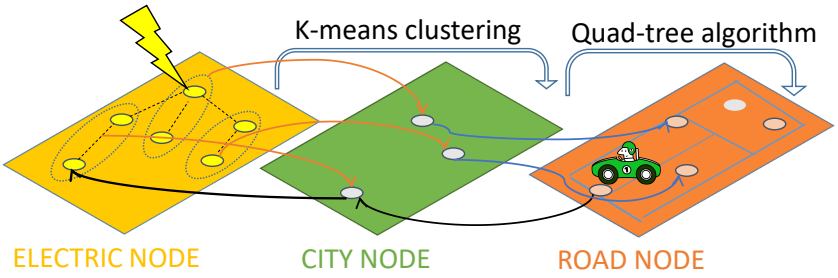

Figure 7.5: Main step to create the System environment

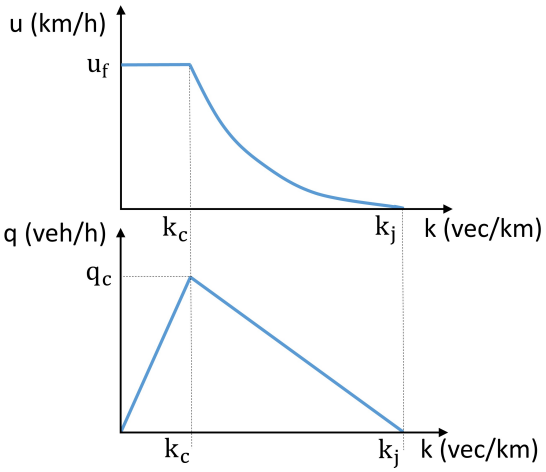

Figure 7.6: Parameters referring to the traffic model

The starting point of our study is the use of two reference distribution system networks as it is really difficult to obtain real electricity distribution grid models, it is quite common to use reference ideal network constructed to guarantee realistic results [63]. The electric grid is composed by electrical nodes and lines characterized by a certain resistance and inductance. Electrical loads are under the nodes of the grid. The nodes characterised by a certain nominal active power $P_{\text{nom}}^{(k)}$ and reactive power $Q_{\text{nom}}^{(k)}$ which are composed by a sum of residential, commercial, agriculture, industrial type of load. Starting from this description, the city layer is

built by using k-means (see figure 7.5) clustering to gather the electrical nodes into a certain number of groups. These new points represent city districts and define the possible interaction of agents. The city layer represents a mid-layer between road network and electric network is compulsory and opens the possibility of more precise sociological and urban descriptions. Finally the road network is obtained starting from the city districts by building a quadratic graph was around the city nodes. An algorithm is implemented such that areas with more city nodes will be surrounded by a bigger number of roads (bigger density of roads), as expected in a typical city area. Every branch is then described by three parameters referring to the traffic (see the top diagram in figure 7.6:

- u_f [km/h]: average travel speed of the vehicle withou traffic (called free mean velocity);
- K_c [veh/km]: minimum vehicle density to make the vehicles starting to decrease velocity due to traffic;
- K_j [veh/km]: road vehicle density that creates road congestion and stops the traffic.

The nodes represent the entry/exit points for the vehicles driven by the agents, and the branches represent the roads of the network.

Dynamic part

The electric grid is solved by means of the Backward-Forward Sweep method every minute for 1 week. The loads comes from typical power profiles of residential, industrial and commercial loads. Voltages and currents are computed and can be compared with permissible values. In fact should remain between 90 and 110 % of nominal value, while current is limited by temperature. In general, for every branch of the grid a maximum temperature can be tolerated by the conductor insulation. The maximum temperature imposes a limit on the maximum current a conductor can withstand, taking into account the ambient temperature, the joule losses, and the heat transfer processes. The city layer does not possess (in the present version) an independent dynamic. It basically serves to construct a consistent road network. The road network is indeed important, being where the interactions of agents (making use of the vehicles objects) work towards the creation of the traffic. The traffic dynamics are modelled following a microscopic traffic pattern method [104] able to trace the vehicle position at every time step. The goal is to compute the instantaneous vehicle density q in every road and subsequently the vector u_i for every vehicle i containing all the average speeds of cars (figure 7.6). With these parameters it is possible to compute the energy consumption of the EV based on

an aerodynamic model of the vehicle itself taken from [109]. The traffic method starts from a list of vehicles that enter the road network graph and update the vehicles position and velocity in every road based on the lines defined in figure 7.6. The possibility of vehicles finishing their journey entering a new road before the one-minute time step is also taken into account.

for one week, every agent is characterized by a series of activities. possible ones are: (i) HOME: agent are at home (ii) WORK: agent is at work (iii) LEISURE: the agent is outside home to perform some social or spare time activity. (iv) ERRAND: the agent is not home for mandatory activity (buying food, pharmacy, bureaucracy, doctor, etc.) (v) OUT: the agent is outside the city/simulated environment (for work, holidays, etc.). (vi) ILL: the agent is ill at home (while in normal conditions should be outside home). The when of these activities depends on the characteristics of each agent. Manifold characteristics define a unique agent:

NODE HOME. It is the city node/district where the agent lives. The assignment of this node is not random, but is obtained by an extraction from the Cumulative Distribution Function (CDF) of residential power P_{res} . So nodes with higher installed residential power have bigger probability to be chosen as HOME of the agent.

NODE WORK. This is composed of a principal node, which is the primary working environment, extracted in the same way as NODE HOME considering the sum of industrial, commercial, tertiary and agricultural powers of city nodes (through a sum on electrical nodes). A second node is extracted to represent a secondary working place which could be used by some agents in some special days.

WORK TYPE. depending on the node where the driver works, the work sector is extracted from the cumulative work power installed. Then, by using real or reasonable statistics, the type of employment is chosen between full time worker, part time worker, and freelance.

SEDENTARINESS. The nodes where agents go to perform non-working actions are actually not fixed, and are extracted trip by trip according to a CDF influenced by three parameters: (a) the distance of the agent from the surrounding nodes; (b) the level of installed commercial power (for ERRANDS), and the tertiary installed power (for LEISURE activities); (c) the sedentary level of the agent, which is the tendency of performing LEISURE and ERRANDS activities far outside home. A high level of SEDENTARINESS means that the agent tends to use the car even to reach near places (from 500 meter to 1.5 km, for shorter paths the agent always goes on foot:

for longer paths the agent always uses the car) and it will anyway try to perform activities near home. The sedentary parameter introduces an exponential condition on the previously computed CDF. FAMILY: this binary flag [0, 1] indicates if a person has a family or is single, since this greatly influences agent activities like ERRAND and LEISURE. The activities at this level, using the first 5 parameters, are divided on an hourly basis. To obtain sub-hourly and minute division the parameter ACCURACY and DELAY are used.

EV USER. Every agent is assigned a vehicle object to perform its activities inside the city. The possibilities are two: private non-electric car, or car-sharing EV. In the latter case, this means that the driver does not own an EV, but makes use of whatever electric vehicle is available. The EV car makes uses of an aerodynamic model to convert the average speed velocity of the power into energy consumed by the EV.

Normally the agent will start its journey considering the hour at which it should arrive at destination, subtracting the ideal time of travel (computed without considering the traffic). The true starting time is computed considering other two time steps: (a) a first extraction (ACCURACY) from a normal distribution with expected value of zero and variance 30 minutes to take into account the possible delay/advance of the agent due to the activity starting time differing from an hourly schedule, (b) a second component (DELAY) which add a stochastic delay (positive or negative) due to driver faults.

EVENTS override all the other activities and could last a DAY or a WEEK. In particular ILL or OUT could be extracted and last one day or one week or a weekend (in case of OUT for short holidays).

In order to create an agent's routine, the actions are divided in three categories: fixed actions, semi-aleatory actions and aleatory actions. Depending mainly on the type of WORK and FAMILY status, every driver has a certain type of fixed actions (for example WORK) in predetermined days and hours of the week. Semi-aleatory actions are instead usually LEISURE or ERRAND activities, for each of which there is a fixed number of hours for the agents to fulfil, but the choice of the specific days and time when it is fulfilled depends on random extractions. A typical example could be the agent with family which two or more times a week will take the children to school before going to work. Finally, aleatory actions have to respect some basic constraints (as maximum number of times and hours) and depend on agent characteristics, but are quite random in nature and give the agent a more realistic routine. An example to explain the semi-aleatory activities is shown in table 7.1. These activities provide a list of vehicle trips to perform with

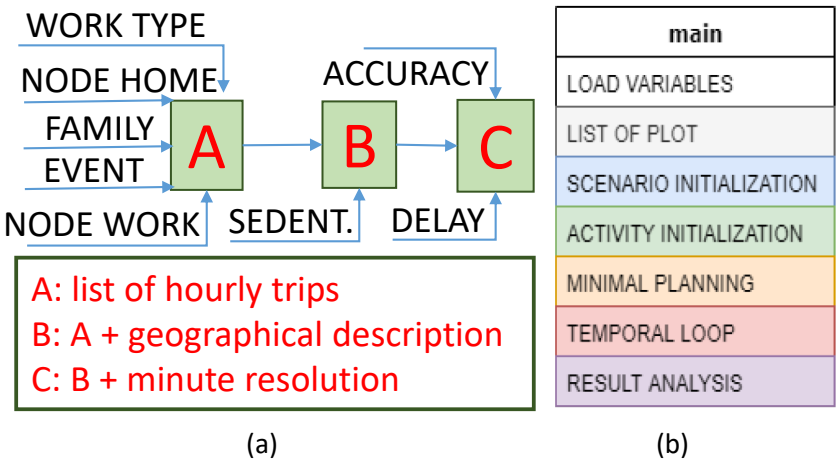

Figure 7.7: A scheme summarizing the driver trip creation procedure. (b) Main temporal loop steps of the simulation

starting times and trip details (see figure 7.7a for a scheme that summarises the approach). Finally the system dynamics are simulated. Figure 7.7b shows the main steps of the tool. In "load variable" the databases and the parameters to define the simulations are loaded. "Scenario initialisation" deals with initialisation" with the creation of the vehicle trip lists. "Minimal planning" is a particular initialisation procedure to choose the number and initial position of EV such that the number is neither too small nor too big with respect to EV users, and positions are consistent with the request of the EV users. Finally in "Temporal loop" the dynamics of the networks are solved.

Acronym	Meaning	Start	End	Prob.	Action
NFWD	No Family-Working days	18	20	0.5	ERRANDS
NFWE	No Family-Week End	20	23	0.6	LEISURE
WFWD	With Family-Working days	18	19	0.4	ERRANDS
WFWE	With Family-Week End	10	13	0.45	LEISURE

Table 7.1: Acronyms and actions for the agents

7.2.2 Case Study and results

The electric grid used is the reference network developed by JRC [142]. The parameters for each road segment were extracted by Gaussian extractions considering four different typologies of roads (for example backbone roads are bigger

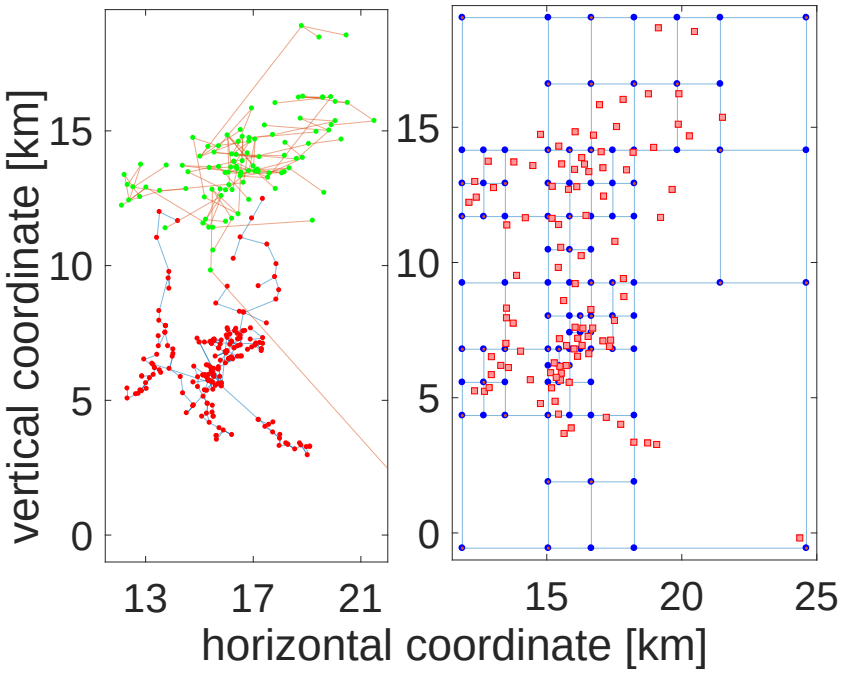

Figure 7.8: Case study road construction

Num. drivers	EV users %	Road type	Power [kW]
1000	10	GOOD	3
5000	30	BAD	6
10000	60		11
20000			13

Table 7.2: Acronyms and actions for the agents

road with high free mean velocity; on the contrary rural roads are characterized by low free mean velocities and low quality parameters). The three networks (electrical, city and road) are shown in figure 7.8. To define the type of work of the agents and their family conditions, and make other reasonable assumptions, data from the Italian institute of statistics and city municipalities were used [98] [1]. A considerable number of simulations were performed by changing the most meaningful parameters. In these scenarios, the EVs recharge with a dumb strategy, which means that they are recharged at a fixed power as soon as they connect to the grid. The parametric analysis is summarised in Table 7.2. GOOD road mean

[1]Statistiche veicoli (in Italian), http://www.comuni-italiani.it

higher free mean velocities and better parameters with respect to bad roads. EV users % represents the percentage of drivers making use of the EV car sharing. Power refers to the power rate at which EVs are recharged once they reach the EV car parking (by hypothesis there is always the possibility to park). All the possible combinations of the parameters were simulated, for a total of 72 simulations (every simulations consists of 7 simulated days). All the simulations were performed in Matlab® in commercial available Desktop computers. A sample of the results that can be obtained from the proposed framework is shown below. In general, the agents tend to live in the city, while particular rural nodes with very high industrial power attract many workers. Figure 7.9 shows the nodes where people live and work for the case of 15000 people. Figure 8 shows the cumulative presence of vehicles in the case of 20000 drivers.

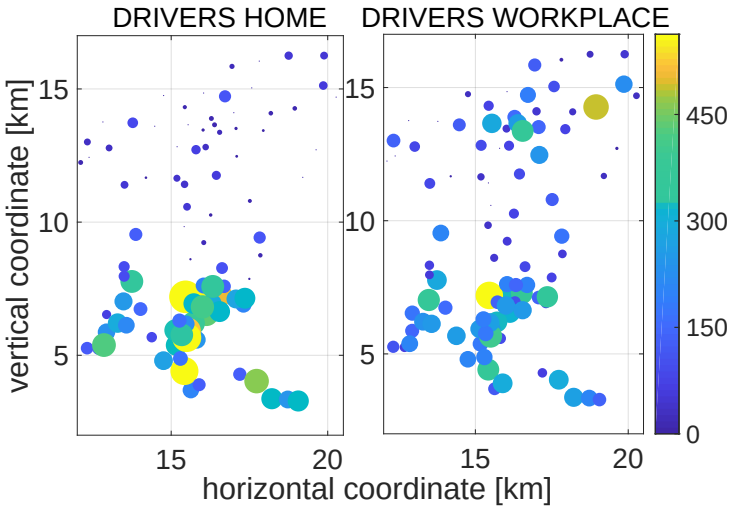

Figure 7.9: Nodes where drivers live and work

Figure 7.10: vehicles presence for one working day

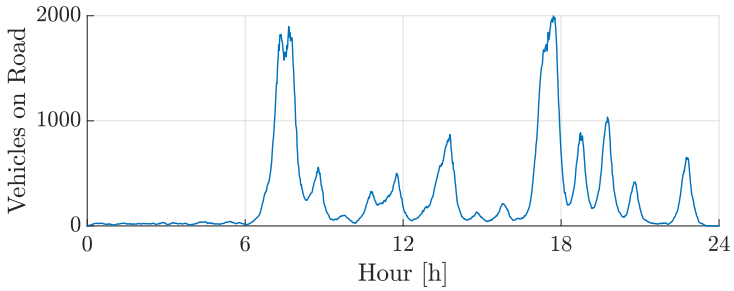

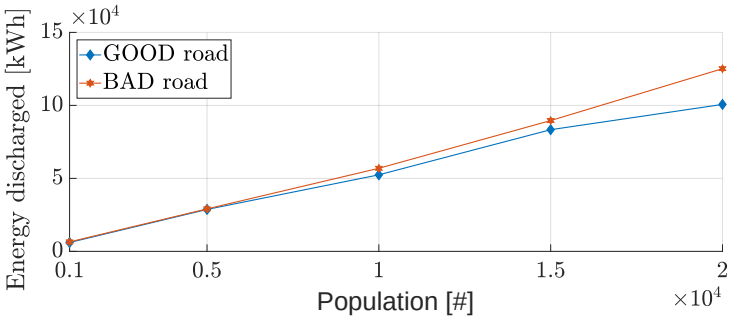

Figure 7.11: total energy spent by EVs considering different populations.

Figure 7.12: spatio-temporal distribution of voltages in the rural network

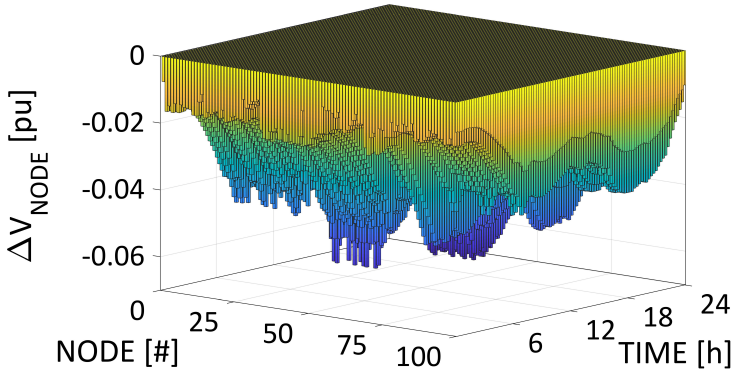

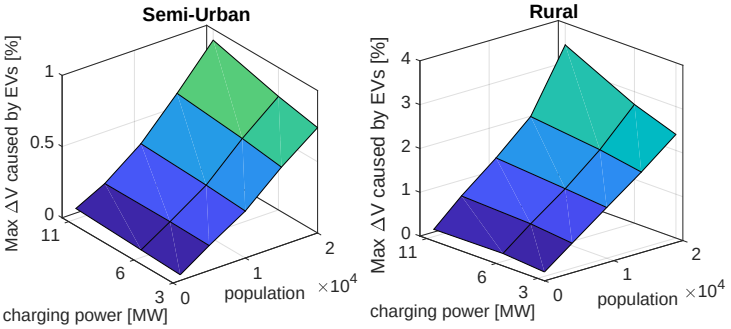

Figure 7.13: $\Delta V_{\max}$ caused by EVs in the grid

Figure 7.14: spatio-temporal distribution of voltages in the rural network

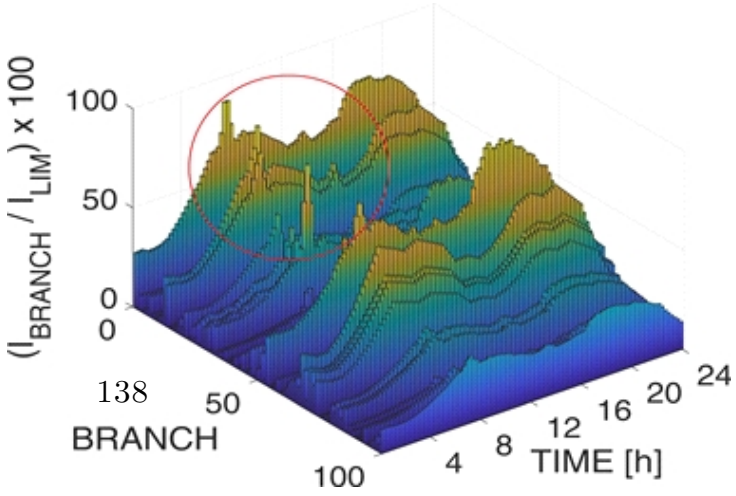

The model is able to grasp the morning and night peak of working days, while the travels along the day are rather variable, less smooth than expected from typical traffic curves [2]. This suggest that new kind of work types could populate the model, such as retired or unemployed people, people who uses the car to work and perform multiple trips a day in not standard hours, and so forth. Moreover a better use of ACCURACY and DELAY parameters can help smoothing the traffic curve. The road characteristics influence the time spent by drivers in the grid and the energy spent by EVs. Figure 7.11 shows the energy discharged by all the EVs in the whole week. The energy discharged is higher when BAD road characteristics are used due to bigger traffic problems and more time spent by the drivers on the road. For what concerns the electric network, Figure 7.12 shows the time-spatial distribution of voltages (computed as $\Delta V_{i,t} = V_{i,t} - V_{\text{nom}}$ for every node i and time step t) for the rural network for one of the days in the case of 20000 people with a recharge power for EVs of 11 kW. The ΔV is caused both by the loads and the EVs recharging. By analysing all the time-spatial series coming from the simulations, it is possible to evaluate that:

- the rural network, due to the resistive nature of the line impedance and less nominal power, tends to be more affected by EV introduction, both in terms of voltages and currents even if the presence of EVs is smaller. The semi-urban network is already characterised by a bigger installed load capacity, which makes more difficult for EVs to affect the grid. Figure 7.13 shows the maximum ΔV caused by EVs. With 20000 people and 11 kW used for recharging, the voltage changes more than 3.5% in the rural network and slightly less than 1% in the semi- urban network.
- The current in the branches almost reaches the thermal limits in the case with 20000 drivers, 60% EV adoption in the rural network (figure 7.14) due to the EV recharging in the morning. In general, EVs could increase the $\frac{I_{\text{BRANCH}}}{I_{\text{lim}}}$ ratio more than 20% in both grids. Adding more EV users will lead to violations of the line thermal limits and, in the case of rural networks, can produce excessively low voltages.

7.3 Second Application: historical data and Day ahead-Real market optimization

In this second study a day ahead-real time management system for an aggregator of EVs was deleopped. The aggregator has the possibility to control all the

[2]Open Mobility data of Turin, http://www.5t.torino.it/open-data.

chargers where the EVs are connected. EVs are always connected when parked, thus vehicles are always connected if not traveling. The algorithm will participate in the Day ahead market making use of EVs use forecasts and optimizing the costs solving an optimization problem. (the problem will be formulated in order to actually perform Energy Arbutrage: Evs could also discharge to the grid if this is convenient). Then in real time a priority based logic will guarantee the respect of the power profile purchased in the day-ahead to avoid unblance which is fined in typical power system markets design. This algorithm is used without the need of formulating an optimization problem. In this way it is possible to manage big EVs system without the need of heavy computational power and communication channels. Schematic of the aggregator operation are shown in figure 7.15.

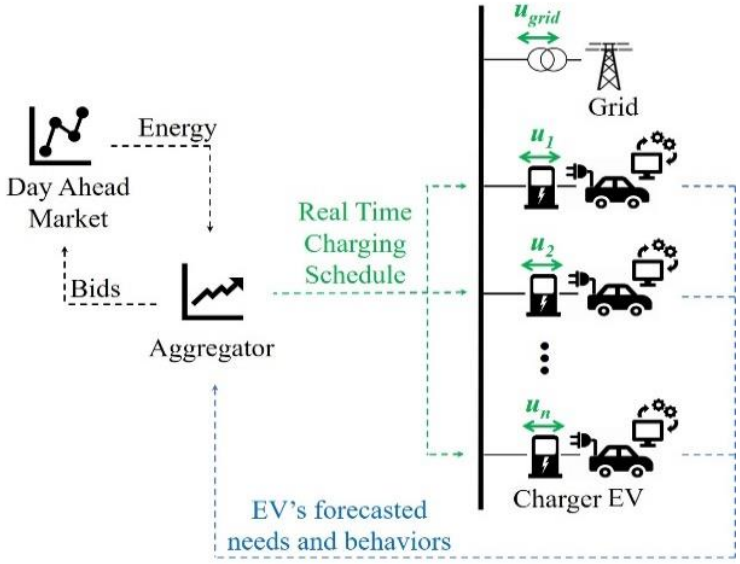

Figure 7.15: Schematic of EVs and aggregator Operation. The quantities $u_1, u_2, \ldots, u_n$ represent the power exchanged by the EVs.

For this demonstrative example actually , only 3 EVs are used and are always controllable in whatever chargers they end up stopping their car. Moreover their travel history and actual travles in simulations comes from car diaries field measurement. Figure 7.16 shows a flowchart containing the subroutine used to estimate the future use of a single EV. Without entering in too much detail, the algorithm order the past travels and for each day of the week identify the statistical mean and the more ordinary days and then applies k-medois clusterizzation in order to predict the typical number of trips, time needed and the energy cost of each travel. The most probable departure times are indicated with $\hat{d}_{\mathrm{j,z}}$, with j

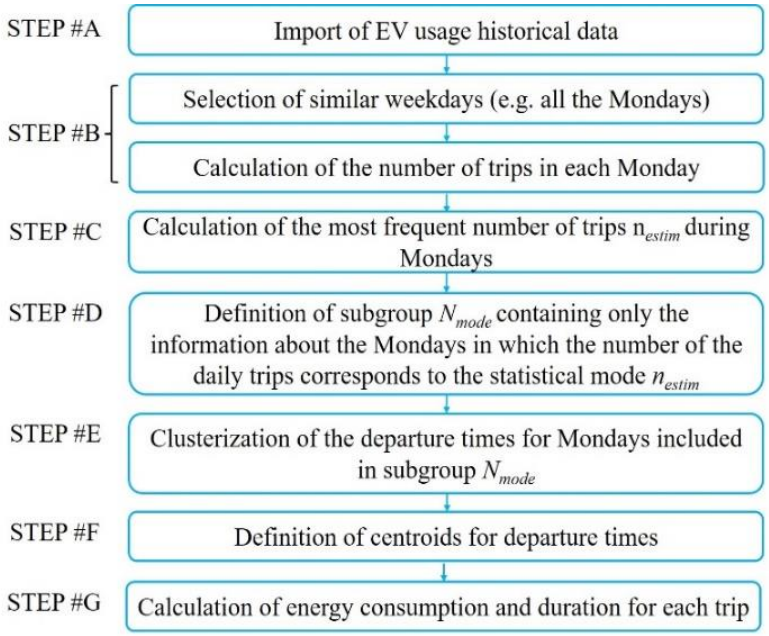

Figure 7.16: EV forecasts subroutine algorithm

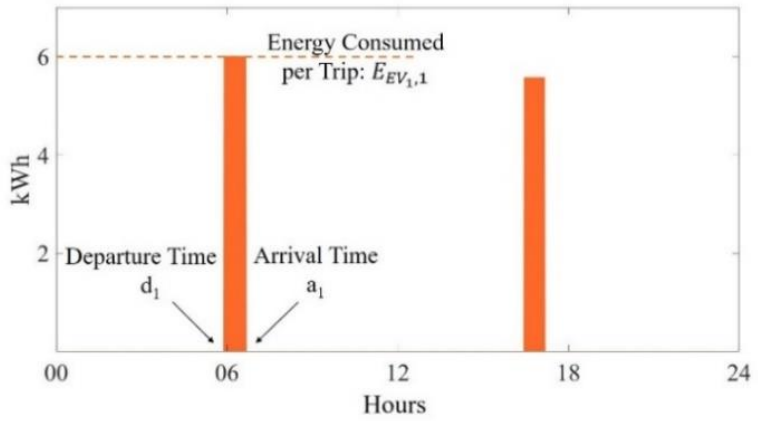

Figure 7.17: Output of the forecasting subroutine of the EV_1 usage profiles

= 1, ... , l where l represents the number of vehicles and z=1, ..., $Num_{\mathrm{EV_j}}$ where $Num_{\mathrm{EV_j}}$ is the number of the trips of the EV_j in the day and ˆ is used in order to identify the variables related to the forecasts. arrival time is indicated by $\hat{a}_{\mathrm{j,z}}$ and energy consumption by $\hat{E}_{\mathrm{EV_{j,z}}}$. An example of a prediction is shown in figure 7.17.

7.3.1 Problem formulation

Charger scheduling

Once the next day forecasted behaviors of the EVs are known, it is necessary to allocate the EVs in the respective chargers. The charger schedule algorithm provides, basing on the forecasts, a binary state signal $\hat{s}_{\mathrm{i,k}}$ which is sent to the aggregator and indicates if at time slot k, an EV is connected to the charger i, as defined in below.

$$\hat{s}_{\mathrm{i,k}} = \begin{cases} 1, & \text{if charger } i \text{ has an EV connected} \\ 0, & \text{if charger } i \text{ has not an EV connected} \end{cases} \tag{7.1}$$

The charger i in which the EVs are allocated during the day is chosen according to the forecasted behaviors in such a way that the charger changes at every departure time while at the end of the day the single EV returns at the charger from which it was parked at the beginning of the day. Fig. 7.18 shows an example of EVs allocation in the chargers. Given that, over the course of the day the single charger i can charge several EVs, thus a dynamic SoC $x_{\mathrm{i,k}}$ associated with the i-th charger needs to be defined. Firstly, the evolution of the energy stored in the EV battery is described by the following model:

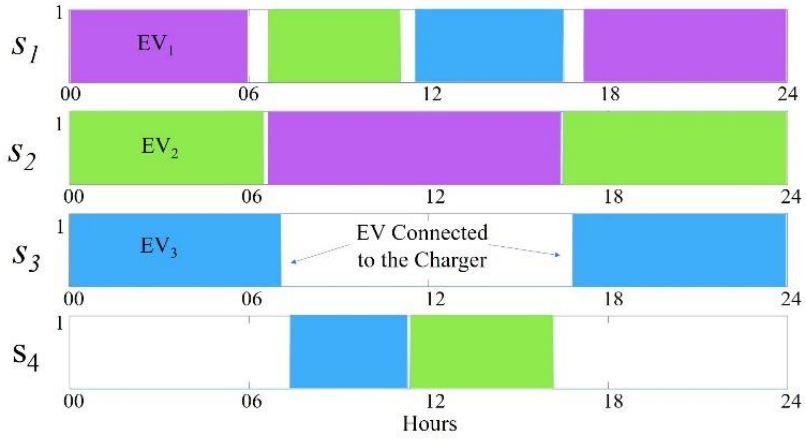

Figure 7.18: Forecasted EVs allocation in the chargers during a day. Different colors correspond to different electric vehicles.

$$\hat{SOC}_{\mathrm{j,k+1}} = \begin{cases} \hat{SOC}_{\mathrm{j,k}} + \Delta t \cdot u_{\mathrm{i,k}}, & \text{if } EV_j \text{ is connected in i} \\ \hat{SOC}_{\mathrm{j,k}} - \hat{E}_{\mathrm{EVj,k}}, & \text{if } k = \hat{d}_{\mathrm{j,z}} \text{ h} \\ \hat{SOC}_{\mathrm{j,k}}, & else \end{cases} \tag{7.2}$$

In Equation 7.2, Δt is the sampling time; $\hat{SOC}_{\mathrm{j,k}}$ is the accumulated energy in the EV_j battery through integration of the power $u_{\mathrm{i,k}}$ delivered from the charger i where the vehicle j is connected; $E_{\mathrm{EV_{j,z}}}$ is the forecasted consumed energy per trip and subtracted when the EV_j leaves the charger i; Therefore, the forecasted charger State of charge $\hat{x}_{\mathrm{i,k}}$ assumes the SoC of the relative connected EV during the charging/discharging operations ($\hat{s}_{\mathrm{i,k}} = 1$) while 0 if no car is plugged. The forecasted $\hat{x}_{\mathrm{i,k}}$ is mathematically defined as in equation below:

$$\hat{x}_{\mathrm{i,k+1}} = \begin{cases} \hat{x}_{\mathrm{i,k}} + \Delta t \cdot u_{\mathrm{i,k}}, & if\ \hat{s}_{\mathrm{i,k}} = 1 \vee \hat{a}_{\mathrm{j,z}} < k < \hat{d}_{\mathrm{j,z}} \\ \hat{SOC}_{\mathrm{j,k}}, & if\ \hat{s}_{\mathrm{i,k}} = 1, \vee k = \hat{a}_{\mathrm{j,z}} \\ \hat{0}, & if\ \hat{s}_{\mathrm{i,k}} = 0, \vee k = \hat{d}_{\mathrm{j,z}} \end{cases} \tag{7.3}$$

Finally, in order to guarantee that each vehicle will leave the charging station with a sufficiently high SoC to allow the performance of the next forecasted travel, the minimum departure $\hat{SOC}_{\mathrm{j,d_{j,z}}}$ is defined in equation below, where $SoC_{\min}$ represents a minimum security level, and a tolerance SoC percentage ΔSoC.

$$\hat{SOC}_{\mathrm{j,d_{j,z}}} = SoC_{\min} + E_{\mathrm{EV_{j,z}}} + \Delta SoC \tag{7.4}$$

Day ahead optimization based on the forecasts

The day ahead strategy evaluates the injected power ui, k at any time k for each charger i based on the forecasted EVs behaviors. Hence, optimality here refers to minimize the station operation costs guaranteeing at least the minimum SoC defined by the forecast of the next trip in equation 7.4. Then, the aggregator solves the following energy arbitrage optimal problem to obtain the charging profile:

$$\min_{u^*} \Delta t \sum_{k=1}^{N} (C_k \cdot \sum_{i=1}^{n} u_{\mathrm{i,k}} \tag{7.5a}$$

$$s.t.\ \textbf{Equ.7.3} \tag{7.5b}$$

$$0 \leq u_{\mathrm{i,k}} \leq \hat{s_{\mathrm{i,k}}} \cdot u_{\mathrm{i,max}}\ \ if\ \hat{SoC}_{\mathrm{j,k}} \leq SoC_{\min} \tag{7.5c}$$

$$-\hat{s_{\mathrm{i,k}}} \cdot u_{\mathrm{i,max}} \leq u_{\mathrm{i,k}} \leq hats_{\mathrm{i,k}} \cdot u_{\mathrm{i,max}}\ \ if\ \hat{SoC}_{\mathrm{j,k}} \geq SoC_{\min} \tag{7.5d}$$

$$0 \leq x_{\mathrm{i,k}} \leq x_{i,max} \tag{7.5e}$$

$$\hat{SoC}_{i,d_{j,i}} \leq x_{\mathrm{i,d_{j,z}}} \leq x_{i,max} \tag{7.5f}$$

$$\forall k = 1, ..., N; \forall i = 1, ..., n; \forall j = 1, ..., l; \forall z = 1, ..., Num_{\mathrm{EV_j}} \tag{7.5g}$$

where,$x_{\mathrm{i,k}}$ are the state variables corresponding to the charger SoC and $u_{\mathrm{i,k}}$ are the manipulated variables corresponding to delivered power profile. Finally, C_k are the energy prices per time step k and are assumed known. Moreover, $u_{\mathrm{i,max}}$

depends on the maximum power that the charger can deliver and the EV can accept. The output of the optimization are the optimized powers $u_{\mathrm{i,k}}$ over the day from each charger i. However, in order to participate at the day-ahead market the aggregator needs to provide its total power profile. Therefore, the optimized day ahead profile $P_{\mathrm{da,k}}$, is defined as follow:

$$P_{\mathrm{da,k}} = \sum_{i=1}^{n} u^{\star}_{\mathrm{i,k}} \tag{7.6}$$

Real time Logic

The real time functioning is operated by a priority-based logic which finally applies the effective charging/ discharging profile to each charger. This logic aims to apply the optimized day-ahead profile by splitting the $P_{\mathrm{da,k}}$ among the different chargers on the base of a defined Priority Index ($PI_{\mathrm{i,k}}$). The Priority Index, is a value, between 0 and 1, which represent the portion of the $P_{\mathrm{da,k}}$ that must be charged by the charger i according to the forecasted charging urgency of the connected vehicle j. It follows that the inverse of $PI_{\mathrm{i,k}}$ represents the discharging availability of each vehicle j as explicated in (7.7) Equation below and it is used in order to define EVs discharging status when aggregators is selling energy to the grid. The $PI_{\mathrm{i,k}}$, in (7.8), is obtained as the mean between other two indexes: the SoC Priority Index $SPI_{\mathrm{i,k}}$ and the Departure Priority Index $DPI_{\mathrm{i,k}}$. The $SPI_{\mathrm{i,k}}$ represents the charging urgency of the vehicle j with respect to its departure energy needs. It is defined in (7.9), as the ratio between the forecasted departure SoC of the vehicle j connected in i at the time step $k(SoC_{\mathrm{j,d}})$, and the sum in j of the forecasted departure state of charge of the other vehicles. In a similar way $DPI_{\mathrm{i,k}}$ is defined in (7.10). This index aims to identify the charging urgency on the base of the next departure time of the vehicle j.

$$u_{\mathrm{i,k}} = \begin{cases} P_{\mathrm{da,k}} \cdot PI_{\mathrm{i,k}}, & if\ P_{\mathrm{da,k}} > 0 \\ P_{\mathrm{da,k}} \cdot \frac{1}{PI_{\mathrm{i,k}}}, & if\ P_{\mathrm{da,k}} \leq 0 \end{cases} \tag{7.7}$$

$$PI_{\mathrm{i,k}} = mean(DPI_{\mathrm{i,k}}; SPI_{\mathrm{i,k}}) \tag{7.8}$$

$$SPI_{\mathrm{i,k}} = \begin{cases} \frac{\hat{SoC_{j,d_{j,z}}}}{\sum_{j=1}^{n} \hat{SoC_{\mathrm{j,d_{j,z}}}}}, & if\ EV_j\ in\ i\ at\ k \\ 0, & else \end{cases} \tag{7.9}$$

$$DPI_{\mathrm{i,k}} = \begin{cases} \frac{1/\hat{d}_{j,z}}{1/\sum_{j=1}^{n} \hat{d_{j,z}}}, & if\ EV_j\ in\ i\ at\ k \\ 0, & else \end{cases} \tag{7.10}$$

$$\forall k = 1, ..., N; \forall i = 1, ..., n; \forall j = 1, ..., l; \forall z = 1, ..., Num_{\mathrm{EV_j}} \tag{7.11}$$

This strategy only divides the available power bought at the day ahead between the cars present in real time. However, if the forecasts are close to the actual EVs behavior, this control will be able to recharge the cars at the right point in order to reach the needed actual SoC for the next trip ($SoC_{\mathrm{j,d_{j,z}}}$).

7.3.2 Case study and results

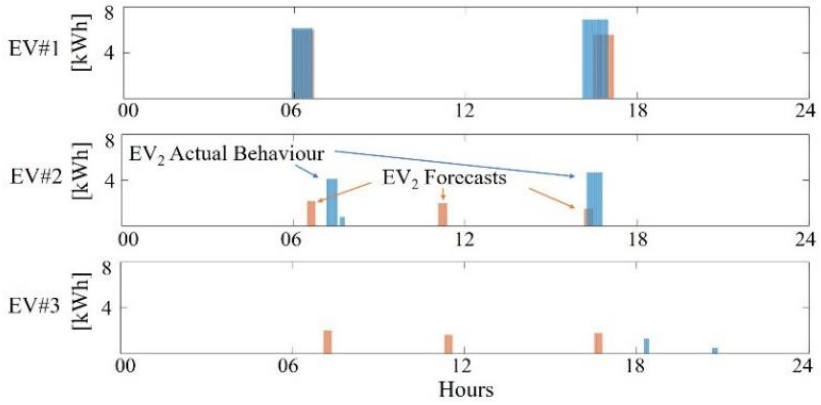

Figure 7.19: EVs usage scenarios: actual (blue) and forecasts (red)

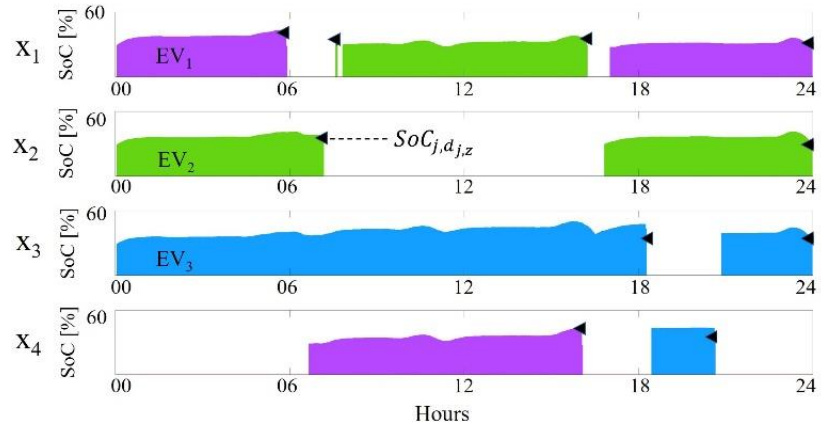

Figure 7.20: EVs allocation and chargers SoC evolution during the day

The proposed methodology is tested on a simple case study with three EVs. The EV historical data have been selected through a clusterization analysis among

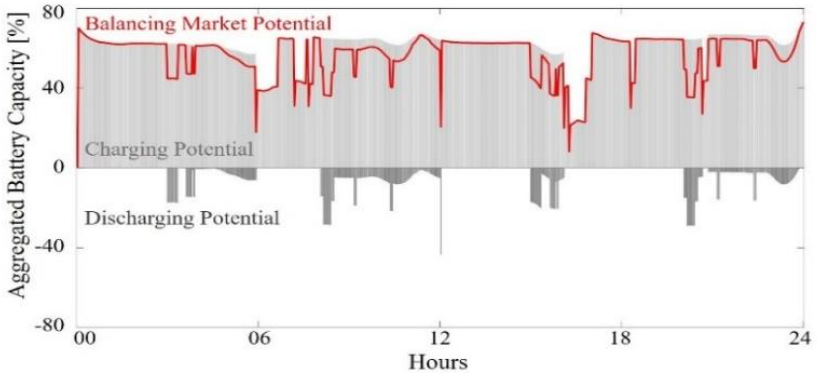

Figure 7.21: Charging, Discharging and Balancing market potential over the day of the simulation for the three EVs

a database composed of 215 EV real usage behaviors available in [3] and covering three years of recording (2013-2015). As a result, EV1, EV2 and EV3 are different and well represent three typical electric vehicle usage profiles. In particular, EV1 represent the highest energy consuming and contemporarily the most systematic usage profile. On the other hand, EV3 represents the lowest energy consumption and contemporarily the most variable usage profile. EV2, represents a medium behavior. Figure 7.19, shows EV1, EV2 and EV3 usage profiles and the respective forecasts. According to the analysis conducted in [69], the chosen battery capacity of each vehicle is 40 kWh, and the considered initial state of charge is assumed to be 30%. The energy prices refer to the December 13th, 2017 Italian market, chosen because it registers the highest prices mean value and contemporarily the highest standard deviation compared to the other days of the year [4].

Since the energy requested from each EV during a day is a marginal part of its installed battery capacity, the power profile that minimizes the cost function (7.5a, makes use of only a small part of the total available battery capacity for the aggregator. Furthermore, under the assumption that the cars are connected to the same aggregator when not traveling, there is no time period where no car is connected. From the above, it follows that the optimized power profile bought at day-ahead market $P_{\mathrm{da,k}}$, results perfectly respected in the real-time operation, thus avoiding any liability to the network. Moreover, in the examined case study, the proposed methodology was always able to guarantee the mobility needs of each EV users. Fig. 7.20, provide an entire overview of the system operation of

[3] My Electric Avenue Data, 2015. [Online]. Available: http://myelectriavenue.info/

[4] GME (Gestore Mercati energetici), Italian Market Operator: https://www.mercatoelettrico.org/En/Default.aspx

the elapsed day operated by the real time logic. In particular, is shown the SoC evolution of the three EVs while it is highlighted the departure State of Charge $\hat{SoC}_{j,d_{j,z}}$, that guarantee the actual EVs trips. For sake of clarity, $SoC_{j,d_{j,z}}$, is calculated similarly to equation 7.4 by using the actual consumed energy per trip $E_{EV_{j,z}}$. From figure 7.20, it can be seen that the state of charge of the EVs at the departure times is always higher than the $SoC_{j,d_{j,z}}$. Table I lists the cost due to the total energy bought from the aggregator to satisfy the mobility needs of its clients and the revenues due to the V2G operations. Moreover, in order to provide the effect of the forecasts and investigate the full potential of the methodology, Table I, shows the costs obtained in the case of exact predictions. The results highlight a cost saving for the aggregator close to 60%. Note that, the deviations in savings between solutions with exact and forecasted EVs information, is just 3%. This suggests that the single EV forecasts errors can be easily mitigated thanks to the EVs aggregated behavior.

7.3.3 integrating frequency control into Priority based logic

As seen in previous chapters, especially fifht and sixth, typical SOC profile of BESSs during PFC varies according to the day and it is composed by three parts: inefficiency, intraday oscillations and mean part. the strategy depicted here to deal with day ahead-real time balancing has to be integrated to deal with frequency control. Some initial hints to how this can happen and how the control algorithm can still be improved:

- work with tolerance ΔSoC: in order to keep a certain amount of SoC margin both in charge and in discharge ΔSoC could be rised to a somewhat mid stand point between $SoC_{\min}$ and $SoC_{\max}$. As for now in order to minimize cost Aggregator makes EVs work at low SoC giving rise to a good potential to charge but not enough space to discharge (see figure 7.21) . A better study of the three components (predicability, forecastability etc...) can generate even better ways to cope with the SoC dynamics.

- Integrate Intraday market participation. Participation to intraday can be integrated in order to better adjust the SoC of EVs in case of too much charging or lower discharging. The current status of electric vehicles average SoC and DPI and SPI index can be used to predict how much energy should be purchased/sell. The more the forecast are good the more is possible to optimize better. The three index could be unified exploiting the concept of laxity introduced in [121].

- In case of aggregators with big EVs numbers, more precisions in forecast and real time control can be gained by passing from a total centralized control in

which forecasts, day ahead and real time goes form a central unit to single EVs to a more decentralized frameworks in which forecasts and dispatching orders pass thorough the use of charging stations (composed by n chargers i).Forecasts and relevant index (average SOC, SPI, DPI) can be reformulate and better used at charging stations level.

Conclusion

Following the chapters order, we may recap the following key points:

- Europe is the most ambitious continent for what concern de-carbonizzation, aiming to reach substantial zero GHG emissions within 2050. Although many efforts are being done, there is still a significant mismatch between our goal and our current direction.
- Converters are going to replace Synchronous Generators due to the increase of RESs and new resources into the grid. System stability can be jeopardized by this change. In particular, Frequency stability depends on the inertia and reserves provided by conventional generation plants. BESS are already being used in order to fulfill fast frequency services in addition to other uses.
- Three categories of studies about BESS performance performing fast frequency control can be conceptualized after a critical review of the literature. Open loop studies are concerned with BESS economics and SoC management. Researchers try to optimize SoC by exploiting variable droop strategies or activating slower resources. More complex attempts make use of multi-units aggregation or BESS participation to multiple services in order to maximize BESS profits. Every solution must be designed taking into account the country specific market rules. The battery model and the degradation process have a great influence on the results. An interesting opportunity for further research could be to devise experimental methodologies in order to recreate empirical models which are able to describe accurately BESS dynamics and degradation maintaining at the same time maintain low computational complexity. The second group is about the impact of BESS after a contingency. The current researches substantially agree in the fact that Rocof control from BESSs can actually work as a substitute for physical inertia, even considering the presence delays and the Phase Locked Loop measurements systems. Hardware in the loop experiments and field tests could add more insights on this issue and in the possible problems arising in

digital controllers performing Rocof control. Voltage Source Converter set-up should also be considered essential for a future converter dominated grid. Distributed control with converter sharing frequency or other control signals is an interesting opportunity which still needs a better focus to evaluate the possibility of gaining more stability for the grid. Finally the last group deals with the impact of BESS during normal operations. A substantial absence of clear and systematic methodologies to reproduce typical frequency variations in the grid was identified. The develop of such a method could help us to evaluate the performance of BESSs and the impact of Variable Droop Strategy or more complex frequency controls on the frequency signal itself.

- In chapter 4 the impact of Rocof and fast PFC by BESSs were assessed. The simulation of the Sardinian Island and the parametric analysis on the two area system showed us how RoCof is useful in smoothing the frequency signal after a contingency, even in the presence of small delays. The performed simulations help us to understand the minimal levels of inertia and reserves to assure that frequency dynamics to be acceptable (especially for what concerns initial RoCof and f_{nadir}). The BESS intervention was dimensioned according to the saturation point of typical Synchronous generators in order to design comparable services. In the Sardian system a 40-50 % decrease in inertia can lead to frequency problems, besides 100 MW of BESSs are more than enough to guarantee good frequency dynamics. Best strategy is to reserve half of the band for RoCof and half for PFC.

- From the simulations in chapter 5, many hints and results can be extracted. By reproducing a real frequency signal in a SFRM it is in fact possible to appreciate that Rocof control has a very small impact under normal grid conditions and that PFC of BESSs is almost comparable to CGs impact. This is due to the slow nature of deterministic frequency deviations which represent the most part of the frequency signal. Moreover, during a contingency Rocof control and PFC are almost complementary with RoCof control being requested within the first 1-2 seconds and PFC being requested slightly after. This suggests that instead of dividing the power bands between the two control channels, the best approach would be to use at the same time the two services with the full bands: during a contingency a double full band will guarantee the best frequency control, while during normal operations RoCof band will be almost no used and it will leave space for PFC.

  The SoC profile of BESSs was investigated during the provision of PFC. This laeds to discover that inefficiencies account much less with respect to intraday swings and SoC decrease or increase, due to the average of the frequency signal. This analysis gives important hints to the best strategy to be devised

for better SoC management. By simplifying the converter dynamics with a power balance over the DC link and using a fast pole to account for converter delays, we can make use of a BESS complete electrical equivalent model together with a computational light SFRM model. Finally few indexes are introduced in order to detect jumps in the irish frequency signal used for the simulations. Jumps will be then analyzed in order to compute and record their frequency range, duration and estimated load mismatch. The starting hypothesis is that jumps are created by TSOs activated reserves and their objective is to re-establish frequency under a certain range. This process is part of the frequency deterministic deviations phenomena.

- In chapter 6, another methodology to create a realistic frequency signal is used in which the goal is to reproduce the average harmonic content of real data. These data are characterized by similar harmonic content in the different days, so that their average behaviour is realistic and can function as a standardized test case. It was also possible to estimate the deterministic and stochastic frequency deviations proportions in the simulated frequency signal. As expected they are about 85 % to 15 % for deterministic slow deviations. BESS PFC efficacy was compared with conventional generation and results just slightly better than fast conventional resources, due to the slow nature of frequency oscillations. In the case of faster frequency dynamics scenarios, BESSs would have much more efficacy. Finally it was possible to simulate the impact of Variable Droop Strategy on the frequency signal. While SoC standard deviation has an appreciable standard deviation decrease (around 6-8 %), the frequency signal remains substantially equal.

- In chapter 7 a complete framework is presented in order to correctly model the impact of EVs in frequency control. An agent based model was developed to create vast scale scenarios simulations with thousand of EVs interacting in road and electric networks. A dumb charging was used to asses the impact of EVs. The impact is not negligible and depends on the R-X ratio of the lines. Voltage changes are up to 3.5% and current in the branches can increase even up to 20 %. This example justify the need for an explicit Distribution System description when evaluating the potential of EVs for frequency control. Bottlenecks at the distribution level can effectively prevent PFC from EVs. A smart strategy for EVs control was presented in the second part considering day ahead energy optimization with real time balancing from the EVs Aggregators. This strategy can be enhanced considering frequency control.

Many possibilities are left as future works. For electric vehicles main steps and

ideas to continue the research have been already presented in Chapter 7. For the sake of brevity I add just a single idea for what concerns BESSs frequency control. By using the frequency recorded data from European Continental system and the frequency reserves data published by ENTSO-E, it could be possible to enhance the model built in Chapter 5 as a Two Area system (Italy and the rest of Europe) similarly to the one proposed in Chapter 4. European system, contrarily to the Irish one, posses secondary and tertiary frequency control. It could be interesting to quantify the BESSs distortion effects in a real electric system due to Variable droop strategy considering also the presence of secondary frequency control and the effects on a Two Area system. With respect to Chapter 6 more than one initial SoC for the various BESSs systems can be considered in the same simulation. For example 10 different values could be chosen to consider all the possible situations that can happen during real operations of the power systems. Rainflow counting can be also used to better evaluate battery degradation.

Bibliography

[1] 50Hertz et al. *TSO proposal for the establishment of common and harmonised rules and processes forthe exchange and procurement of balancing capacity for frequency containment reserves (fcr) in accordance with article 33 of commission regulation (eu) 2017/ 2195 establishing a guideline on electricity balancing*. 2018. URL: https://docstore.entsoe.eu/Documents/Network%5C%20codes%5C%20documents/NC%5C%20EB/FCR_%20Proposal-Article%5C%2033_1_EBGL_20180426_FV.PDF (visited on 10/01/2020).

[2] Atinuke Ademola-Idowu and Baosen Zhang. "Optimal Design of Virtual Inertia and Damping Coefficients for Virtual Synchronous Machines". In: *2018 IEEE Power & Energy Society General Meeting (PESGM)*. IEEE. 2018, pp. 1–5.

[3] International Energy Agency. "World energy Outlook". In: *Paris, France* (2018).

[4] Samir M Alhejaj and Francisco M Gonzalez-Longatt. "Impact of inertia emulation control of grid-scale BESS on power system frequency response". In: *2016 International Conference for Students on Applied Engineering (ICSAE)*. IEEE. 2016, pp. 254–258.

[5] PM Rocha Almeida, Filipe Joel Soares, and JA Peças Lopes. "Electric vehicles contribution for frequency control with inertial emulation". In: *Electric Power Systems Research* 127 (2015), pp. 141–150.

[6] M Hadi Amini, Mohsen Parsa Moghaddam, and Orkun Karabasoglu. "Simultaneous allocation of electric vehicles' parking lots and distributed renewable resources in smart power distribution networks". In: *Sustainable Cities and Society* 28 (2017), pp. 332–342.

[7] Paul M Anderson and Aziz A Fouad. *Power system control and stability*. John Wiley & Sons, 2008.

[8] Philip M Anderson and Mahmood Mirheydar. "A low-order system frequency response model". In: *IEEE Transactions on Power Systems* 5.3 (1990), pp. 720–729.

[9] Göran Andersson. "Modelling and analysis of electric power systems". In: *ETH Zurich* (2008), pp. 5–6.

[10] A Anisie and Boshell F. "Utility Scale Batteries: Innovation Landscape Brief". In: *International Renewable Energy Agency: Abu Dhabi, UAE* (2019).

[11] *Annual Energy Outlook 2019 with projections to 2050*. Tech. rep. US Energy Information Administration, 2019.

[12] Francesco Arrigo, Marco Merlo, and Ferdinando Parma. "Fourier transform based procedure for investigations on the grid frequency signal". In: *2017 IEEE PES Innovative Smart Grid Technologies Conference Europe (ISGT-Europe)*. IEEE. 2017, pp. 1–6.

[13] F Arrigo et al. "Assessment of primary frequency control through battery energy storage systems". In: *International Journal of Electrical Power & Energy Systems* 115 (2020), p. 105428.

[14] Simone Barcellona and Luigi Piegari. "Lithium ion battery models and parameter identification techniques". In: *Energies* 10.12 (2017), p. 2007.

[15] Roberto Benato et al. "Large-scale electrochemical energy storage in high voltage grids: Overview of the Italian experience". In: *energies* 10.1 (2017), p. 108.

[16] Hassan Bevrani. *Robust power system frequency control*. Springer, 2014.

[17] Yuankai Bian et al. "Demand side contributions for system inertia in the GB power system". In: *IEEE Transactions on Power Systems* 33.4 (2017), pp. 3521–3530.

[18] Fabio Bignucolo et al. "Integration of lithium-ion battery storage systems in hydroelectric plants for supplying primary control reserve". In: *Energies* 10.1 (2017), p. 98.

[19] E Bompard et al. *Report on opportunities and options for PtG in power systems*.

[20] Theodor S Borsche, Juan de Santiago, and Göran Andersson. "Stochastic control of cooling appliances under disturbances for primary frequency reserves". In: *Sustainable Energy, Grids and Networks* 7 (2016), pp. 70–79.

[21] Theodor S Borsche, Andreas Ulbig, and Göran Andersson. "Impact of frequency control reserve provision by storage systems on power system operation". In: *IFAC Proceedings Volumes* 47.3 (2014), pp. 4038–4043.

[22] Theodor Borsche, Andreas Ulbig, and Goran Andersson. "A new frequency control reserve framework based on energy-constrained units". In: *2014 Power Systems Computation Conference*. IEEE. 2014, pp. 1–7.

[23] Theodor Borsche et al. "Power and energy capacity requirements of storages providing frequency control reserves". In: *2013 IEEE Power & Energy Society General Meeting*. IEEE. 2013, pp. 1–5.

[24] Claudio Brivio, Stefano Mandelli, and Marco Merlo. "Battery energy storage system for primary control reserve and energy arbitrage". In: *Sustainable Energy, Grids and Networks* 6 (2016), pp. 152–165.

[25] Paul Vincent Brogan et al. "Effect of BESS Response on Frequency and RoCoF During Underfrequency Transients". In: *IEEE Transactions on Power Systems* 34.1 (2018), pp. 575–583.

[26] Ye Cai et al. "Self-sustainable community of electricity prosumers in the emerging distribution system". In: *IEEE Transactions on Smart Grid* 8.5 (2016), pp. 2207–2216.

[27] Silvia Canevese, Adriano Iaria, and Marco Rapizza. "Impact of fast primary regulation and synthetic inertia on grid frequency control". In: *2017 IEEE PES Innovative Smart Grid Technologies Conference Europe (ISGT-Europe)*. IEEE. 2017, pp. 1–6.

[28] S Canevese et al. "Battery Energy Storage Systems for frequency regulation: Simplified aging evaluation". In: *2017 6th International Conference on Clean Electrical Power (ICCEP)*. IEEE. 2017, pp. 291–297.

[29] Jun Cao et al. "Optimal sizing and control strategies for hybrid storage system as limited by grid frequency deviations". In: *IEEE Transactions on Power Systems* 33.5 (2018), pp. 5486–5495.

[30] Pantelis Capros et al. "EU Reference Scenario 2016-Energy, transport and GHG emissions Trends to 2050." In: (2016).

[31] Pantelis Capros et al. "Outlook of the EU energy system up to 2050: The case of scenarios prepared for European Commission's "clean energy for all Europeans" package using the PRIMES model". In: *Energy strategy reviews* 22 (2018), pp. 255–263.

[32] Smart Grid Coordination CEN-CENELEC-ETSI. "Group.(2012)". In: *Smart Grid Reference Architecture* (2012), pp. 1–107.

[33] Shuaixun Chen et al. "Penetration rate and effectiveness studies of aggregated BESS for frequency regulation". In: *IEEE Transactions on Smart Grid* 7.1 (2015), pp. 167–177.

[34] Bolong Cheng and Warren B Powell. "Co-optimizing battery storage for the frequency regulation and energy arbitrage using multi-scale dynamic programming". In: *IEEE Transactions on Smart Grid* 9.3 (2016), pp. 1997–2005.

[35] Yunzhi Cheng et al. "Dynamic available AGC based approach for enhancing utility scale energy storage performance". In: *IEEE Transactions on Smart Grid* 5.2 (2014), pp. 1070–1078.

[36] *China Renewable Energy Outlook*. Tech. rep. Energy Research Institute of Academy of Macroeconomic Research and China National Renewable Energy Centre, 2018.

[37] Woo Yeong Choi and Kyung Kook. "Impact Analysis of BESS for Providing Frequency Response in Korean Power System". In: Oct. 2017.

[38] European Commission. *Commission Regulation (EU) 2017/1485 of establishing a guideline on electricity transmission system operation*. 2017.

[39] M Coppo et al. "The Italian smart grid pilot projects: Selection and assessment of the test beds for the regulation of smart electricity distribution". In: *Electric Power Systems Research* 120 (2015), pp. 136–149.

[40] Dennis W Dees, Vincent S Battaglia, and André Bélanger. "Electrochemical modeling of lithium polymer batteries". In: *Journal of power sources* 110.2 (2002), pp. 310–320.

[41] Nicholas DeForest, Jason S MacDonald, and Douglas R Black. "Day ahead optimization of an electric vehicle fleet providing ancillary services in the Los Angeles Air Force Base vehicle-to-grid demonstration". In: *Applied energy* 210 (2018), pp. 987–1001.

[42] Maurizio Delfanti, Davide Falabretti, and Marco Merlo. "Energy storage for PV power plant dispatching". In: *Renewable Energy* 80 (2015), pp. 61–72.

[43] Gauthier Delille, Bruno Francois, and Gilles Malarange. "Dynamic frequency control support by energy storage to reduce the impact of wind and solar generation on isolated power system's inertia". In: *IEEE Transactions on sustainable energy* 3.4 (2012), pp. 931–939.

[44] Florian Dörfler, John W Simpson-Porco, and Francesco Bullo. "Breaking the hierarchy: Distributed control and economic optimality in microgrids". In: *IEEE Transactions on Control of Network Systems* 3.3 (2015), pp. 241–253.

[45] Mohammad Dreidy, H Mokhlis, and Saad Mekhilef. "Inertia response and frequency control techniques for renewable energy sources: A review". In: *Renewable and Sustainable Energy Reviews* 69 (2017), pp. 144–155.

[46] Adam Dyśko et al. "Assessment of Risks Resulting from the Adjustment of ROCOF Based Loss of Mains Protection Settings Phase II". In: *University of Strathclyde, ref: NGC/LOM/TR/2013-001b* (2013).

[47] EirGrid/SONI. *DS3 Joint Grid Code Working Group Position Paper on RoCoF*. Tech. rep. 2012.

[48] EirGrid/SONI. *RoCoF Modification Proposal - TSOs' Recommendations*. Tech. rep. 2012.

[49] Eirgrid and SONI. *All-island ten year transmission forecast statement*. 2017.

[50] P Energy. "Rate of change of frequency (ROCOF)-review of TSO and generator submissions final report". In: (2013).

[51] Jonas Engels, Bert Claessens, and Geert Deconinck. "Techno-economic analysis and optimal control of battery storage for frequency control services, applied to the German market". In: *Applied energy* 242 (2019), pp. 1036–1049.

[52] ENTSO-E. "Continental Europe significant frequency deviations". In: (2019).

[53] ENTSO-E. *Frequency Stability Evaluation Criteria for The Synchronous Zone of Continental Europe*. 2016.

[54] ENTSO-E. *Network Code on Emergency and Restoration*. 2017. URL: http://www.entsoe.eu/network_codes/load/ (visited on 10/07/2019).

[55] ENTSO-E. *Network Code on Load-Frequency Control and Reserves*. 2013. URL: http://www.entsoe.eu/network_codes/load/ (visited on 10/07/2019).

[56] ENTSO-E. *Network Code on System Operations*. 2017. URL: http://www.entsoe.eu/network_codes/load/ (visited on 10/07/2019).

[57] ENTSO-E. *Supporting Document for the Network Code on Load-Frequency Control and Reserves*. 2013. URL: https://www.acer.europa.eu/Official_documents/Acts_of_the_Agency/Annexes/ (visited on 10/07/2019).

[58] Mircea Eremia and Mohammad Shahidehpour. *Handbook of electrical power system dynamics: modeling, stability, and control*. Vol. 92. John Wiley & Sons, 2013.

[59] Joint Investigation Team EURELECTRIC—ENTSO-E. "Deterministic Frequency Deviations—Root Causes and Proposals for Potential Solutions". In: *EURELECTRIC: Brussels, Belgium* (2011).

[60] Michele Falco et al. "Agent-based Modelling to Evaluate the Impact of Plug-in Electric Vehicles on Distribution Systems". In: *2019 International Conference on Smart Energy Systems and Technologies (SEST)*. IEEE. 2019, pp. 1–6.

[61] Ricardo Fernandes. "Simulation of a Subcritical Power Plant using a Boiler Following Control sequence". In: (2012).

[62] Masoud Hajiakbari Fini and Mohamad Esmail Hamedani Golshan. "Determining optimal virtual inertia and frequency control parameters to preserve the frequency stability in islanded microgrids with high penetration of renewables". In: *Electric Power Systems Research* 154 (2018), pp. 13–22.

[63] Marco Giacomo Flammini et al. "Interaction of consumers, photovoltaic systems and electric vehicle energy demand in a Reference Network Model". In: *2017 International Conference of Electrical and Electronic Technologies for Automotive*. IEEE. 2017, pp. 1–5.

[64] Johannes Fleer and Peter Stenzel. "Impact analysis of different operation strategies for battery energy storage systems providing primary control reserve". In: *Journal of Energy Storage* 8 (2016), pp. 320–338.

[65] Johannes Fleer et al. "Techno-economic evaluation of battery energy storage systems on the primary control reserve market under consideration of price trends and bidding strategies". In: *Journal of Energy Storage* 17 (2018), pp. 345–356.

[66] *Frequency Stability Evaluation Criteria for The Synchronous Zone of Continental Europe*. Tech. rep. ENTSO-E, 2016.

[67] Ana Gadea, Mattia Marinelli, and Antonio Zecchino. "A market framework for enabling electric vehicles flexibility procurement at the distribution level considering grid constraints". In: *2018 Power Systems Computation Conference (PSCC)*. IEEE. 2018, pp. 1–7.

[68] Helena Gerard, Enrique Rivero, and Daan Six. "Basic schemes for TSO-DSO coordination and ancillary services provision". In: *SmartNet Deliv. D* 1 (2016), p. 3.

[69] Francesco Giordano et al. "Self-consumption improvement for a nanogrid with photovoltaic and vehicle-to-home technologies". In: *2018 IEEE International Conference on Environment and Electrical Engineering and 2018 IEEE Industrial and Commercial Power Systems Europe (EEEIC/I&CPS Europe)*. IEEE. 2018, pp. 1–6.

[70] Francisco M Gonzalez-Longatt. "Effects of fast acting power controller of BESS in the system frequency response of a multi-machine system: probabilistic approach". In: *2018 IEEE Innovative Smart Grid Technologies-Asia (ISGT Asia)*. IEEE. 2018, pp. 798–803.

[71] Josep M Guerrero et al. "Hierarchical control of droop-controlled AC and DC microgrids—A general approach toward standardization". In: *IEEE Transactions on industrial electronics* 58.1 (2010), pp. 158–172.

[72] Mohammad Hesam Hafezi, Lei Liu, and Hugh Millward. *Modeling Activity Scheduling Behavior of Travelers for Activity-Based Travel Demand Models*. Tech. rep. 2018.

[73] Hua Han et al. "Review of power sharing control strategies for islanding operation of AC microgrids". In: *IEEE Transactions on Smart Grid* 7.1 (2015), pp. 200–215.

[74] Sekyung Han, Soohee Han, and Kaoru Sezaki. "Optimal control of the plug-in electric vehicles for V2G frequency regulation using quadratic programming". In: *ISGT 2011*. IEEE. 2011, pp. 1–6.

[75] Jesus C Hernández et al. "Primary frequency control and dynamic grid support for vehicle-to-grid in transmission systems". In: *International Journal of Electrical Power & Energy Systems* 100 (2018), pp. 152–166.

[76] Tim Hilgert et al. "Modeling week activity schedules for travel demand models". In: *Transportation Research Record* 2666.1 (2017), pp. 69–77.

[77] Linbin Huang et al. "A virtual synchronous control for voltage-source converters utilizing dynamics of DC-link capacitor to realize self-synchronization". In: *IEEE Journal of Emerging and Selected Topics in Power Electronics* 5.4 (2017), pp. 1565–1577.

[78] IEEE. "IEEE standard for synchrophasors for power systems". In: *IEEE Standard* 37 (2005), pp. 118–2005.

[79] Wardah Inam et al. "Stability, control, and power flow in ad hoc dc microgrids". In: *2016 IEEE 17th Workshop on Control and Modeling for Power Electronics (COMPEL)*. IEEE. 2016, pp. 1–8.

[80] IRENA. *Battery Storage for Renewables: Market Status and technology outlook*. 2016.

[81] C ISO. "What the duck curve tells us about managing a green grid". In: *Calif. ISO, Shap. a Renewed Futur* (2012), pp. 1–4.

[82] Pietro Iurilli, Claudio Brivio, and Marco Merlo. "SoC management strategies in Battery Energy Storage System providing Primary Control Reserve". In: *Sustainable Energy, Grids and Networks* 19 (2019), p. 100230.

[83] Seyedmahdi Izadkhast, Pablo Garcia-Gonzalez, and Pablo Fri********** "An aggregate model of plug-in electric vehicles for primary frequency control". In: *IEEE Transactions on Power Systems* 30.3 (2014), pp. 1475–1482.

[84] Seyedmahdi Izadkhast et al. "Design of plug-in electric vehicle's frequency-droop controller for primary frequency control and performance assessment". In: *IEEE Transactions on Power Systems* 32.6 (2017), pp. 4241–4254.

[85] Hyeondeok Jo et al. "Development of frequency control performance evaluation criteria of BESS for ancillary service: A case study of frequency regulation by KEPCO". In: *2017 IEEE Innovative Smart Grid Technologies-Asia (ISGT-Asia)*. IEEE. 2017, pp. 1–5.

[86] Ali Jokar et al. "Review of simplified Pseudo-two-Dimensional models of lithium-ion batteries". In: *Journal of Power Sources* 327 (2016), pp. 44–55.

[87] Mostafa Kazemi and Hamidreza Zareipour. "Long-term scheduling of battery storage systems in energy and regulation markets considering battery's lifespan". In: *IEEE Transactions on Smart Grid* 9.6 (2017), pp. 6840–6849.

[88] Mostafa Kazemi et al. "Operation scheduling of battery storage systems in joint energy and ancillary services markets". In: *IEEE Transactions on Sustainable Energy* 8.4 (2017), pp. 1726–1735.

[89] Ruud Kempener and Eric Borden. "Battery storage for renewables: Market status and technology outlook". In: *International Renewable Energy Agency, Abu Dhabi* (2015), p. 32.

[90] Thongchart Kerdphol et al. "Robust virtual inertia control of an islanded microgrid considering high penetration of renewable energy". In: *IEEE Access* 6 (2017), pp. 625–636.

[91] M Khalid and AV Savkin. "An optimal operation of wind energy system for frequency control based on model predictive control". In: *Renewable energy* 48 (2012), pp. 127–132.

[92] Vaclav Knap et al. "Sizing of an energy storage system for grid inertial response and primary frequency reserve". In: *IEEE Transactions on Power Systems* 31.5 (2015), pp. 3447–3456.

[93] Michael Koller et al. "Review of grid applications with the Zurich 1 MW battery energy storage system". In: *Electric Power Systems Research* 120 (2015), pp. 128–135.

[94] Benjamin Kroposki et al. "Achieving a 100% renewable grid: Operating electric power systems with extremely high levels of variable renewable energy". In: *IEEE Power and Energy Magazine* 15.2 (2017), pp. 61–73.

[95] Prabha Kundur et al. "Definition and classification of power system stability". In: *IEEE transactions on Power Systems* 19.2 (2004), pp. 1387–1401.

[96] Prabha Kundur, Neal J Balu, and Mark G Lauby. *Power system stability and control*. Vol. 7. McGraw-hill New York, 1994.

[97] H-J Kunisch, KG Kramer, and H Dominik. "Battery energy storage another option for load-frequency-control and instantaneous reserve". In: *IEEE Transactions on Energy Conversion* 3 (1986), pp. 41–46.

[98] *Lavoro e Retribuzioni, occupazioni dipendenti e retribuzioni*. Tech. rep. Italian Institute of Statistichs, 2017.

[99] Rachel Lee et al. "A closed-loop analysis of grid scale battery systems providing frequency response and reserve services in a variable inertia grid". In: *Applied Energy* 236 (2019), pp. 961–972.

[100] Bei Li et al. "Coordinated scheduling of a gas/electricity/heat supply network considering temporal-spatial electric vehicle demands". In: *Electric Power Systems Research* 163 (2018), pp. 382–395.

[101] Tao Liu, David J Hill, and Congchong Zhang. "Non-disruptive load-side control for frequency regulation in power systems". In: *IEEE transactions on smart grid* 7.4 (2016), pp. 2142–2153.

[102] Mihai Sănduleac Lucian Toma and Stefan Andrei Baltac. *Deliverable 2.1. Review of relevance of current techniques to advanced frequency control*. Tech. rep. RESERVE European project, 2017.

[103] Charles M Macal and Michael J North. "Agent-based modeling and simulation". In: *Proceedings of the 2009 Winter Simulation Conference (WSC)*. IEEE. 2009, pp. 86–98.

[104] Sven Maerivoet and Bart De Moor. "Cellular automata models of road traffic". In: *Physics reports* 419.1 (2005), pp. 1–64.

[105] Yuri V Makarov et al. "Sizing energy storage to accommodate high penetration of variable energy resources". In: *IEEE Transactions on sustainable Energy* 3.1 (2011), pp. 34–40.

[106] Jürgen Marchgraber, Wolfgang Gawlik, and Günter Wailzer. "Reducing SoC-Management and losses of battery energy storage systems during provision of frequency containment reserve". In: *Journal of Energy Storage* 27 (2020), p. 101107.

[107] Uros Markovic et al. "Lqr-based adaptive virtual synchronous machine for power systems with high inverter penetration". In: *IEEE Transactions on Sustainable Energy* (2018).

[108] Uros Markovic et al. "Optimal Sizing and Tuning of Storage Capacity for Fast Frequency Control in Low-Inertia Systems". In: *2019 International Conference on Smart Energy Systems and Technologies (SEST)*. IEEE. 2019, pp. 1–6.

[109] Charalampos Marmaras, Erotokritos Xydas, and Liana Cipcigan. "Simulation of electric vehicle driver behaviour in road transport and electric power networks". In: *Transportation Research Part C: Emerging Technologies* 80 (2017), pp. 239–256.

[110] Olivier Mégel, Johanna L Mathieu, and Göran Andersson. "Maximizing the potential of energy storage to provide fast frequency control". In: *IEEE PES ISGT Europe 2013*. IEEE. 2013, pp. 1–5.

[111] Francesca Madia Mele et al. "Impact of variability, uncertainty and frequency regulation on power system frequency distribution". In: *2016 Power Systems Computation Conference (PSCC)*. IEEE. 2016, pp. 1–8.

[112] Pascal Mercier, Rachid Cherkaoui, and Alexandre Oudalov. "Optimizing a battery energy storage system for frequency control application in an isolated power system". In: *IEEE Transactions on Power Systems* 24.3 (2009), pp. 1469–1477.

[113] Federico Milano. "A python-based software tool for power system analysis". In: *2013 IEEE Power & Energy Society General Meeting*. IEEE. 2013, pp. 1–5.

[114] Federico Milano. *Power system modelling and scripting*. Springer Science & Business Media, 2010.

[115] Federico Milano and Álvaro Ortega Manjavacas. *Converter-based Energy Storage Systems: Context, Modelling and Dynamic Analysis*. Cambridge University Press, 2019.

[116] Federico Milano et al. "Foundations and challenges of low-inertia systems". In: *2018 Power Systems Computation Conference (PSCC)*. IEEE. 2018, pp. 1–25.

[117] Markus Mirz et al. "Dynamic phasors to enable distributed real-time simulation". In: *2017 6th International Conference on Clean Electrical Power (ICCEP)*. IEEE. 2017, pp. 139–144.

[118] Iman Naziri Moghaddam and Badrul Chowdhury. "Optimal sizing of hybrid energy storage systems to mitigate wind power fluctuations". In: *2016 IEEE Power and Energy Society General Meeting (PESGM)*. IEEE. 2016, pp. 1–5.

[119] Carmelo Mosca et al. "Mitigation of frequency stability issues in low inertia power systems using synchronous compensators and battery energy storage systems". In: *IET Generation, Transmission & Distribution* 13.17 (2019), pp. 3951–3959.

[120] Yunfei Mu et al. "Primary frequency response from electric vehicles in the Great Britain power system". In: *IEEE Transactions on Smart Grid* 4.2 (2012), pp. 1142–1150.

[121] Yorie Nakahira et al. "Smoothed least-laxity-first algorithm for ev charging". In: *Proceedings of the Eighth International Conference on Future Energy Systems*. 2017, pp. 242–251.

[122] Nebojsa Nakicenovic et al. "Energy scenarios". In: *World Energy Assessment of the United Nations* (2000).

[123] Emil Namor et al. "Control of battery storage systems for the simultaneous provision of multiple services". In: *IEEE Transactions on Smart Grid* 10.3 (2018), pp. 2799–2808.

[124] Daniel E Olivares et al. "Trends in microgrid control". In: *IEEE Transactions on smart grid* 5.4 (2014), pp. 1905–1919.

[125] Australian Energy Market Operator. *International review of frequency control adaptation*. Tech. rep. 2016.

[126] Australian Energy Market Operator. *Quaterly Energy Dynamics - Q1 2019*. 2019.

[127] Alvaro Ortega and Federico Milano. "Combined Frequency and RoCoF Control of Converter-Interfaced Energy Storage Systems". In: *IFAC-PapersOnLine* 52.4 (2019), pp. 240–245.

[128] Alvaro Ortega and Federico Milano. "Frequency control of distributed energy resources in distribution networks". In: *IFAC-PapersOnLine* 51.28 (2018), pp. 37–42.

[129] Alvaro Ortega and Federico Milano. "Modeling, simulation, and comparison of control techniques for energy storage systems". In: *IEEE transactions on Power Systems* 32.3 (2016), pp. 2445–2454.

[130] Alvaro Ortega and Federico Milano. "Stochastic transient stability analysis of transmission systems with inclusion of energy storage devices". In: *IEEE Transactions on Power Systems* 33.1 (2017), pp. 1077–1079.

[131] Álvaro Ortega and Federico Milano. "Comparison of different PLL implementations for frequency estimation and control". In: *2018 18th International Conference on Harmonics and Quality of Power (ICHQP)*. IEEE. 2018, pp. 1–6.

[132] Álvaro Ortega and Federico Milano. "Impact of frequency estimation for VSC-based devices with primary frequency control". In: *2017 IEEE PES Innovative Smart Grid Technologies Conference Europe (ISGT-Europe)*. IEEE. 2017, pp. 1–6.

[133] Álvaro Ortega et al. "Hardware-in-the-Loop Validation of the Frequency Divider Formula". In: *2018 IEEE Power & Energy Society General Meeting (PESGM)*. IEEE. 2018, pp. 1–5.

[134] Erik Ørum et al. “Future system inertia”. In: *ENTSOE, Brussels, Tech. Rep* (2015).

[135] Alexandre Oudalov, Daniel Chartouni, and Christian Ohler. “Optimizing a battery energy storage system for primary frequency control”. In: *IEEE Transactions on Power Systems* 22.3 (2007), pp. 1259–1266.

[136] J Palermo. “International review of frequency control adaptation”. In: *Australian Energy Market Operator* (2016).

[137] Georgios Papaefthymiou and Ken Dragoon. “Towards 100% renewable energy systems: Uncapping power system flexibility”. In: *Energy Policy* 92 (2016), pp. 69–82.

[138] European Parliament and Council. *Directive (EU) 2019/944 of the European Parliament and of the Council of 5 June 2019 on common rules for the internal market for electricity and amending Directive 2012/27/EU*. 2019.

[139] F Parma et al. “A tool to investigate the PV and storage plants effective integration in the European interconnected transmission network”. In: *2013 International Conference on Clean Electrical Power (ICCEP)*. IEEE. 2013, pp. 254–261.

[140] Bala Kameshwar Poolla, Saverio Bolognani, and Florian Dörfler. “Optimal placement of virtual inertia in power grids”. In: *IEEE Transactions on Automatic Control* 62.12 (2017), pp. 6209–6220.

[141] Vasileios Poulios et al. “Optimal placement and sizing of battery storage to increase the PV hosting capacity of low voltage grids”. In: *International ETG Congress 2015; Die Energiewende-Blueprints for the new energy age*. VDE. 2015, pp. 1–8.

[142] Giuseppe Prettico et al. “Distribution system operators observatory: From european electricity distribution systems to representative distribution networks”. In: *JRC report EUR 27927 EN* (2016).

[143] P Ralon et al. “Electricity storage and renewables: costs and markets to 2030”. In: *International Renewable Energy Agency: Abu Dhabi, UAE* (2019).

[144] Miguel Ramı**********rez et al. “Placement and sizing of battery energy storage for primary frequency control in an isolated section of the Mexican power system”. In: *Electric Power Systems Research* 160 (2018), pp. 142–150.

[145] Giuliano Rancilio et al. “Modeling a Large-Scale Battery Energy Storage System for Power Grid Application Analysis”. In: *Energies* 12.17 (2019), p. 3312.

[146] Simon Remppis et al. “Influence of 15-minute contracts on frequency deviations and on the demand for balancing energy”. In: *International ETG Congress 2015; Die Energiewende-Blueprints for the new energy age*. VDE. 2015, pp. 1–7.

[147] *Results of the EUCO3232.5 scenario on Member States*. Tech. rep. European Commission, 2019.

[148] Michel Rezkalla, Michael Pertl, and Mattia Marinelli. “Electric power system inertia: requirements, challenges and solutions”. In: *Electrical Engineering* 100.4 (2018), pp. 2677–2693.

[149] Michel Rezkalla et al. “Trade-off analysis of virtual inertia and fast primary frequency control during frequency transients in a converter dominated network”. In: *2016 IEEE Innovative Smart Grid Technologies-Asia (ISGT-Asia)*. IEEE. 2016, pp. 890–895.

[150] David Rosewater and Summer Ferreira. “Development of a frequency regulation duty-cycle for standardized energy storage performance testing”. In: *Journal of Energy Storage* 7 (2016), pp. 286–294.

[151] David Rosewater, Paul Scott, and Surya Santoso. “Application of a uniform testing protocol for energy storage systems”. In: *2017 IEEE Power & Energy Society General Meeting*. IEEE. 2017, pp. 1–5.

[152] Sandro Rubino et al. “Advanced control of inverter-interfaced generation behaving as a virtual synchronous generator”. In: *2015 IEEE Eindhoven PowerTech*. IEEE. 2015, pp. 1–6.

[153] Ehsan Samadani et al. “Empirical modeling of lithium-ion batteries based on electrochemical impedance spectroscopy tests”. In: *Electrochimica Acta* 160 (2015), pp. 169–177.

[154] Benjamin Schafer, Marc Timme, and Dirk Witthaut. “Isolating the impact of trading on grid frequency fluctuations”. In: *2018 IEEE PES Innovative Smart Grid Technologies Conference Europe (ISGT-Europe)*. IEEE. 2018, pp. 1–5.

[155] Marc Scherer. “Frequency control in the European power system considering the organisational structure and division of responsibilities”. PhD thesis. ETH Zurich, 2016.

[156] Robert Schmidt et al. “Revenue-optimized Marketing of electric Vehicles’ Flexibility Options”. In: *International ETG-Congress 2019; ETG Symposium*. VDE. 2019, pp. 1–6.

[157] R Schwerdfeger et al. "Approach for load frequency control participation by decentralized energy devices". In: *2015 IEEE Power & Energy Society General Meeting*. IEEE. 2015, pp. 1–5.

[158] Ioan Serban, Remus Teodorescu, and Corneliu Marinescu. "Energy storage systems impact on the short-term frequency stability of distributed autonomous microgrids, an analysis using aggregate models". In: *IET Renewable Power Generation* 7.5 (2013), pp. 531–539.

[159] AA Shaltout and KA Abu Al-Feilat. "Damping and synchronizing torque computation in multimachine power systems". In: *IEEE transactions on power systems* 7.1 (1992), pp. 280–286.

[160] Qingxin Shi, Fangxing Li, and Hantao Cui. "Analytical method to aggregate multi-machine SFR model with applications in power system dynamic studies". In: *IEEE Transactions on Power Systems* 33.6 (2018), pp. 6355–6367.

[161] B Shoeiby et al. "Dynamics of droop-controlled microgrids with unequal droop response times". In: *2013 Australasian Universities Power Engineering Conference (AUPEC)*. IEEE. 2013, pp. 1–6.

[162] Lakshmi Srinivasan et al. "Provision of frequency control by a BESS in combination with flexible units". In: *2018 IEEE International Energy Conference (ENERGYCON)*. IEEE. 2018, pp. 1–6.

[163] Karl Stein et al. "Characterization of a Fast Battery Energy Storage System for Primary Frequency Response". In: *Energies* 11.12 (2018), p. 3358.

[164] Daniel-Ioan Stroe et al. "Operation of a grid-connected lithium-ion battery energy storage system for primary frequency regulation: A battery lifetime perspective". In: *IEEE transactions on industry applications* 53.1 (2016), pp. 430–438.

[165] Insight_E energy think tank. *How Can batteries Support Eu electricity System*. 2016.

[166] Ali Tayyebi et al. "Gridforming converters–inevitability, control strategies and challenges in future grid applications". In: *International Conference on Electricity Distribution (CIRED)*. 2018.

[167] *Technical report on Member State results of the EUCO policy scenarios*. Tech. rep. E3MLAB and IIASA, 2016.

[168] Terna. *Allegato A15 al Codice di Rete; Regolazione Frequenza Potenza*. 2008.

[169] Terna. *Progetto pilota riserva ultra-rapida di frequenza*. 2019.

[170] Terna. *Terna pilot projects. [Online].* URL: http://www.terna.it/en-gb/sistemaelettrico/progettipilotadiaccumulo.aspx (visited on 10/01/2020).

[171] Terna. *Terna UVAM pilot project. [Online].* URL: https://www.terna.it/it/sistema-elettrico/progetti-pilota-delibera-arera-300-2017-reel/progetto-pilota-uvam (visited on 10/01/2020).

[172] Andreas Thingvad, Charalampos Ziras, and Mattia Marinelli. "Economic value of electric vehicle reserve provision in the Nordic countries under driving requirements and charger losses". In: *Journal of Energy Storage* 21 (2019), pp. 826–834.

[173] Pieter Tielens and Dirk Van Hertem. "The relevance of inertia in power systems". In: *Renewable and Sustainable Energy Reviews* 55 (2016), pp. 999–1009.

[174] Lucian Toma et al. "On the virtual inertia provision by BESS in low inertia power systems". In: *2018 IEEE International Energy Conference (ENERGYCON)*. IEEE. 2018, pp. 1–6.

[175] Politecnico di Torino. *Deliverable 1.4. Use Case Definition for Research in Frequency and Voltage Control*. Tech. rep. RESERVE European project, 2017.

[176] Politecnico di Torino and RESERVE partners. *Deliverable 1.1. Scenarios & architectures for 100% RES and roles of sector actors*. Tech. rep. RESERVE European project, 2016.

[177] Christoph Trabert, Andreas Ulbig, and Göran Andersson. "Model predictive frequency control employing stability constraints". In: *2015 American Control Conference (ACC)*. IEEE. 2015, pp. 5678–5685.

[178] Operation Handbook UCTE. *Appendix 1, Load-frequency Control and Performance*. 2009.

[179] Willem Uijlings, DNV KEMA Ltd Cathedral Street, and SE London. *An independent analysis on the ability of Generators to ride through Rate of Change of Frequency values up to 2Hz/s*. Tech. rep. s. Technical report, Uijlings, 2013.

[180] Andreas Ulbig et al. "General frequency control with aggregated control reserve capacity from time-varying sources: The case of PHEVs". In: *2010 IREP Symposium Bulk Power System Dynamics and Control-VIII (IREP)*. IEEE. 2010, pp. 1–14.

[181] Andreas Ulbig et al. "Predictive control for real-time frequency regulation and rotational inertia provision in power systems". In: *52nd IEEE Conference on Decision and Control*. IEEE. 2013, pp. 2946–2953.

[182] Ivan Vera and Lucille Langlois. "Energy indicators for sustainable development". In: *Energy* 32.6 (2007), pp. 875–882.

[183] Petr Vorobev et al. "Deadbands, Droop and Inertia Impact on Power System Frequency Distribution". In: *IEEE Transactions on Power Systems* (2019).

[184] Evangelos Vrettos, Frauke Oldewurtel, and Göran Andersson. "Robust energy-constrained frequency reserves from aggregations of commercial buildings". In: *IEEE Transactions on Power Systems* 31.6 (2016), pp. 4272–4285.

[185] Xiongfei Wang et al. "A review of power electronics based microgrids". In: *Journal of Power Electronics* 12.1 (2012), pp. 181–192.

[186] Rashid A Waraich et al. "Plug-in hybrid electric vehicles and smart grids: Investigations based on a microsimulation". In: *Transportation Research Part C: Emerging Technologies* 28 (2013), pp. 74–86.

[187] Tobias Weißbach, Simon Remppis, and Hendrik Lens. "Impact of current market developments in Europe on deterministic grid frequency deviations and frequency restauration reserve demand". In: *2018 15th International Conference on the European Energy Market (EEM)*. IEEE. 2018, pp. 1–6.

[188] Bolun Xu et al. "Modeling of lithium-ion battery degradation for cell life assessment". In: *IEEE Transactions on Smart Grid* 9.2 (2016), pp. 1131–1140.

[189] Weijia Yang et al. "Wear reduction for hydropower turbines considering frequency quality of power systems: a study on controller filters". In: *IEEE Transactions on Power Systems* 32.2 (2016), pp. 1191–1201.

[190] Alireza Zakariazadeh, Shahram Jadid, and Pierluigi Siano. "Multi-objective scheduling of electric vehicles in smart distribution system". In: *Energy Conversion and Management* 79 (2014), pp. 43–53.

[191] Rafael Zárate-Miñano, Marian Anghel, and Federico Milano. "Continuous wind speed models based on stochastic differential equations". In: *Applied Energy* 104 (2013), pp. 42–49.

[192] Antonio Zecchino et al. "Enhanced primary frequency control from EVs: a fleet management strategy to mitigate effects of response discreteness". In: *IET Smart Grid* 2.3 (2019), pp. 436–444.

[193] Fang Zhang et al. "Assessment of the effectiveness of energy storage resources in the frequency regulation of a single-area power system". In: *IEEE Transactions on Power Systems* 32.5 (2017), pp. 3373–3380.

[194] Hongcai Zhang et al. “Evaluation of achievable vehicle-to-grid capacity using aggregate PEV model”. In: *IEEE Transactions on Power Systems* 32.1 (2016), pp. 784–794.

[195] Qing-Chang Zhong et al. “Self-synchronized synchronverters: Inverters without a dedicated synchronization unit”. In: *IEEE Transactions on power electronics* 29.2 (2013), pp. 617–630.

[196] Yue Zhou, Meng Cheng, and Jianzhong Wu. “Enhanced frequency response from industrial heating loads for electric power systems”. In: *IEEE Transactions on Industrial Informatics* 15.6 (2018), pp. 3388–3399.

This Ph.D. thesis has been typeset by means of the TEX-system facilities. The typesetting engine was pdfLATEX. The document class was `toptesi`, by Claudio Beccari, with option `tipotesi=scudo`. This class is available in every up-to-date and complete TEX-system installation.